Evaluation of FcR-directed immunotherapeutic strategies to manipulate macrophages in *in vitro* and *ex vivo* models of chronic inflammation

Von der Fakultät für Mathematik, Informatik und Naturwissenschaften der RWTH Aachen University zur Erlangung des akademischen Grades eines Doktors der Naturwissenschaften genehmigte Dissertation
vorgelegt von

Master of Science Biotechnology

Radoslav Mladenov

aus Stara Zagora (Bulgarien)

Berichter: Universitätsprofessor Dr. Rainer Fischer

Universitätsprofessor Dr. Jürgen Bernhagen

Tag der mündlichen Prüfung: 20.12.2016

Dulcius ex asperis

A Latin phrase meaning "sweeter after difficulties".

Summary

Macrophages are a fundamental part of the immune system and are responsible for diverse physiological processes including inflammation, tissue repair and homeostasis. Displaying extraordinary diversity and plasticity, macrophages are clustered in an intricate model, with two extremes – pro-inflammatory (M1) versus anti-inflammatory (M2) phenotypes. Mirroring the Th1/Th2 dichotomy, M1/M2 participate in initiation of the inflammation process and guide it until final resolution. While the M1 phenotype dominates in the early inflammation phase by initiating and orchestrating the immune response, a transition towards predominance of the M2 phenotype occurs at the final stage, which is important for resolution, tissue repair, and final healing. However, in a variety of immune-mediated inflammatory diseases, like rheumatoid arthritis, chronic cutaneous inflammation, this M1/M2 balance is disturbed and a persistency of M1 arrests the pro-inflammatory phase, contributing directly to the chronicity. To address the lack of available strategies for a targeted treatment of the mentioned diseases, in this thesis an emphasis will be put on the development of novel immunotherapeutical approaches. Recently, our group showed in a series of experiments that CD64-directed depletion of M1 using recombinant ETA'-based immunotoxin (IT) was able to reverse this increased M1/M2 ratio. This approach could be utilized in order to influence pathogenic changes of the M1/M2 ratio in a therapeutic setting.

In this thesis, first “proof-of-concept” in the human system is demonstrated by testing the IT-treatment *ex vivo* using biopsies from patients with chronic skin inflammation (atopic dermatitis or chronic diabetic wounds). Next to normalizing the M1/M2 ratio as reported in the previous *in vivo* animal study, also the cytokine levels (e.g. IL-6 and IL-10) could successfully be normalized towards the anti-inflammatory profile. Furthermore, the collected data in this work provides additional evidence for the large macrophage heterogeneity as well as plasticity demonstrated by the ability of M1 to be functionally repolarized into the M2 direction and *vice versa*. This key observation points towards a potential novel therapeutic approach with regard to macrophages-targeted therapy: the modulation, rather than the elimination of M1 macrophages. Unlike the CD64-targeting IT therapy, the immunomodulation aims to intervene in the inflammation process and restores the cytokine balance without affecting the macrophage viability. Therefore, two immunomodulatory fusion proteins were designed to target CD64, the distinctive marker for M1, and deliver two different human effector proteins - thioredoxin 1 (Trx-1) and suppressor of cytokine signaling 2 (SOCS-2). The constructs were genetically engineered as C-terminal fusion partners to H22(scFv), expressed in HEK293T c ells and

purified using affinity chromatography. The identity and binding specificity of the macrophage immunomodulatory proteins (MIMPs) were successfully confirmed using SDS-PAGE followed by Coomassie staining, western blotting, and flow cytometry, respectively. Primary macrophages were derived from human PBMCs and used to investigate the immunomodulatory activity of both MIMPs. Two different experimental approaches termed "priming" and "treatment" were used *in vitro* — which represent both application paths – systemic and local, respectively. While H22(scFv)-Trx-1 failed to induce substantial repolarization, H22(scFv)-SOCS-2 successfully attenuated the expression of pro-inflammatory cytokines in M1 (e.g. IL-6, IL-12, TNF-α and IL-1β). In addition, it also induced secretion of anti-inflammatory IL-10. However, H22(scFv)-Trx-1 was able to attenuate the oxidative stress in M1. Furthermore, priming of non-polarized macrophages with both MIMPs proved successful in prevention of the later polarization into the M1-like phenotype upon stimulation with wound exudate. Herein the superior effect of H22(scFv)-SOCS-2 was again demonstrated by the substantial induction of IL-10 production. In the future, the clinical relevance of these findings should be confirmed in *ex vivo* experiments using human biopsies or in an appropriate preclinical animal model.

In a parallel line of exploration, the suitability of the Fc-alpha receptor (FcαR, CD89) for immunotherapy-targeting macrophages was investigated *in vitro*. To that aim, the receptor density of CD89 and CD64 was determined by flow cytometry. Although CD89 was expressed at lower levels than CD64 on both M1 and M2, it was preferentially expressed by M1. To develop CD89-targeted immunotherapy, an IT comprising a CD89-binding scFv and ETA' was recombinantly expressed and subsequently affinity purified. Successful binding, internalization and receptor-dependent cytotoxicity of this IT was confirmed on $CD89^+$ pro-monocytic cell lines (HL-60, THP-1, MonoMac-1 and U937), whereby IC_{50} values tended to be dependent on the nature of the stimulus (e.g. IFN-γ or TNF-α). Nevertheless, the CD89(scFv)-ETA' failed to induce apoptosis in primary human PBMC-derived macrophages regardless of their phenotype, but these findings revealed possible utilization of the CD89-directed IT in the context of myeloid leukemia, neutrophilia and similar diseases.

In conclusion, results of this thesis provide new insights into the immunomodulation of macrophages using a well validated CD64-targeted delivery system as well as the function of SOCS-2 and Trx-1 in the context of polarized macrophages during chronic inflammation. The CD64 but not the CD89 path in combination with a suitable effector payload comprises a promising therapeutic strategy for inflammatory diseases, strengthening the immunotherapeutic armamentarium.

Zusammenfassung

Makrophagen stellen einen wesentlichen Teil des angeborenen Immunsystems dar und spielen eine entscheidende Rolle bei der Regulation von Entzündung, Immunabwehr, Geweberegeneration und Homöostase. Sie zeichnen sich durch enorme Diversität und Plastizität aus: Makrophagen sind in einem komplexen Modell gruppiert mit zwei Extremen– pro-inflammatorischer (M1) gegenüber anti-inflammatorischem (M2) Phänotyp. Die Th1/Th2-Dichotomie wiederspiegelnd sind M1/M2 an der Einleitung eines entzündlichen Prozesses beteiligt und begleiten ihn bis zur finalen Auflösung. Während der M1-Phänotyp in der frühen Entzündungsphase durch Orchestrierung der Immunantwort dominiert, tritt ein Übergang zur M2-Dominanz in der späteren Phase ein, die für die Förderung der Gewebereparatur und Heilung von wesentlicher Bedeutung ist.

Jedoch in einer Vielzahl von immunvermittelten Entzündungserkrankungen, wie der rheumatoiden Arthritis oder der chronischen Hautentzündung, ist das M1/M2-Gleichgewicht gestört und eine Persistenz von M1 arretiert die pro-inflammatorische Phase, was letztendlich zu einem chronischen Aktivierungszustand führt. Um den Mangel an verfügbaren Strategien für die gerichtete Behandlung der aufgeführten Erkrankungen zu adressieren, wird in dieser Studie ein Schwerpunkt auf die Entwicklung von neuen immuntherapeutischen Ansätzen gesetzt. In Vorarbeiten wurde in erster Linie in Mausexperimenten gezeigt, dass die CD64-gerichtete Elimination von M1 unter Verwendung von rekombinantem ETA'-b asierten Immuntoxin (IT) in der Lage ist, das zunehmende M1/M2-Verhältnis umzukehren.

In dieser Arbeit wurde dieser Entwicklungsprozess von Makrophagen-gerichteten Therapieansätzen weiter fortgesetzt. Als Konzeptnachweis für das humane System wurde eine IT-Behandlung *ex vivo* an Biopsien von Patienten mit chronischen Hautentzündungen (atopische Dermatitis oder chronische diabetische Wunden) durchgeführt. Dabei wurde neben Normalisierung des M1/M2-Verhältnisses wie in der früheren *in vivo*-Studie auch der Zytokinspiegel (insbesondere IL-6 und IL-10) in Richtung der entzündungshemmenden Phase verschoben. Darüber hinaus stellten die in dieser Arbeit gesammelten Daten erste zusätzliche Beweise für die immense Heterogenität und Plastizität der Makrophagen dar: hier wurde dokumentiert, dass M1 funktionell fähig sind, in Richtung M2 umzupolarisieren und umgekehrt. Dieses weltweit erstmals dargestellte Schlüsselmerkmal eröffnet das Potenzial für einen neuartigen therapeutischen Ansatz: die Makrophagen-gerichteten Immunmodulation und nicht unbedingt eine Elimination von Makrophagen. Im Gegensatz zur CD64-spezifischen IT-Therapie soll die Immunmodulation so in den Entzündungsprozess eingreifen, dass das Zytokingleichgewicht wieder hergestellt wird, ohne die Makrophagenviabilität einzuschränken.

Zu diesem Zweck wurden zwei immunmodulatorische Fusionsproteine entwickelt, die gegen den distinkten M1-Oberflächenmarker - CD64 - gerichtet sind. Als Fusionspartner dieser Makrophagen-immunomodulatorischen Proteine (MIMP) wurden zwei verschiedene humane Effektorproteine - Thioredoxin 1 (Trx-1) und Suppressor of Cytokine Signaling 2 (SOCS-2) hergestellt. Diese wurden genetisch als C-terminale Fusionspartner an das anti-CD64 Antikörperfragment H22(scFv) fusioniert, rekombinant in HEK293T exprimiert und durch Affinitätschromatographie gereinigt. Die Identität und Bindungsspezifität beider MIMP wurde mittels SDS-PAGE mit Coomassie-Färbung und Western Blotting, sowie Durchflusszytometrie bestätigt. Primäre Makrophagen wurden aus humanen PBMCs isoliert und für die Untersuchung der immunmodulatorischen Aktivität beider MIMPs verwendet. Zwei verschiedene experimentelle Ansätze wurden *in vitro* durchgeführt – Vorbehandlung (priming) und Nachbehandlung (treatment). Dadurch wurden die beiden möglichen Applikationswege repräsentiert: systemisch *versus* lokal. Während H22(scFv)-Trx-1 keine erhebliche Repolarisation von Makrophagen auslösen konnte, war H22(scFv)-SOCS-2 nicht nur in der Lage die Expression von pro-inflammatorischen Zytokinen in M1 (IL-6, IL-12, TNF-α und IL-1β) erfolgreich zu verringern, sondern auch die Sekretion des anti-inflammatorischen Zytokins IL-10 zu induzieren. Unabhängig davon ermöglichte eine Vorbehandlung unpolarisierter Makrophagen mit beiden MIMPs eine Blockade für eine Polarisierung in M1-Richtung nach Stimulation mit Wundexsudat. In diesem Ansatz konnte wiederum eine deutlich bessere Wirkung von H22(scFv)-SOCS-2 durch eine signifikante Induktion der IL-10 Produktion gezeigt werden. In der Zukunft sollte die klinische Relevanz dieser präliminären Befunde in *ex vivo*-Experimenten mit menschlichen Biopsien oder in einem geeigneten präklinischen Tiermodell bestätigt werden.

In einer parallelen *in vitro*-Untersuchung wurde die Eignung des Fc-alpha-Rezeptors (FcαR, CD89) für eine alternative, Makrophagen-gerichtete Immuntherapie untersucht. Dafür wurde die Rezeptordichte von CD89 und CD64 mittels Durchflusszytometrie gemessen. Obwohl CD89 im Vergleich zu CD64 auf M1 und M2 in geringeren Konzentrationen exprimiert wurde, war CD89 markant für M1. Für die CD89-gerichtete Immuntherapie wurde ein korrespondierendes anti-CD89 Antikörperfragment an ETA' fusioniert, in *E. coli* exprimiert und durch Affinitätschromatographie gereinigt. Erfolgreiche Bindung, Internalisierung und Dosis-abhängige Zytotoxizität der generierten IT konnte auf $CD89^+$ monozytären Zelllinien (HL-60, THP-1, MonoMac-1 und U937) bestätigt werden. Die IC_{50}-Werte korrelierten mit dem eingesetzten Stimulus (z.B. IFN-γ oder TNF-α). Allerdings zeigte das generierte CD89(scFv)-ETA' keine zytotoxische Wirkung auf primären Makrophagen unabhängig von ihrem Phänotyp.

Obwohl sich auf Grund dieses Ergebnissen CD89(scFv)-ETA' nicht für die Behandlung von Makrophagen-vermittelten Erkrankungen eignet, könnte dieses IT nichtsdestotrotz eine Anwendung bei anderen Erkrankungen wie z.B. myeloide Leukämie, Neutrophilie u.a. finden.

Zusammenfassend liefern die Ergebnisse dieser Arbeit erste Einblicke für eine mögliche Immunmodulation von Makrophagen durch neue, CD64-spezifische rekombinante Fusionsproteine. Hier wurden insbesondere die Kombination und die Funktion von SOCS-2 und Trx-1 im Zusammenhang mit einer induzierbaren Makrophagenpolarisation im Kontext der chronischen Entzündung dargestellt. Hierdurch eröffnet sich nicht nur ein vielversprechender und innovativer neuer Behandlungsansatz für Entzündungserkrankungen, sondern auch eine Vergrößerung der Palette des immuntherapeutischen Instrumentariums.

Table of contents

Acknowledgements

First and foremost, I would like to express my greatest thanks to my doctoral advisor **Prof. Dr. Rainer Fischer** for supervising this thesis and for supporting me throughout my academic education.

I am deeply thankful to **Prof. Dr. Jürgen Bernhagen** for agreeing to co-supervise me. I would like to thank **Prof. Dr. Dr. Stefan Barth** for giving me the chance to start my project in his department.

I wish also to thank **Prof. Dr. Lothar Elling** for agreeing to act as a co-referent.

I am indebted to **Dr. Theo Thepen** for allowing me to work in his group, for practically supervising this project, and for critically reading this thesis. Thank you also for taking the time to answer my questions, for giving me valuable advices and for giving me working freedom during the last years.

Many thanks go to **Prof. Dr. Jörn Schmitz, Dr. Christoph Stein, Dr. Birgit Orthen, Dr. Rolf Fendel,** and **Dr. Michael Huhn** for the additional support of this work, all the valuable suggestions and for their encouragement in difficult phases as well as for valuable discussions.

My special thanks go to my friend and colleague **Dr. Dmitrij Hristodorov** and **his family**. Thank you for the solid friendship, cheering humor and great time in and outside the lab!

Iam very grateful to my colleagues – **Sonja, Lea, Chris, Karinna, Alda, Eric, Judith, Hannes, Tobi, Steffi, Manal,** and the rest of the PhD students in Fraunhofer IME. One might say that I´ve seen them in the past 3 years more often than anyone else.

For their kind help in the lab, I am very grateful to **Reinhard, Anh-Tuan, Severin,** and **Kai.**

I would like to thank **both my students – Tim** and **Fabian** not only for doing a lot of valuable work within the project but also I am thankful for their solid friendship and data output!

Last but not least, I would like to say thank you to **my parents - Julia and Asen,** who supported me despite the great distance to my native country.

Finally, I would like to thank **my girlfriend Desislava** for always encouraging me, understanding me, and being the woman behind my success.

The support in form of scholarship by the Jürgen Manchot Foundation is gratefully acknowledged.

I Introduction

I.1. Chronic inflammatory diseases hamper the modern society

The most common chronic condition in adults is called multimorbidity. This concept encompasses the coexistence of multiple chronic diseases or conditions, which are responsible for seven out of ten deaths each year. The treatment of people with chronic diseases accounts for 86% of the USA's health care costs [3]. Chronic conditions such as diabetes, chronic inflammatory skin diseases (e.g. atopic dermatitis (AD) and chronic diabetic wounds (CDWs)), rheumatoid arthritis (RA), and multiple sclerosis (MS) have a strong chronic inflammatory component and lay a heavy burden on health with a socio-economic impact worldwide [4, 5]. Inflammation plays an important role in the most common causes of death worldwide, including atherosclerotic cardiovascular disease, cancer, and chronic obstructive lung disease. Unfortunately, the increasing rates of these chronic systemic illnesses suggest that inflammation caused by excessive and inappropriate activation of the innate immune system is unable to respond appropriately to danger signals that are new in the context of evolution [6]. This leads to unresolved or chronic inflammatory activation of the body also termed immune-mediated inflammatory diseases (IMID). In its nature, inflammation is designed to protect and recover the human body from invaders. It has been long known that inflammation is a self-limiting and controlled process of the immune system (IS). In general it is defined by an initial trigger followed by an acute inflammatory stage, pathogen clearance and finalized by resolution phase. Under the control of immune and tissue cells, the inflammation should follow strictly the healing course. However, in many cases the complex network of the inflammation process suffers dysfunctions of different nature, which lead induction or worsening of the above mentioned pathologies.

In a "Nature" review, Serhan *et al.* described specialized pro-resolving mediators (SPMs), which are produced during the acute inflammatory response and have important roles in orchestrating the resolution of tissue inflammation [7-9]. These endogenous SPMs (e.g. lipoxins, protectins, resolvins, etc.) act as checkpoint controllers in inflammation and introduce, and fine-tune the resolution course – a process termed as "resoleomics" [10, 11]. Considering the modern pandemic increase of chronic medical illnesses involving chronic inflammation, it has become apparent that these resolution mechanisms are not achieving their potential resolving capacity [12]. As an explanation for the explosion in rates of chronic unresolving inflammation, Bosma-den Boer raises the hypothesis that recent drastic changes in lifestyle including diet, especially over-nutrition and psycho-emotional stress, are responsible for

inflammation and for disturbances in the healing process. In addition, current interventions like persistent use of anti-inflammatory medication and even antibiotics potentially suppress the final resolution of inflammation. The persistent stress factors of recent lifestyle changes have pushed the IS into a constant state of activity, leading to chronically unresolved inflammation and increased vulnerability for chronic disease [12]. While the adaptation of the human organism to lifestyle changes is a biologic process in need of several generations ahead, modern scientists are challenged before long to develop new pharmaceutical products for treatment of IMIDs.

I.2. Challenging the fundamental macrophage dogma

Highlighting the key portion of Ilya Metchnikoff´s Nobel Prize finding for physiology or medicine in 1908, George Bernard Shaw (1856-1950) opined in his play named "The Doctor's Dilemma" that "There is at the bottom only one genuine scientific treatment for all diseases and that is to stimulate the phagocytes". G.B. Shaw's exhortation to stimulate the phagocytes raised solid debates at that time whenever or not host IS might have a universal mode of action against viruses, microbial and neoplastic cells. More than a century later, the "early" phagocytes turned out to be a cluster of immune cells capable of "professional" phagocytosis (e.g. monocytes (MO), macrophages (MΦ), neutrophils (NΘ)), but there are also "non-professional" phagocytes including epithelial cells, endothelial cells, fibroblasts, and mesenchymal cells [13]. Being an important part of the cellular innate IS the MO and MΦ have - as potent phagocytes - crucial and distinct roles in tissue homeostasis and immunity. Until recently, a fundamental dogma established by van Furth's mononuclear phagocyte system (MPS) concept in 1968 [14] postulated that the homeostasis of tissue-resident MΦ relies on the constant recruitment of blood MO. As such, MO and MΦ were considered as two closely related cell types that arise from a continuum of differentiation. However, although MO give rise to MΦ under certain circumstances and environments, a recent study has challenged the generalized applicability of this dogma by showing that most tissue MΦ originate and are maintained independently of MO input [15]. Thus, it is now considered that tissue-resident MΦ are able to self-maintain locally throughout adult life with minimal contribution from circulating MO. Apart from their origin, when activated, MΦ count among all immune cells as the most potent cytokine producers in human immune system and thus, major orchestrators in inflammation [16]. Furthermore, MΦ can undergo a diverse program of polarization, which depending on the microenvironment dictates their effector functions [17]. First evidenced by Sutterwala *et al.* in 1998 the M1/M2 paradigm was officially proposed by Mills *et al.* in 2000. Accordingly, MΦ can acquire a

classical M1 polarization, upon encountering microbial products (e.g. LPS) or inflammatory cytokines (e.g. interferon-gamma (IFN-γ)), or an alternative M2 polarization in response to IL-4 or IL-13. The hallmarks of M1 macrophages are overexpression of surface (e.g. CD32, CD64, CD68 and CD14) and soluble (IL-12, IL-6, TNF-α and IL-1β) markers, upregulation in the production of reactive nitrogen and oxygen species (RNS and ROS), and potent antigen presentation via major histocompatibility complex (MHC) I and II classes [18]. Alternatively polarized MΦ (M2) are further classified into different subsets (M2a, M2b, and M2c) based on the type of stimulation and the subsequent expression of surface molecules and cytokines. The M2a profile exhibits a wound-healing and tissue repairing activity, which is influenced by Th-2 cells. Regulatory M2b appear similar to M2a upon activation by regulatory T-cells and various stimuli, such as immuno-complexes and glucocorticoids. Following induction by IL-10, the M2c contribute in suppression of immune responses and tissue remodeling. M2 markers include surface CD206, CD163, CD301, and CD273 [19]. More recently, the human MΦ activation was clustered in a complex model (**Figure 1B**), which has widely expanded the previous simplified M1/M2 model (**Figure 1A**) [20, 21]. Based on analysis of MΦ transcriptomes the multispectral model by Xue *et al.* demonstrates the extraordinary MΦ plasticity and heterogeneity.

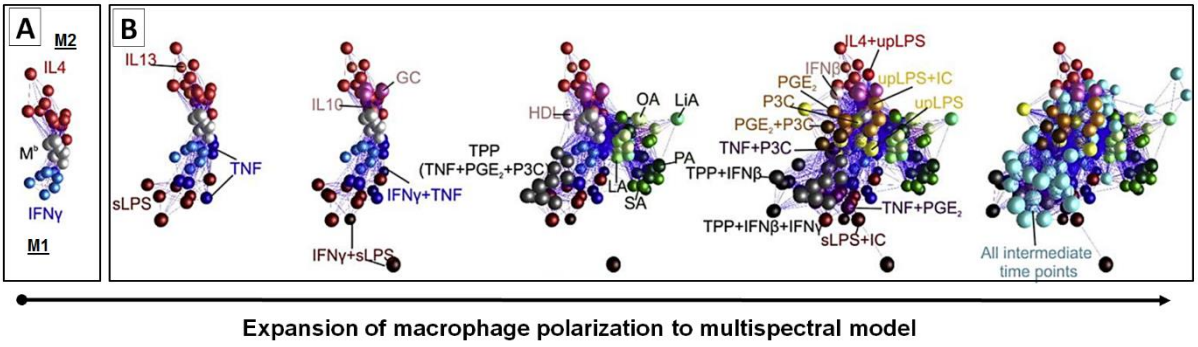

Figure 1: MΦ polarization presented in a novel spectrum model
Xue *et al.* stimulated human MΦ with diverse activation signals, acquiring a data set of 299 MΦ transcriptomes. Analysis of this data set extended the current M1 versus M2-polarization model **(A)** and revealed a spectrum of MΦ activation states **(B)** depending on added stimulus (e.g. LPS, IL-10, etc.) [20].

I.3. MΦ phenotypes in pathophysiology

Macrophages play a beneficial role in pathogenic and homeostatic clearance, which includes the potent induction and regulators of immune responses and also the essential role in the orchestration of many metabolic functions in health and disease. However, alongside the diverse roles in protective immunity and homeostasis MΦ also contribute to many pathological processes (e.g. chronic inflammatory diseases). Many disease models are based on the distinction of MΦ subtypes in regard to the disease location (e.g. alveolar MΦ versus synovial

MΦ) [22, 23]. However, recent evidence of the functional and phenotypic similarity between the pathologic MΦ subtypes in different diseases raised the possibility of considerable simplification of different models. Consequently, the two sites of the same coin - the M1 versus M2 types of MΦ – comprise a simple bipolar model to better understand and discriminate the positive from negative impact during some of the classic IMIDs (e.g. wound healing, RA, MS, etc.). As illustrated in **Figure 2**, there is plenty of evidence in the literature pointing either directly to pro-inflammatory M1 MΦ or M1-related cytokines (e.g, TNF-α, interleukin (IL)-1, IL-6, etc.) in variety of IMIDs such as: ankylosing spondylitis (AS) [24] , atherosclerosis [25], AD [26], CDWs [27], inflammatory bowel disease (IBD) [28, 29], kidney disease [30, 31], MS [32, 33], pancreatitis [34], RA [35, 36] and stomach infections [37]. Due to the dominance of MΦ in the mentioned diseases, researchers have just recently introduced the concept of MΦ-mediated inflammatory disorders [38], which covers parts of the IMIDs. However, this term is still new to the immunological society and needs time to become popular. Although the exact underlying defect(s) in many of the IMIDs is still unknown [39], it is clear that persistent cytokine secretion is causing a vicious circle, which augments the inflammation and also leads to chronic pain by directly activating nociceptive sensory neurons [40, 41]. Recently, Xue *et al*.

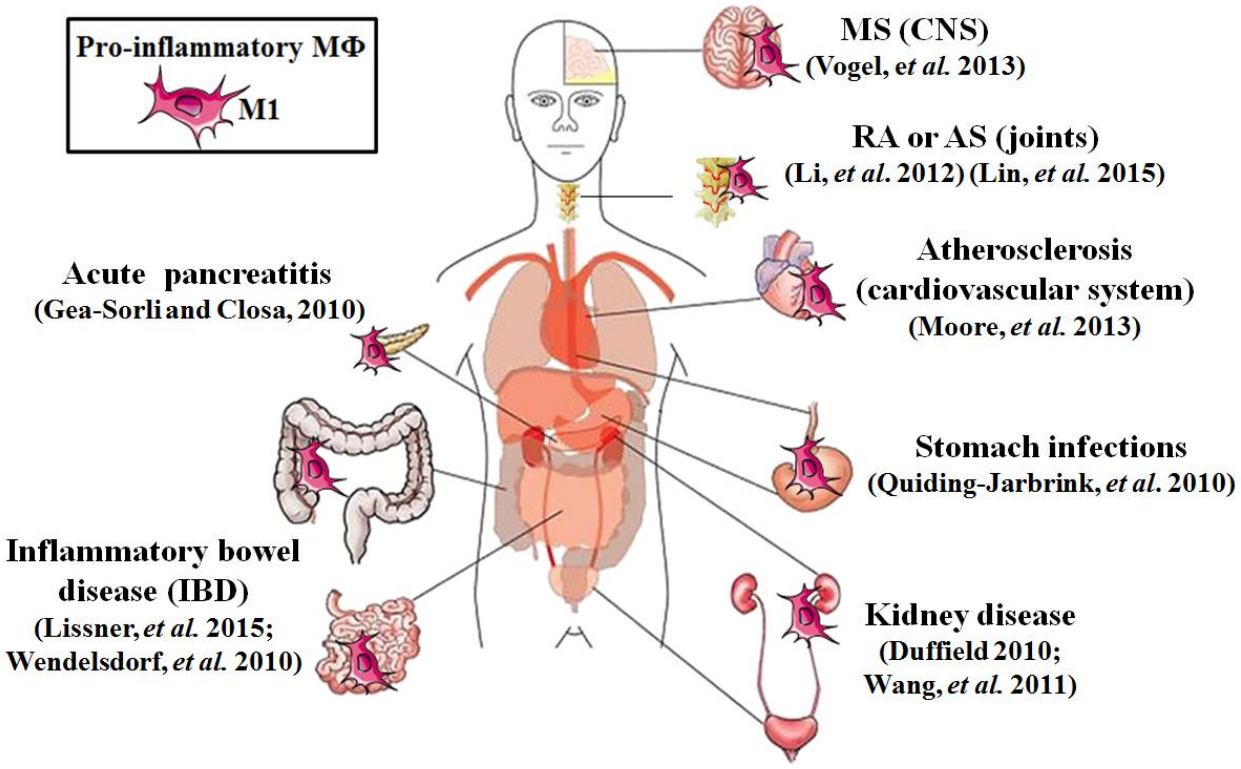

Figure 2: IMIDs are marked by strong dominance of pro-inflammatory MΦ (M1).
Map of human body indicating most abundant inflammatory diseases associated with dominance of M1 MΦ. Image adaptation is designed by Radoslav Mladenov. The original image source is http://images.tutorvista.com/content/feed/u72/body2.JPG.

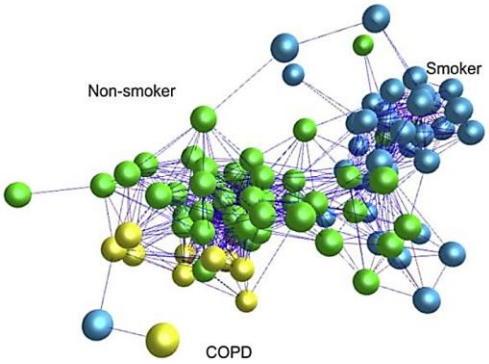

Figure 3: Dynamics of MΦ´ phenotypes in health and disease. MΦ undergo dynamic phenotype changes during disease (e.g. COPD) or habits (e.g. smoking). Xue *et al*. performed further a study of the correlation network of human alveolar MΦ (n = 100) from two studies [43, 44] using 374 genes differentially expressed between nonsmokers (n = 39) and smokers (n = 49) or COPD (n = 12) patients [20].

confirmed the phenotype dynamics of MΦ during diseases or even habits in a transcriptome analysis of alveolar MΦ from non-smokers, smokers or patients with chronic obstructive pulmonary disease (COPD) (**Figure 3**) [20, 42]. As expected, this study revealed three distinct transcriptional programs in MΦ from the three groups being assigned to three different clusters. For example, unlike non-smokers, in smokers the gene modules associated with glucocorticoids [45] as well as free fatty acids and IL-4 were significantly enriched, which suggests a complex stimuli network. Interestingly, the study revealed for COPD patients a complete loss of the enriched modules observed in smokers. However, a module linked to IFN-γ stimulation was strongly depleted in alveolar MΦ from both - smokers and COPD patients. In conclusion, this study sets an important building block in understanding the multiple mechanisms and complex gene controlling caused by the environment. Moreover, the broader transcriptome analysis brings new insights of how the transcriptional network operates differently from normal during certain disease. In the future studies should be extended to compare extensive transcriptome analysis from the same tissues in homeostasis and pathophysiology in order to develop suitable models for new therapeutic strategies in human disease [20]. Therefore, as also Ginhoux and Jung reckon in their recent "Nature" review, there is much interest in the potential of manipulating these cells for therapeutic benefit. Interventions might aim to deplete MO/MΦ when their effects are detrimental or, alternatively, to boost their activity when it is advantageous [46].

I.4. Inflammation biomarkers related to macrophages

Inflammatory MO/MΦ selectively traffic to the sites of inflammation, produce inflammatory cytokines and chemokines, and thereby actively orchestrate and contribute to both local and systemic inflammation. Thus, in this study a panel of mediators is analyzed, which is actively involved in inflammation and thus assigned to the MΦ population: IL-1β, IL-6 IL-12, TNF-α, GM-CSF, IL-10, IL-4, IL-13, TGF-β, MIP-1α, MIP-1β, and CXCL-10.

I.4.1. Soluble mediators in inflammation associated with MΦ

Interleukin 12

The interleukin 12 (IL-12) family includes IL-12, IL-23, IL-27, and IL-35. Biologically active IL-12 is a disulfide-linked heterodimeric 70 kDa cytokine composed of a 35 kDa (p35) and a 40 kDa (p40) subunit. The p35 subunit is a member of the IL-6 superfamily and is secreted in response to IFN-γ and upon stimulation via TLR-3, TLR-4 or TLR-7 axis. The p40 subunit is secreted either as a monomer or homodimer, whereas it is regulated independently of p35 [47]. The IL-12 p70 IL-12 is a strong pro-inflammatory cytokine produced by APCs, which can be dendritic cells (DCs), MΦ and also B-cells. The IL-12 is involved in a feedback loop between T-cells and APCs since IL-12 induces IFN-γ production by T-cells, which facilitate also Th1 differentiation [48, 49].

Interleukin-6

The interleukin-6 (IL-6) is a multi-functional cytokine involved in regulation of immune responses, acute phase reactions and hematopoiesis. IL-6 is a pleiotropic cytokine and it is usually not produced constitutively by normal cells, but its expression is promptly induced by a variety of cytokines, bacterial products (e.g. LPS) or viral infections. Among the strongest producers are MΦ, DCs, and T-cells. It acts on a wide range of tissues, regulating growth, differentiation and also polarization status depending on the nature of the target cells [50, 51]. Next to diagnostic marker, IL-6 has emerged as a therapeutic target. Anti-IL-6 therapeutics showed efficient neutralization of IL-6 production *in vivo* and, thus far, proved safe and useful in inflammatory diseases [52].

Tumor necrosis factor - alpha

Tumor necrosis factor (TNF-α) is a pro-inflammatory cytokine involved in systemic inflammation and is an important cytokine for the acute phase reaction. It is primarily released by MΦ, but it can also be produced by many other cell types such as $CD4^+$ T-cells, NK cells, NΘ, mast cells, eosinophils, and neurons. The expression of other cytokines, chemokines, ROS, RNS, and prostaglandins is stimulated by TNF-α [53]. It is able to induce fever, apoptosis, cachexia, inflammation and to inhibit tumorigenesis and viral replication [54]. Excessive production of TNF-α is associated with high severity grade in a series of IMIDs (e.g. IBD, RA, psoriasis, etc.) and, therefore, a range of anti-TNF biologics form the current standard of care for these indications [55].

Interleukin-1

The interleukin 1 (IL-1) belongs to an important family of biologically active proteins derived by mononuclear cells participating in inflammation. There are two distinct types of IL-1 – IL-1α and IL-1β. They share similarities such as molecular weight, biological effects and same receptors on target cells. IL-1β causes a number of different auto-inflammatory syndromes and, moreover, it induces cyclooxygenase-2 (PTGS2/COX2), which contributes to inflammatory pain hypersensitivity in the central nervous system (CNS) [56]. Main producers of IL-1 cytokines are MΦ and MO, but als other immune cells (e.g. T-cells, NΘ). IL-1 can be conditionally expressed by fibroblasts, epithelial and endothelial cells. Their biological properties include pyrogenicity, bone resorption, antigen presentation to T-cells and stimulation of B- and T-cells proliferation [57, 58].

Granulocyte - macrophage colony - stimulating factor

Granulocyte - macrophage colony - stimulating factor (GM-CSF) is a monomeric glycoprotein stimulating the generation and function of NΘ, eosinophils and MO/MΦ. It functions as a cytokine and is secreted mostly by MΦ and T-cells. Other cell types such as mast cells, NK cells, endothelial cells, and fibroblasts are reported to produce it in low amounts. It stimulates hematopoiesis of MO and granulocytes (NΘ, eosinophils, and basophils) [59]. GM-CSF has been found to be relevant in poorly or not healing wounds, pulmonary inflammation, and variety of cancers (e.g. human prostate and renal cancer, hematological malignancies, lung cancer, etc.) [60, 61].

Interleukin-10

The interleukin-10 (IL-10) protein is a homodimeric anti-inflammatory cytokine. It is associated with pleiotropic effects in immunoregulation and inflammation. It is produced mainly by MΦ and T-cells. IL-10 has the ability to block the synthesis of pro-inflammatory cytokines such as IFN-γ, IL-2, IL-3, TNF-α, and GM-CSF and it is also a potent suppressor of several effector and accessory functions of immune cells including MΦ, T-cells and NK cells [62]. However, IL-10 is stimulatory towards Th2-cells and mast cells. Furthermore, it stimulates B-cell maturation and antibody production. While the presence of IL-10 in cancer environment is correlated with increased immune tolerance and poor prognosis, it has been demonstrated in IMIDs that recombinant human IL-10 ameliorates the inflammation in the context of Crohn's disease, psoriasis, and others [63, 64].

Interleukin-4

IL-4 is an immunoregulatory cytokine in the size varying between 15 and 19 kDa, representing variable glycosylation. There are gene and structural association of IL-4 with IL-13, IL-5 and GM-CSF [65]. IL-4 has a multifaceted role in regulation of hematopoiesis, inflammation, and the development of effector T-cell responses. Moreover, IL-4 is a key regulator in humoral and adaptive immunity. It is produced mainly by Th2 cells, but there is evidence of mast cells and MΦ that secrete IL-4 [65-67].

Interleukin-13

Interleukin 13 (IL-13) is a non-glycosylated protein with a molecular weight of 12 kDa. It is a pleiotropic cytokine, whose spectrum of action encompasses B-cells, mononuclear phagocytes, and large granular lymphocytes. IL-13 is secreted by MΦ, DCs, NK cells, and to some extend by conditioned T-cells [68]. IL-13 inhibits the production of a series of cytokines like IL-1, IL-6, TNF-α, and IL-8 by activated human MO/MΦ. As it has immunoregulatory functions, IL-13 is also involved in some human diseases such as asthma, systemic sclerosis, and some inflammatory diseases [69].

Transforming growth factor – beta

Transforming growth factor – beta (TGF-β) is secreted by many cell types, including MΦ, in a latent form - complexed with two other polypeptides, latent TGF-beta binding protein (LTBP) and latency-associated peptide (LAP). It is synthesized as a precursor that contains LAP at the N-terminus and mature TGF-β at the C-terminus [70]. Therefore, LAP levels correlate with the TGF-β ones. It is involved in many cellular functions, including the control of cell growth, cell proliferation, cell differentiation and apoptosis. In chronic or impaired wounds, the exogenous addition of TGF-β superfamily members accelerates the healing process [71, 72].

Macrophage inflammatory proteins

Macrophage inflammatory proteins (MIP) are chemotactic cytokines and belong to the family of cysteine-cysteine chemokines. There are two major forms, MIP-1α and MIP-1β that are produced by MΦ in response to bacterial endotoxins [73], and both also act as coactivators of MΦ when combined with IFN-γ. Although highly homologous in structure, MIP-1α and MIP-1β differ in their function. MIP-1α stimulates strong antigen-specific responses, while MIP-1β promotes antibody responses. Both chemokines are associated with M1-related immune response [74].

Interferon gamma-induced protein 10

Interferon gamma-induced protein 10 (IP-10) is an 8.7 kDa chemokine, also called CXCL10. It is secreted by several cell types including MO, MΦ, endothelial cells and fibroblasts in response to IFN-γ. CXCL10 triggers chemoattraction of MO, MΦ, T-cells, NK cells, and DCs. It promotes T-cell adhesion to endothelial cells, antitumor activity, and inhibition of bone marrow colony formation and angiogenesis [75-77].

I.4.2. Surface markers for investigation of MΦ phenotype

The selection of surface markers for discrimination between M1 and M2 phenotype is based on results from previous investigation. Recently, it was demonstrated that CD14 and CD64 are overexpressed on M1 phenotype, whereas CD301 and CD206 are distinct M2 markers [18]:

CD14

CD14 has two forms - one is anchored to the membrane by a glycosylphosphatidylinositol tail (mCD14) and the other is a soluble form (sCD14). Soluble CD14 appears after shedding of mCD14 or sCD14 is directly secreted from intracellular vesicles. CD14 acts as a co-receptor (along with the Toll-like receptor TLR 4 and MD-2) for the detection of LPS. CD14 is expressed mainly by MΦ and to a much lesser extend by DCs and NΘ. CD14 is upregulated in response to LPS [78].

CD64

Human FcγRI (CD64) is a 72-kDa transmembrane glycoprotein composed of three extracellular Ig-like domains (EC1-3), a single transmembrane spanning region, and a short cytoplasmic tail. The EC2 domain and especially the degree of hydrophobicity essentially contributes to the higher affinity in binding IgG Abs. To trigger cellular activation upon IgG binding, CD64 requires an accessory chain known as the common FcR γ-chain, which possesses an immunoreceptor tyrosine-based activation motif (ITAM). CD64 overexpression is induced by TLR agonization and IFN-γ pathway, which assigns it to markers of M1 phenotype [79-81].

CD206

CD206 (also known as mannose receptor) is a C-type lectin strongly present on the surface of M2 MΦ as response to IL-4 polarization. It is also expressed by immature DCs and rarely observed on human dermal fibroblasts and keratinocytes. CD206 recognizes terminal mannose, N-acetylglucosamine and fucose residues on glycylated proteins from bacterial

sources, which play an important role in innate immunity. In addition, CD206 helps in recycling and clearance of glycoproteins [82-84].

CD301

CD301 is a member of the C-type lectin/C-type lectin-like domain (CTL/CTLD) superfamily. It has functions in cell adhesion, cell-cell signaling, glycoprotein turnover, and roles in inflammation and immune response. *In vitro* studies demonstrate the CD301 expression in response to type II cytokines. However, it has also been suggested that CD301 is induced by dermal microenvironment on MΦ independent of IL-4/IL-13 signaling [18, 85].

I.5. Antibody-based therapeutic approaches in chronic inflammatory diseases

Current therapeutic approaches for selective immunointervention in IMIDs focus mainly on targeted neutralization of the pro-inflammatory cytokines [86]. Therefore, therapies using neutralizing antibodies or soluble receptor fusion proteins were on the top-line of global prescription drugs in 2014. AbbVie's Humira® (tumor necrosis factor (TNF-α) - blocking monoclonal antibody (mAb) - Adalimumab) was the top global product of 2014, with global sales of US$11.8 billion. In the top 10 were also Amgen's Enbrel® (TNF-α receptor fused to IgG1 constant domain – Etanercept) and Johnson & Johnson/Merck's Remicade® (TNF-α blocking monoclonal antibody- Infliximab) acquiring together more than US$16 billion [87]. Although this therapeutic strategy is quite efficient, it is an expensive treatment, since it requires multiple applications with high dosage of neutralizing units due to the excessive serum amount and continuous production of soluble and membrane-bound TNF-α [88]. Next to some adverse-effects (e.g. neutropenia and infections), the targeted therapy is often inefficient due to interactions between the Fcγ domain of the full-length anti-TNF-α mAbs and Fcγ receptors (e.g. CD64) [89]. Moreover, capturing the anti-TNF-α by CD64 via the Fcγ domain induces a tyrosine phosphorylation cascade leading to a pro-inflammatory downstream reaction, which counteracts the positive effects from neutralizing TNF-α [90]. A therapeutic approach, which does not inhibit the specific inflammatory cytokine but rather the producing cells, would ultimately be more efficient and likely require a much lower dosage. Accordingly, our approach was focused on directly targeting the cells producing the negative inflammatory mediators, which in case of IMIDs´ pathogenesis points to the M1 subdivision, whereas the M2 counterpart is associated with resolution of inflammatory processes [91].

I.6. Human FcγRI (CD64) as target for immunotherapy

CD64 is conditionally expressed on most myeloid cells including MO, MΦ, and DCs, but although granulocytes show no expression of CD64, the expression can be induced upon activation [92, 93]. Human CD64 is capable of binding monomeric IgG1 (K_D=1.54 x 10^{-9}), IgG3 (K_D=1.64 x 10^{-9}) and IgG4 (K_D=2.94 x 10^{-9}) - but not IgG2 [94, 95]. Interestingly, while mouse FcγRs efficiently bind human IgG subclasses, human FcγRs bind mouse IgG subclasses poorly [96]. In addition, binding of monomeric IgG is sufficient for internalization and recycling of the receptor, while phagocytosis is induced upon cross-linking. These characteristics meet the requirements for CD64 as a target for direct IT treatment. The potential of CD64-targeted therapy of chronic inflammatory diseases has been reported in previous studies, in which CD64 has been used as a target molecule for the directed delivery of cytotoxic payload (e.g. Ricin A and Pseudomonas exotoxin A) [97, 98]. In addition, CD64-directed ITs have been proven successful in M1-depletion using not only the bacterial truncated exotoxin A (ETA'), but also human effector proteins (e.g. angiogenin or microtubule-associated protein (MAP)) [99, 100].

I.7. Depletion of inflammation-associated MΦ through CD64 targeting

In the past decades, several mAbs have been generated against human CD64 recognizing different epitopes. The murine mAb m22 binds with high affinity and the binding is not inhibited by blocking with human IgG1, the Fc class that shows strongest binding to CD64 [101]. Due to their high immunogenicity, murine antibodies are not suitable for repeated application in humans. Therefore, m22 was humanized by CDR-grafting onto human V region frameworks. The resulting H22 mAb displayed equivalent binding specificity, affinity and functionality as the murine original m22 mAb [102]. The first CD64-targeting antibody drug conjugate (ADC) was composed of the full size H22 mAb and two chemically linked Ricin A toxin molecules. Although preliminary tests showed a low cytotoxic profile on the pro-monocytic cell line U937, the desired specific pro-apoptotic effect were observed after stimulation with IFN-γ [103, 104]. However, the IgG1 Fc-tail of the H22 mAb enables recognition and binding through all Fcɣ receptors (FcɣR) including to the high affinity CD64, the medium affinity (CD32) and low affinity (CD16) FcγR, which in turn might lead to non-specific targeting [105]. Another major drawback of the H22 mAb RicinA ADC is the excessive size of 210 kDa, which limits the extravasation from blood and the tissue penetration. Furthermore, both RicinA molecules were chemically linked to the Fc tail of the H22 mAb, which has a negative influence on the pharmacokinetics of the ADC [106]. To meet the requirements in terms of CD64-restricted specificity and reduced size of the construct, a single

chain variable fragment (scFv) derived from H22 mAb was generated by molecular design and genetic engineering [107]. This format can be used as a targeting unit for specific delivery of an effector molecule as part of immunotoxin (IT), human cytolytic fusion proteins (hCFP) or ADC [108]. This format can be used as a targeting unit for specific delivery of an effector molecule as part of immunotoxin (IT), human cytolytic fusion proteins (hCFP) or antibody drug conjugates (ADC) [109]. In the late 1990s, the truncated version of exotoxin A from *Pseudomonas aeroginosa* replaced the plant RicinA toxin, which was introduced as second generation ITs [110]. ETA' is a modified bacterial enzyme that irreversibly ribosylates a posttranslationally modified unique histidine residue called diphthamide. This causes an inactivation of the elongation factor-2 (EF-2) and thus, already at very low-toxin concentrations protein translation is efficiently blocked leading to apoptosis-driven cell death [111]. The ETA'-based ITs are genetically linked constructs, which allow production by bacterial fermentation and high-affinity purification. The recombinant ETA'-based ITs fused to H22(scFv) (noted as H22(scFv)-ETA') was introduced in therapeutic approaches against leukemia, chronic cutaneous inflammation in mice and ischemic-reperfusion injury in rats [98, 107, 112]. In both preclinical studies on inflammation the ITs demonstrated successful elimination of the $CD64^+$ activated MΦ, later identified as the pro-inflammatory M1. Furthermore, these studies showed that H22(scFv)-ETA' specifically targets the M1 population and moreover, elimination of M1 is a valuable approach for ameliorating strong inflammation processes. A follow-up investigation recently showed that the ITs induce an M1-restricted cytotoxic effect, but spare the M2 population *in vitro*. However *in vivo*, the M1/M2 ratio was strongly reversed towards the anti-inflammatory M2 population [113]. Nevertheless, ETA'-based ITs have some major disadvantages like immunogenicity and collateral toxicity (e.g. hepatotoxicity, vascular leakage, etc.), which according to reports from several clinical trials appear to be the major limitation factors [114].

A substantial improvement in the concept of IT-based immunotherapy is the generation of fully-human ITs, called human cytolytic fusion proteins (hCFPs). In the past few years, CD64-directed hCFPs bearing effector molecules like granzyme B and angiogenin proved successful in targeted elimination of human M1 and showed comparable IC_{50} values to the ETA'-based ITs [100, 115]. On top of that the recently reported H22(scFv)-fusion to microtubule associated protein (MAPtau) showed efficient killing of proliferating M1 in mouse and human models of chronic skin inflammation. M2 population remained unaffected by the CD64-directed intervention, and the M1/M2 ratio was reversed up to 100-fold towards the M2 prevalence [116]. Indeed, the aforementioned suggestion by Ginhoux and Jung to manipulate

MΦ during IMIDs is already a proven fact by our previous *in vitro* and *in vivo* findings [116]. Moreover, to bring the concept a step further, the present work proposes a more elegant way to intervene in chronic inflammation, which so far lacks any parallels in the literature – the immunomodulation of MΦ. Instead of eliminating M1 cells with CD64-targeted cytotoxic constructs, the manipulation of M1 cells is carried out using the H22(scFv) moiety, but linked to an immunomodulatory protein (e.g. suppressor of cytokine signaling).

I.8. Effector domains used for generation of immunomodulatory proteins

The plasticity and flexibility of the activation state are key features of MΦ [113, 117]. Tissue MΦ acquire a distinct phenotypic and functional profile in response to signals derived from microbes, viruses, damaged tissues, and activated immune cells (e.g. T- or natural killer (NK) cells) [118]. The effect of different signals is conveyed by different signaling pathways, which ultimately induce the transcription of different genes encoding either pro- or anti-inflammatory cytokines [19]. For example, IFN-γ and lipopolysaccharides (LPS) act through STAT1 (signal transducers and activators of transcription 1) and TLR4 (Toll-like receptor 4) signaling, respectively, activate the expression of IL-12, nitric oxide synthase 2 (NOS2), and TNF-α. In contrast, the IL-4-induced M2 polarization counteracts the effect of interferon-responsive factor 3 (IRF-3) and activates STAT6 promoting transcription of anti-inflammatory genes including arginase 1 (Arg1), PPARγ (peroxisome proliferator-activated receptor gamma), SOCS (suppressor of cytokine signaling), and Kruppel-like factor 4 (KLF-4) [119-121]. This shows that SOCS and KLF4 are involved in the feedback inhibition of STAT1 and the NF-κB pathway, respectively [120, 121]. The interactions of the cytokine networking and the associated intracellular signaling in MΦ suggest that intervention might bring new perspectives regarding the therapeutic control of IMIDs.

I.8.1. Suppressor of cytokine signaling proteins as feedback regulators

SOCS is a family of proteins (SOCS1-7 and CIS (cytokine-induced signal transducer and activator of transcription (STAT) inhibitor)) that regulate signaling downstream of a variety of receptors [122]. Early studies showed that transcription of CIS, SOCS1, SOCS2, and SOCS3 is increased in response to cytokine stimulation. Furthermore, the SOCS proteins inhibit cytokine-induced signaling pathways and are, therefore, part of a classical negative feedback circle. SOCS proteins modulate signaling by several mechanisms including inactivation of the Janus kinases (JAKs), blocking access of the STATs to receptor binding sites, and ubiquitination of diverse signaling proteins with subsequent targeting to the proteasome [123].

Moreover, SOCS proteins regulate MΦ and DC activation next to being essential for T-cell development and differentiation. SOCS proteins can be induced by variety of cytokines and factors such as IL-2, IL-3, erythropoietin, granulocyte macrophage colony-stimulating factor (GM-CSF), IFN-γ, etc. and inhibit through a negative feedback loop the cytokine signal transduction [40]. Current evidence indicates that CIS and SOCS1-3 are most often associated with regulation of cytokine receptor signaling through the JAK-STAT pathway, while SOCS4-7 predominantly regulate growth factor receptor signaling [124]. To inhibit the signaling, the SH2 domain of SOCS-1 can directly bind the activation loop of JAK [125]. Furthermore, it has been reported that SOCS-1 binds the type I IFN receptor and the IFN-γ receptor, which might serve as a powerful suppression of IFN signaling [126, 127]. There is already substantial evidence that SOCS-2 and 3 diametrically control MΦ polarization. Spencer *et al*. showed in a knock-out mouse model the importance of SOCS-2 for the anti-inflammatory phenotype of MΦ, whereas SOCS-3 had a rather pro-inflammatory activity [128]. In addition, SOCS-2 is critical for the anti-inflammatory activity of important mediators such as the above-mentioned SPMs (e.g. lipoxins). The molecular mechanism behind this process has yet not been clarified [129]. Recently, Arnold *et al.* reported involvement of SOCS-3 in fine-tuning *in vitro* and *in vivo* the MΦ polarization towards M1 function via its effects on intracellular signaling pathways including PI3K (Phosphoinositide 3-kinase) and NF-κB (nuclear factor kappa-light-chain-enhancer of activated B cells) [130]. While SOCS1-3 all act as feedback cytokine regulators, SOCS-1 and SOCS-3 but not SOCS-2 attenuate insulin signaling leading to insulin resistance and, thereby, might contribute to type 2 diabetes (T2D) [131]. Therefore, the focus of the present work was set on the generation of a recombinant MIMP composed of H22(scFv) genetically fused to the more apt SOCS-2 protein. The size of the resulting fusion protein is predicted to be at around 53 kDa.

I.8.2. Thioredoxin-1 as an anti-oxidant and anti-inflammatory mediator

Thioredoxins (Trx-s) are a group of small ubiquitous proteins that are key regulators of cellular redox balance. The mammalian Trx family includes the secreted and cellular protein (Trx-1), the mitochondria-specific Trx-2, the Trx-like cytosolic protein p32TrxL, a truncated version of Trx-1 known as Trx80, and the thioredoxin-related protein 14, TRP-14 [132]. Trx-1 is secreted by lymphocytes, hepatocytes, fibroblasts, and several tumor cells [133]. Trx-1 is a 12 kDa protein that acts as a growth factor, a cofactor that provides reducing equivalents, a transcriptional regulator, and also has anti-oxidative, anti-apoptotic, and anti-inflammatory properties. Expression of Trx-1 is increased under various stress conditions such as hypoxia

and viral and bacterial infections. Depending on its localization, it can act in different pathways. For instance, outside of cells Trx-1 influences cell growth and chemotaxis. In the cytoplasm it acts as an antioxidant and a reductant cofactor and in the nucleus it regulates the activity of transcription factors [134]. In the 1990s Sachi *et al.* showed that sun-exposed skin demonstrated enhanced expression of Trx-1, which seems to be a protective response to oxidative damage [135]. The cellular reduction-oxidation state is regulated by the Trx-interacting protein by binding and inhibiting Trx-1 in a redox-dependent fashion [136]. Interestingly, recombinantly expressed Trx-1 downregulates the expression of several important inflammatory genes, such as IL-1, TNF-α, IL-6, and IL-8 in LPS *in vitro* activated MΦ [137]. Moreover, a direct association of Trx-1 with MΦ migration inhibitory factor (MIF) was reported, suggesting that Trx-1 on the cell surface serves as binding molecule or receptor component for MIF and that it inhibits MIF–mediated inflammatory signals (e.g. monocyte chemoattractant protein (MCP)-1) [138, 139]. Furthermore, in a murine atherosclerosis model, intravenous (i.v.) application of human Trx-1 increased the number of M2 at the site of the plaques. In the same study, Trx-1 induced both CD206 and IL-10 expression indicating a phenotype population shift towards M2 in the context of a disease model [139]. Moreover, in a different model using transgenic mice the overexpression of human Trx-1 attenuated focal ischemic brain damage and increased the resistance to various oxidative stresses, leading to longer survival compared to untreated littermates [140, 141]. Interestingly, another study provides evidence that a truncated form of Trx-1 called Thioredoxin80 (Trx-80) promotes rather the M1-phenotype and thus, enhances atherosclerosis [142]. Taken together, based on the evidence regarding downregulation of the several inflammatory cytokine genes combined with proven antioxidant properties, Trx-1 presents a promising fusion candidate for CD64-directed immunomodulatory therapy. The size of the resulting fusion protein is predicted to be at around 45 kDa.

I.9. FcαR (CD89) as a new target for MΦ-directed immunotherapy

While CD64 is well investigated in respect to different pathologies, the Fc-alpha receptor (FcαRI, CD89) remains rather unexplored. CD89 shares some structural similarities with CD64 and also requires the common FcR γ-chain for signal transduction. However, FcαRI binds with equally low affinity (K_D=1-5 x 10^{-7}) all forms of immunoglobulin A: IgA1, IgA2 and secretory IgA (sIgA) [143]. Under normal physiological conditions CD89 is present on MO, MΦ, NΘ, and eosinophils. Its biological function is to interact with IgA-opsonized targets, triggering several immunological defense processes, e.g. phagocytosis, antibody-dependent cell-mediated cytotoxicity (ADCC), antibody-dependent cell-mediated phagocytosis (ADCP), and

stimulation of inflammatory mediators [144]. In many human tissues, most $CD89^+$ cells are NΘ or MO/MΦ. Furthermore, although MO in the blood express relatively high levels of CD89, most tissue MΦ (particularly those located in the gut lamina propria) tend not to express CD89 on the surface, with a parallel downregulation of CD14 [145]. This suggests that the abundance of CD89 depends on the differentiation stage of myeloid cells. Thus far, the abundance and density of CD89 expression on tissue maturing MO and MΦ in the context of IMIDs is poorly investigated. Therefore, the final part of this work is focused on analysis of the presence of CD89 on different phenotypes of MΦ and, furthermore, the suitability of CD89 as a target for MΦ-directed immunotherapy in the aspect of inflammation.

I.10. Motivation, aims and objectives

Due to the demographic transition towards an overall older population, the portion of people with age-associated risk of developing chronic inflammatory diseases (or IMIDs) increased dramatically, and IMIDs can inflict devastating degenerative effects throughout the body [146]. There is also a tendency for rapidly increasing intake and need of new medications, which already challenges the healthcare system worldwide. Therefore, novel strategies for efficient therapeutic intervention need to be developed in the near future. This problem was addressed by the "Skinheal" project, as part of the "Markets of the future" program of the Fraunhofer-Gesellschaft (Fraunhofer Society). Within this project, the Fraunhofer Institute for Molecular Biology and Applied Ecology (IME) focuses on the role of MΦ as potential targets in chronic inflammation and, in particular, on the development of immunotherapeutic strategies using biological constructs. MΦ are an important part of the innate immune system. They are remarkably plastic cells able to adapt to micro-environmental changes acquiring distinct polarization phenotypes coined M1 and M2. During normal inflammation, M1 prevail in the early phase orchestrating the first defense and the recruitment of effector cells, whereas M2 are more abundant at the late stage resolving the inflammation and mediating tissue repair. In chronic inflammatory diseases, the balance between M1 and M2 is disturbed leading to the predominance of M1 cells that arrest the inflammatory response in the initial phase and prevent the entry into the next finalizing phase. So far, the "Skinheal" project demonstrated the selective elimination of M1 MΦ by the CD64-targeted IT H22(scFv)-ETA', both *in vitro* and *in vivo* in a transgenic mouse model for chronic cutaneous inflammation.

To extend the previous achievements, the aim of this doctoral thesis was first to perform a "proof of concept" in a human system using skin biopsies from patients with a chronic skin condition. Furthermore, based on the evidence confirming the heterogeneity and plasticity of

the MO/MΦ lineage, a novel strategy to intervene in chronic inflammation was explored. Instead of eliminating the M1 population with CD64-targeted cytotoxic constructs, a more elegant immunomodulation of M1 was accomplished using the same targeting moiety linked to an immunomodulatory protein (e.g. SOCS-2 or Trx-1). The fusion proteins were targeted in a unique fashion to a specific cell population. The novel macrophage immunomodulatory proteins (MIMPs) were generated using the same production and preparation platform as already described for other H22(scFv)-fused constructs. Since the effector domains are of human nature, a focus was set on *in vitro* experiments using human PBMC-derived MΦ. The analysis of biomarkers (surface markers and cytokines) was primarily carried out by flow cytometry. Furthermore, the MΦ functionality was established by phagocytosis and oxidative stress assays. In a parallel line of experiments, it was determined whether the myeloid CD89 biomarker, recently described in context of leukemia, is present on polarized MΦ in sufficient amounts for targeted immunotherapy. As done for CD64-directed ETA' ITs in previous studies, delivery and phenotype-specific cytotoxicity by targeting of CD89 will be analyzed. To that aim, the CD89(scFv)- ETA' (~70 kDa) construct was generated, expressed in *Escherichia coli* (*E. coli*), purified and characterized *in vitro*, which includes binding to target cells, cell viability, and cytoxicity mechanisms. A detailed overview of the workflow scheme is illustrated in **Figure 4** (next page). The sections indicate the work packages performed in parallel, which in combination comprise this doctoral thesis.

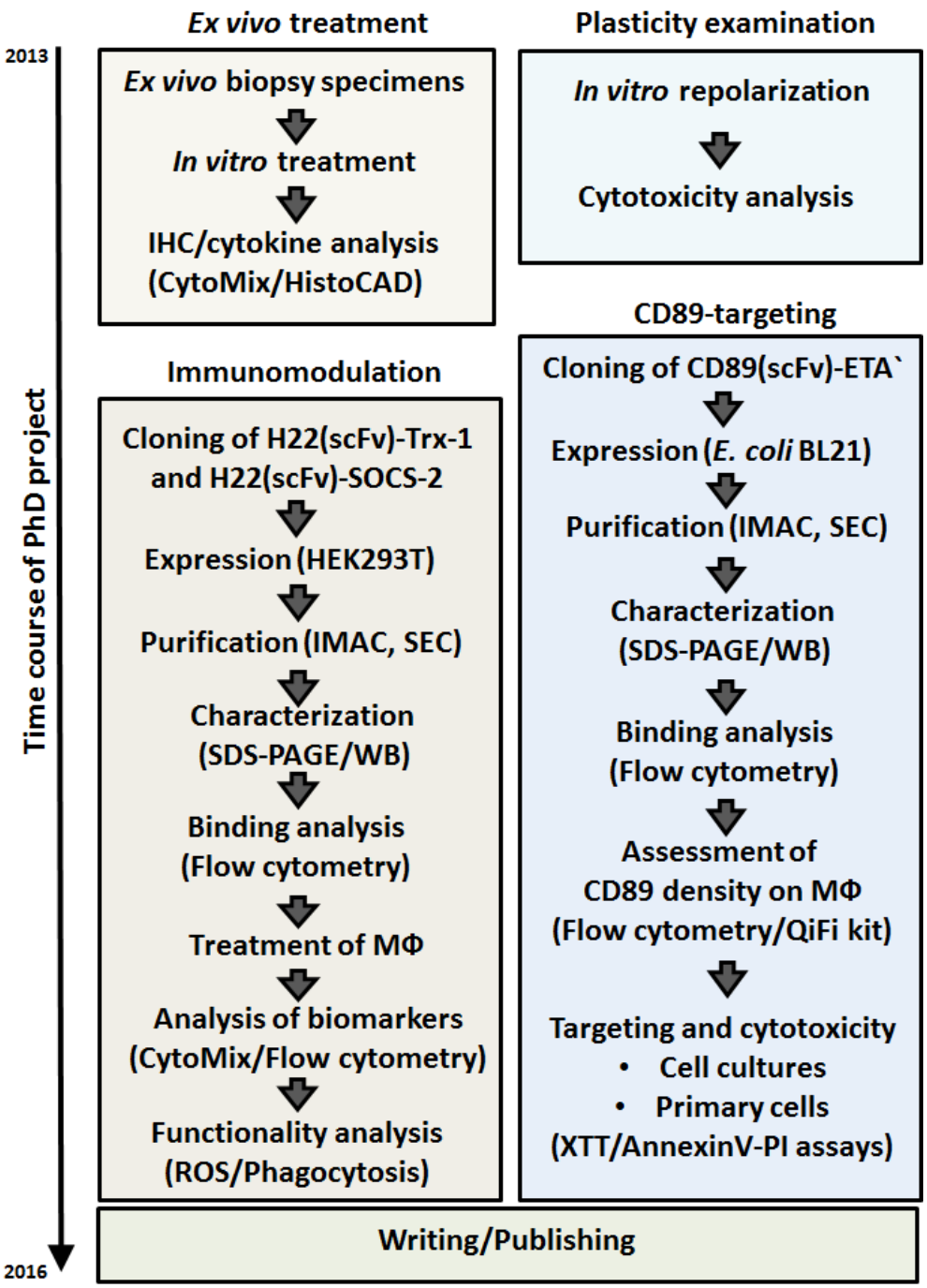

Figure 4: Overview of project milestones.
Workflow is arranged chronologically from top to bottom. Abbreviations: MΦ, macrophage; XTT, cell viability assay; PI, propidium iodide; SDS-PAGE, sodium dodecylsulfate polyacrylamide gel electrophoresis; WB, western blotting; IHC, immunohistochemistry; ROS, reactive oxygen species.

II Materials and Methods

II.1. Materials

II.1.1. Chemicals and consumables

Unless otherwise noted, all chemicals and consumables were purchased from the following manufacturers: eBioscience (Frankfurt am Main, Germany); Peprotech (Hamburg, Germany); Invitrogen (Leek, Niederlande); New England BioLabs (Frankfurt am Main, Germany); Sigma-Aldrich (München, Germany); Thermo Fisher Scientific (Waltham, USA); MWG-Biotech (Martinsried, Germany); Roche (Mannheim, Germany); Dickinson Bioscience (Heidelberg, Germany); Qiagen (Hilden, Germany); GE Healthcare (Freiburg, Germany); Fermentas (Vilnius, Lithuania); Promega (Mannheim, Germany); Carl Roth (Karlsruhe, Germany); Merck (Darmstadt, Germany); BioRad (München, Germany); Corning Inc. (Hagen, Germany); Hewlett Packard (Ratingen, Germany); Eppendorf (Hamburg, Germany); Millipore (Schwalbach am Taunus, Germany); Novagen (Darmstadt, Germany); Sarstedt (Nümbrecht, Germany); B. Braun (Melsungen, Germany); Schott-Glaswerke GmbH (Berlin, Germany); Serva (Heidelberg, Germany); Whatman (Freiburg, Germany); VWR (Darmstadt, Germany); Labomedic (Bonn, Germany); Nalgene (Waltham, USA); Sartorius (Sartorius, Hanau); Life Technologies (California, USA); Kisker Biotech (Steinfurt, Germany); Menzel (Braunschweig, Germany); Southern Biotech (Birmingham, USA); Greiner (Solingen, Germany); Origene (Rockville, USA); and AppliChem (Darmstadt, Germany).

II.1.2. Buffers, media and solutions

Buffers and stock solutions were prepared according to standard procedures using deionized water (dH_2O). Ready-to-use RPMI1640 medium was purchased from Invitrogen (Waltham, USA). Ampicillin (Sigma-Aldrich) was prepared as stock solutions, filter-sterilized (0.2 μm) and added to cooled down media to a final concentration of 1 mg/l. Zeocin® (Invitrogen) was added to the medium of transfected cells in a final concentration of up to 100 μg/mL. Human blocking serum was purchased from Sigma-Aldrich. The composition of all common buffers is summarized below. The recipes are according to Sambrook [147] and Coligan [148].

Table 1. Buffers and media

Buffer	Composition	Concentration	
TGS (pH 8.3)	Tris-HCl (pH 8.3)	25	mM
	Glycin	192	mM
	SDS	0.1	%(w/v)
TAE (pH 8.2)	Tris	40	mM
	Glacial acetic acid (pH 8.2)	5.7	%(v/v)
	EDTA	10	mM
Coomassie Staining Solution	Coomassie Brilliant Blue G-250	0.25	%(v/v)
	Methanol	50	%(v/v)
	Glacial acetic acid	9	%(v/v)
Coomassie Destaining Solution	Methanol	10	%(v/v)
	Glacial acetic acid	10	%(v/v)
5x Protein Loading Buffer	Tris-HCl (pH 6.8)	62.5	mM
	Glycerol	30	%(v/v)
	SDS	4	%(w/v)
	Bromphenol Blue	0.05	%(w/v)
	β-Mercaptoethanol (reducing)	10	%(v/v)
SDS PAGE Gel	Acrylamide/Bisacrylamide (30/1)	12	%(w/v)
(separating gel)	Tris-HCl (pH 8.8)	375	mM
	SDS (10%w/v)	0.1	%(w/v)
	TEMED	0.1	%(v/v)
	APS	0.1	%(w/v)
SDS PAGE Gel	Acrylamide/Bisacrylamide (30/1)	5	%(w/v)
(stacking gel)	Tris-HCl (pH 8.8)	150	mM
	SDS (10%w/v)	0.1	%(w/v)
	TEMED	0.1	%(v/v)
	APS	0.1	%(w/v)
SOC	Peptone	2.0	%(w/v)
	Yeast extract	0.5	%(w/v)
	NaCl	10	mM
	KCl	25	mM
	$MgCl_2$	10	mM
	$MgSO_4$	10	mM
	Glucose	20	mM

Buffer	**Composition**	**Concentration**	
Binding Buffer (pH 7.5)	Na_2HPO_4	200	mM
(Ni-NTA purification)	NaCl	1	M
	Imidazole	5	mM
Wash Buffer (pH 7.5)	Na_2HPO_4	50	mM
(Ni-NTA purification)	NaCl	1	M
	Imidazole	25	mM
Elution Buffer (pH 7.5)	Na_2HPO_4	50	mM
(Ni-NTA purification)	NaCl	1	M
	Imidazole	500	mM
Blotting Buffer (pH 8.4)	Tris-HCl (pH 8.4)	25	mM
	Glycine	192	mM
	Methanol	20	%(v/v)
AP Buffer (pH 9.6)	Tris-HCl (pH 9.6)	100	mM
	NaCl	100	mM
	$MgCl_2$	5	mM
Lysogeny Broth (LB – medium)	Peptone	1.0	%(w/v)
(pH 7.0)	Yeast extract	0.5	%(w/v)
	NaCl	1	%(w/v)
	Agar (agar plates)	1.5	%(w/v
Terrific Broth (TB medium)	Peptone	1.0	%(w/v)
(pH 7.0)	Yeast extract	0.5	%(w/v)
	NaCl	1	%(w/v)
10x Phosphate Buffer	K_2HPO_4	0.72	M
(for TB medium)	KH_2PO_4	0.17	M
10x RBC lysis buffer	NH_4Cl	1,55	mM
	$KHCO_3$	1	mM
	EDTA	0.1	mM
10x AnnexinV binding buffer	HEPES/NaOH (pH 7.4)	100	mM
	NaCl	1.4	M
	$CaCl_2$	25	mM

Buffer	Composition	Concentration	
10x PBS (pH 7.4)	NaCl	1.37	M
	KCl	27	mM
	Na_2HPO_4 x $12H_2O$	81	mM
	KH_2PO	15	mM
10x PBST (pH 7.4)	1x PBS	1.37	M
	Tween 20	0.5	%(v/v)

II.1.3. Chromatography resin and membranes

An XK16-20 column filled with IMAC Sepharose 6 Fast Flow resin (GE Healthcare) was used for the enrichment of histidine (His)-tagged proteins via immobilized metal ion affinity chromatography (IMAC). Preparative size exclusion was carried out using an XK16-70 column packed with Superdex™ 75 resin. Vivaspin Ultrafiltration Devises 30K (Sartorius) were used to concentrate the purified proteins. For sterile filtration 0.2 µm PVDF Durapore Membrane syringe filters (Sarstedt) were used.

II.1.4. Enzymes and reaction kits

Restriction enzymes (e.g. *Not*I and *Blp*I), T4 DNA ligase and Q5 High-Fidelity DNA Polymerase were purchased from New England BioLabs and used according to manufacturer´s instructions. The following kits were used:

Table 2. Names and suppliers of kits

Name	Composition
NucleoSpin Plasmid Kit	Macherey-Nagel
NucleoSpin Extract II Kit	Macherey-Nagel
Gentra Puregene Mouse Tail Kit	Qiagen

II.1.5. Antibodies and recombinant proteins

Antibodies were used for detection of recombinant proteins on western blots, for analysis of expression levels of surface markers on mammalian cells by flow cytometry, and for staining selected surface receptors using IHC and immunofluorescence assays. Carrier-free, ultrapure and biologically active Thioredoxin-1 (#P10599) was purchased from R&D Systems. The antibodies used in this thesis are listed in **Table 3**.

Table 3. Antibodies used in this thesis.

Name	Supplier	Application
Mouse anti-Penta-His AlexaFluor488	Qiagen	WB
Mouse-anti-Penta-His	Qiagen	WB
Goat-anti-Mouse-AP	Sigma	WB
Goat-anti-Rat-AP	Sigma	WB
Rat-anti-Human SOCS-2	Biolegend	WB
Mouse-anti-Human CD14:FITC	eBioscience	FC, IHC
Mouse-anti-Human CD64 [10.1]:FITC	Biolegend	FC, IHC
Mouse-anti-Human CD64 [10.1]:APC	Biolegend	FC, IHC
Mouse-anti-Human CD301:FITC	Biolegend	FC, IHC
Mouse-anti-Human CD206:RPE	Biolegend	FC, IHC
Mouse-anti-Human CD89:RPE	Biolegend	FC, IHC
Mouse-anti-Human Thioredoxin	AbD Serotec	WB
Goat-anti-Rabbit:FITC	Sigma	FC
Mouse IgG1 Isotype Control: FITC	eBioscience	FC
Mouse IgG1 Isotype Control: RPE	eBioscience	FC

Abbreviations: WB, western blotting; FC, flow cytometry; IHC, immunohistochemistry.

II.1.6. Synthetic oligonucleotids

Synthetic oligonucleotides were synthesized by MWG-Biotech and used for DNA amplification by polymerase chain reaction (PCR). The sequences of all oligonucleotides used in this thesis are listed below. The complete gene sequences of CD89(scFv), Trx-1 and SOCS-2 are listed in section VI.6.

Table 4. Sequences of oligonucleotides used for PCR in this thesis

#	Name	Sequence
1	H22-seq-forw	GTACCGACTTCACCTTCACC
2	pMS-seq-rev	CAG CTG GCC CTC GCA G
3	hCD64f	TTAAGCATTTCCCTAATGACTATGA
4	hCD64r	ACTACCCTCCAAAAAACATCTAAG
5	T7-prom-forw	AATACGACTCACTATAG

II.1.7. Vectors

The underlying DNA vectors for all molecular cloning procedures were either pMS for mammalian expression [149] or pMT for bacterial expression, which is derived from the bacterial expression vector pET27b (Novagen) [107]. All cloning work was adapted to the characteristics

of the chosen vectors, such as corresponding restriction sites, and performed according to standard methods (II.2). The vector maps and the sequences of all constructs are listed in the appendix.

II.1.8. Biological material

II.1.8.1. Bacterial strains

E.coli DH5α was used for all intermediate cloning steps and for amplification of plasmid DNA. *E.coli* BL21(DE3) was used for the expression of recombinant proteins. Bacterial stocks were obtained from New England Biolabs.

Table 5. Name and genotypes of used *E.coli* strains

#	Strain name	Genotype
1	DH5α	*fhuA2 Δ(argF-lacZ)U169 phoA glnV44 Φ80 Δ[150]M15 gyrA96 recA1 relA1 endA1 thi-1 hsdR17*
7	BL21(DE3)	*fhuA2 [lon] ompT gal (λ DE3) [dcm] ΔhsdS;* DE3 = *λ sBamHIo ΔEcoRI-B int::(lacI::PlacUV5::T7 gene1) i21 Δnin5*

II.1.8.2. Mammalian cell lines

The following mammalian cell lines were used for the functional analysis of recombinant proteins:

Table 6. Cell lines used in this thesis.

Name	Characteristics	Reference
HL-60	Human $CD64^+$ promonocytic leukemia cell line	ATCC Nr. CCL-240
THP-1	Human $CD64^+$ promonocytic leukemia cell line	ATCC Nr. TIB-202
MonoMac-1	Human $CD64^+$ promonocytic leukemia cell line	DSMZ Nr. ACC-252
U937	Human $CD64^+$ promonocytic leukemia cell line	ATCC CRL-1593.2
Ramos	Human $CD89^-$ and $CD64^-$ Burkitt's lymphoma derived cell line	ATCC Nr. CRL-1596

Abbreviations: ATCC, American Type Culture Collection; DSMZ, Deutsche Sammlung von Mikroorganismen und Zellkulturen.

II.1.8.3. Primary MΦ

Primary peritoneal mouse MΦ and PBMC-derived human MΦ were used for the functional analysis of recombinant proteins. All experiments on human PBMC were conducted with the approval of the Clinical Research Ethics Board of the RWTH Aachen University and University hospital in Aachen.

II.1.8.4. Human patient material

Human skin biopsy were collected at the Sankt Franziskus Hospital in Aachen and at the Katharinen Hospital in Stuttgart according to the guidelines of the ethical committee of the University Hospital Aachen and Katharinen Hospital Stuttgart, respectively. The wound exudates from five T2D patients (**Table 7**) were kindly provided by Dipl. Biol. (t.o.) Sibylle Thude and Prof. Dr. Ralf Lobmann, Medical Director, Department of Endocrinology, Diabetology and Geriatrics, Civil Hospital of Stuttgart in accordance with the guidelines of the ethical committee of the Civil Hospital of Stuttgart, Germany. Written consent was obtained from every individual patient. Serum was obtained fully anonymously from previously untreated leukemia patients or healthy blood donors, after receiving informed consent and with the approval of the Clinical Research Ethics Board of the University of Aachen.

Table 7: Parameters of the five diabetic patients being the exudate source

Sample ID	Year of birth	Gender	Wound state	Age of wound	Local medication
001	1933	male	chronic	5 weeks	No
002	1942	female	chronic	2 years	No
003	1947	female	chronic	3 years	No
004	1928	female	chronic	11 months	No
005	1952	female	chronic	6.5 weeks	No

II.1.9. Equipment and software

All equipment used in this thesis:

Balances: Precision and analysis balances, Talent: TE601, TE64-0CE, Talent TE3102S, (Sartorius)

Cell counter: Casy1 (Scharfe System)

Cell washer: Rotolavit Cell Washer (Hettich Lab Technology)

Centrifuges: Table centrifuge 5415D and 5415R (Eppendorf), Multifuge 3 S-R / 1S (Heraeus Instruments), Avanti J-25I Centrifuge (Beckman Coulter), Rotina 420R (Hettich Lab Technology)

Chromatography Equipment: Äkta Purifier (GE Healthcare)

Cryostat: Cryostat CM 3050 (Leica)

Rocker/Shaker: Eppendorf Thermomixer comfort, Eppendorf Thermostat 5320

Electrophoresis and Blotting: Mini Protean III Gel Chamber, Protein Gel-Apparatus and Supplies Mini PROTEAN II™, Gel Air Dryer, Mini Trans-Blot, Mini Trans-Blot Cell (all BioRad)

Flow Cytometer: FACSCalibur (Becton Dickinson)

Hoods: Hera Safe HS12 (Kendro)

Incubators: Thermomixer compact (Eppendorf AG), Incubator Function Line Type UT12 (Heraeus Instruments), CD210 (Binder)

Microscopes: TCS SP5 Confocal Microscope (Leica), DMIL Inverted Microscope with Mercury Fluorescence Light Source (Leica), DM2000 (Leica)

PCR Thermocyclers: Primus 96 Plus (MWG-Biotech), Programmable Thermal Controller PTC-200™ (MJ Research Inc.)

Sequencer: ABI Prism 3730 Capillary-Sequencer (Applied Biosystems)

Software: Graph Pad Prism v5.0, Unicorn v5.2, AIDA Image Analyzer, CLC Main Workbench v7.5, Lasergene, Microsoft Office 2010, Cyflogic v1.2.1, Adobe Photoshop CS5.1 Extended, WinMDI v2.8, eBioscience Flow Analytics

Sonication: Sonication Probe UW2070 (Bandelin Electronic)

Spectrophotometer: Epoch Microplate Spectrophotometer (BioTek), Tecan Genios Pro

Transilluminator: Molecular Imager Gel Doc XR System (BioRad)

Vibratome: Vibrating Blade Microtome Leica VT1200S (Leica)

Vortex: Vortex-Genie 2 (Scientific Industries Inc.)

Water Baths: TE31025, TE12000 (Sartorius)

II.2. Methods

II.2.1. Recombinant DNA technology

II.2.1.1. Transformation of *E. coli* DH5α by heat shock

Chemically competent *E. coli* bacteria (40 µL aliquots) were thawed on ice and mixed gently with 50 ng of the plasmid DNA. The mixture was then incubated on ice for 30 min and heat shocked at 42°C for 30 s. Thereafter, the transformation was accomplished by recovering the bacteria with 400 µL of LB medium supplemented with 20 mM glucose and incubated at 37°C with shaking (400 rpm) for 45 min. The bacteria was centrifuged at 1000 x g and resuspended in 300 µL fresh LB medium supplemented with appropriate antibiotics. Finally, 50 µL of the cells were plated onto LB agar supplemented with appropriate antibiotics and incubated at 37°C overnight. Due to the lower transformation efficiency in the case of ligated plasmid DNA the whole mixture was plated.

II.2.1.2. Growth and maintenance of E. coli DH5α

LB medium containing the appropriate antibiotic (50 µg/mL) was inoculated with a single recombinant colony of *E. coli* and grown overnight at 37°C with vigorous shaking (225 rpm). Individual colonies of *E.coli* DH5α were picked on LB agar plates containing the matching antibiotic. Plates were briefly stored at 4°C and for long storage at -80°C glycerol stocks were prepared using overnight culture transferred into sterile fresh LB medium supplemented with final 20% (v/v) glycerol.

II.2.1.3. Isolation of plasmid DNA from *E. coli*

Plasmid DNA was purified using the NucleoSpin Plasmid Kit (Macherey-Nagel) according to the manufacturer´s instructions and stored at -20°C in elution buffer.

II.2.1.4. Quantification of DNA

DNA concentration was determined by measuring the E_{260nm} and purity of the nucleic acid was determined by measuring the $E_{260nm/280nm}$ ratio, which is 1.8 or higher for pure DNA.

II.2.1.5. Restriction of DNA

DNA was incubated with the corresponding restriction enzyme and buffer in a heating block at standard 37°C for 20min for analytical and 2 h for preparative digestion. Digestion with *Sfi*I was conducted at 50°C for 2h. Restriction endonucleases, 10x restriction buffers and bovine serum albumin [151] solution were obtained from New England BioLabs.

II.2.1.6. Ligation of DNA

The ligation of DNA fragments (II.2.1.5) was performed using final 200-400 U of T4 DNA Ligase (400,000 U/mL; New England BioLabs) dissolved in 10x ligase buffer system as recommended in the manufacturer's protocol to a final volume of 20 µl. The recommended amount of vector was 40-50 ng. Six-fold molar excess of insert DNA to vector DNA was used to ensure successful ligation. The ligation reaction was carried out at 15°C overnight followed by heat shock transformation in *E. coli.*

II.2.1.7. Agarose gel electrophoresis

Agarose gel electrophoresis was used to isolate DNA fragments after separation of plasmid DNA, restriction fragments and PCR products. Therefore, 1.2% (w/v) agarose gels were prepared in TAE buffer containing 0.5 µg/mL ethidium bromide. DNA containing samples were loaded with OrangeG Loading Buffer (New England BioLabs). The 2-Log DNA ladder (New England

BioLabs) was used to evaluate sample size and fragments integrity. DNA was visualized at 302 nm and documented using a Molecular Imager Gel Doc XR System (BioRad). Agarose blocks containing the DNA fragments of interest were excised from the preparative gel on an UV transilluminator with a sterile blade. DNA extraction was performed using a NucleoSpin Extract II kit (Macherey-Nagel) according to the manufacturer´s guidelines and stored at -20°C.

II.2.1.8. DNA sequencing and analysis

Sequence analysis was carried out at the Fraunhofer IME sequencing facility using an ABI Prism 3700 Capillary-Sequencer (Applied Biosystems) with BigDye™ cycle sequencing terminator chemistry and the Applied Biosystems Sequencing Analysis Program. The sequences were analyzed using CLC Main Workbench software.

II.2.2. Production of recombinant proteins

II.2.2.1. Prokaryotic periplasmic expression under osmotic stress conditions

Recombinant CD89(scFv)-ETA' was expressed in *E. coli* BL21(DE3) cells. To enhance solubility, folding and final yield of the recombinant protein, periplasmic stress expression in the presence of compatible solutes was used as previously described [152]. Briefly; after transformation, selection and pre-culturing (26°C, 180 rpm) the main culture of bacteria was grown to an E_{600nm} of 1.6 in TB medium supplemented with 0.5 mM $ZnCl_2$. Osmotic stress was induced by adding 500 mM D-sorbitol, 10 mM betaine monohydrate and 4% (w/v) NaCl plus 40% (v/v) TB medium containing 0.5 mM $ZnCl_2$. After incubation at 26°C for 45 min with shaking (180 rpm), protein expression was induced with 2 mM IPTG. Bacteria were harvested 16 - 18 h after induction by centrifugation (4000 × g, 10 min, 4°C) and frozen at –80°C overnight. The frozen pellet was resuspended at 4°C in preparation buffer (75 mM Tris-HCl, 300 mM NaCl, 5 mM DTT, 10 mM EDTA, 10% (v/v) glycerol, pH 8.0) containing a complete protease inhibitor cocktail (Roche) and sonicated five times for 60 s at 200 W. Cell debris was removed by centrifugation (24,000 × g, 20 min, 4°C). DTT, EDTA and diverse metabolic chemicals were removed by dialysis against phosphate-buffered saline (PBS) plus 0.4 M NaCl (pH 7.4) at 4°C overnight. The bacterial lysate was supplemented with 5 mM imidazole in order to minimize unspecific binding during the protein purification by IMAC.

II.2.2.2. Eukaryotic expression using human embryo kidney cells (HEK293T)

Roti®-Fect (Carl Roth) was used for liposome-mediated transfection of HEK293T cells according to the manufacturer's instructions. Briefly, for each transfection approach 3×10^5 cells

per well in 3 mL R10 medium were seeded in a 6-well plate and cultivated under standard conditions. After 18 h the transfection mix was prepared by adding 2 µg of plasmid DNA and 20 µL of Roti®-Fect to 400 µL serum-free RPMI 1640 (Gibco BRL, Eggstein, Germany). The cells were washed with DPBS (Gibco BRL, Eggstein, Germany) and resuspended in 3 mL serum-free RPMI. The prepared mixture was added carefully to the HEK293T cells and these were incubated for 4 h under serum-free standard conditions for an optimal uptake of the liposome-DNA-complex. Thereafter, serum conditions were restored by adding sterile FCS to a final concentration of 10% (v/v). The transfected cells were incubated under standard cell culture conditions and viability was controlled by light microscopy. The fluorescence of the reporter protein (eGFP) was monitored daily and after reaching 70-80% of the adherent cells a selective pressure was induced incrementally by adding Zeocin® (Invitrogen) in a final concentration up to 100 µg/mL. Expression of desired recombinant fusion proteins was monitored by western blotting and binding analysis of the cell supernatant. Expansion of the most efficiently transfected cell cultures was conducted stepwise using T25, T75 and Triple flasks. Supernatant of the final expansion stage was collected and stored at 4°C under sterile conditions.

II.2.2.3. Immobilized Metal Ion Affinity Chromatography (IMAC)

Recombinantly expressed proteins tagged with poly-histidine tail were enriched by IMAC on an Äkta Purifier System (GE Healthcare) using IMAC Sepharose 6 Fast Flow resin (GE Healthcare) loaded with Ni^{2+} cations.

II.2.2.3.1. Purification of bacterial lysate

Bacterial lysate was cleared by vacuum filtration using a 1 µm Whatman filter (Sartorius) before loading onto a ready-to-use XK16-20 column at a flow rate of 1 mL/min. After loading, the column was washed with wash buffer (20 mM imidazole) until the baseline was reached. Elution was carried out at a flow rate of 1 mL/min using elution buffer (500 mM imidazole). Finally, the eluted protein fraction was concentrated using a Vivaspin Ultrafiltration Device 30K (Sartorius) in preparation for size exclusion chromatography (SEC).

II.2.2.3.2. Purification of supernatant of the MIMP-expressing cell culture

Supernatant of the MIMP-expressing cell culture was adjusted to optimal binding conditions using 4x binding buffer (pH 7.4). Vacuum filtration using 0.45 µm membrane filter (Sartorius) was used to clarify the supernatant prior to loading onto a ready-to-use XK16-20 column at a flow rate of 0.5-1 mL/min overnight. After complete loading, the column was washed with wash buffer (20 mM imidazole) until the baseline was reached and the elution was carried out at a flow rate of 1 mL/min using elution buffer (500 mM imidazole). The elution fraction was

concentrated using a Vivaspin Ultrafiltration Device 30K (Sartorius) in preparation for size exclusion chromatography (SEC).

II.2.2.4. Preparative size exclusion chromatography (SEC)

Preparative SEC was carried out on an Äkta Purifier System (GE Healthcare) using an XK16-70 column packed with SuperdexTM 75 (GE Healthcare). PBS (pH 7.4) buffer was used for the mobile phase at a flow rate of 1.0 mL/min. Protein elution was monitored at E_{280nm}. Collected fractions were analyzed by sodium dodecylsulfate polyacrylamide gel electrophoresis (SDS-PAGE) for protein size and purity. Selected fractions were then combined, concentrated, filter-sterilized (0.2 µm), aliquoted and stored at either 4°C or –20°C.

II.2.2.5. Protein analysis

II.2.2.5.1. Sodium dodecylsulfate polyacrylamide gel electrophoresis (SDS-PAGE)

Discontinuous SDS-PAGE was used for the separation of protein samples under reducing conditions. Therefore, the protein samples were diluted in PBS (pH 7.4) and 5x protein loading buffer in a ratio of 1:5. After heating the samples at 95°C for 5 min, proteins were separated electrophoretically at 170 Volts for 70 min in a Mini-PROTEANII chamber (BioRad) under 1x TGS buffer conditions. Thereafter, protein bands were visualized by staining with Coomassie Staining Solution for 20 min at room temperature (RT). Non-specific background staining was removed by washing with Coomassie Destaining Solution until the protein bands were clearly visible.

II.2.2.5.2. Western blotting

The identification of SDS-PAGE separated proteins (II.2.2.5.1) was performed by specific antibodies (table 3) using western blotting. Briefly, proteins were transferred from the polyacrylamid gel onto a Whatman® nitrocellulose membrane (Sigma) using an Xcell II Blot Module (BioRad) for electro-tank blotting at 300 mA for 60 min in transfer buffer. Thereafter, the nitrocellulose membrane was blocked with 5% (w/v) milk powder (Roth) for 1 h at RT or 4°C overnight. Afterwards, the membrane was washed three times with 1x PBST and incubated with the primary antibody (Table 3) shaking at 4 °C overnight. The membrane was washed as described above and the primary antibody was detected using an alkaline phosphatase-conjugated anti-mouse-IgG mAb (1:5,000; Sigma). A secondary antibody was incubated for 1 h at RT and afterwards the blot was extensively washed with 1x PBST. Prior to staining with NBT/BCIP substrate (Life Technologies), the membrane was equilibrated in 1x AP buffer for 5 min at RT. After visualization of the protein bands the membrane was washed with dH_2O and dried. A

CanoScan 8800F scanner [153] software was used to digitalize the blots. Pre-stained broad range protein markers (New England BioLabs) were used as a reference.

II.2.2.5.3. Quantification of purified proteins

Purified proteins (II.2.2.3) were quantified using the Roti-Nanoquant (Roth) Bradford Assay according to the manufacturer's instructions. Known BSA concentrations were used for establishment of the standard curve. The final calculation of protein concentration was performed using Microsoft Excel 2007.

II.2.3. *In vitro* biological work

II.2.3.1. Cell culture with mammalian cells

Mammalian cell lines were cultivated in complete medium (RPMI1640) supplemented with 10% (v/v) fetal calf serum (FCS) (BioChrom), 50 µg/mL penicillin and 100 µg/mL streptomycin (all Invitrogen). Cell cultures were incubated at 37°C, 100% humidity and 5% CO_2, and were split twice a week. The cell number was monitored using a Casy cell counter (Schaerfe System). Before CD64-targeting experiments were conducted, the receptor expression was augmented by stimulating the HL-60 and THP-1 cells with 100 U/mL IFN-γ for 24 h.

II.2.3.1.1. Isolation of peritoneal murine MΦ

Murine MΦ were extracted by a peritoneal lavage. Mice were injected with 1 mL of 2% (w/v) BioGel P-100 (BioRad) into C57/BL6 wild type or hCD64tg mice to induce sterile inflammation and influx of MΦ into the peritoneal cavity. After 3 days, the mice were sacrificed and the MΦ were isolated out of the peritoneal cavity using 5 mL ice-cold PBS (pH 7.4). After lysis of red blood cells using 1 x RBC buffer for 15 min on ice, MΦ were washed with PBS and cultured at a concentration of up to 1.0×10^6 cells/mL in complete medium in T75 tissue culture flasks for 4 h. Thereafter, non-adherent cells were removed by washing with cold PBS (pH 7.4) and MΦ were detached by incubation with cold 0.5 mM EDTA in PBS (pH 7.4) for 10 min on ice. An appropriate number of cells was then seeded into assay plates and incubated overnight.

II.2.3.2. Isolation of primary human MΦ

Human MO were isolated from buffy coats provided by the University hospital in Aachen; sample collection was performed according to the guidelines of the ethical committee. The content of a buffy coat (approximately 150 mL) was diluted equivolumetrically with sterile PBS and 35 mL of the resulting dilution was carefully added to 15 mL pre-pipetted Bicoll separating

solution (d=1.1g/mL, BioChrom). Gradient separation was performed at 800 × g for 30 min at RT with minimal acceleration and deceleration rates. The monocytic cell layer was isolated, washed with PBS at RT and cultured overnight as described above. Non-adherent cells (e.g. B- and T-cells) were removed by two mild washing steps. Finally, adherent cells were harvested by scraping in pre-warmed standard medium.

II.2.3.3. *In vitro* polarization of primary MΦ

II.2.3.3.1. Murine MΦ

The polarization of murine MΦ into either M1 or M2 phenotypes was conducted by a single stimulation step. MΦ were stimulated towards M1 using 100 U/mL murine IFN-γ (Peprotech) and 1 µg/mL LPS (Sigma). MΦ were polarized to M2 using 20 ng/mL murine IL-4 (Peprotech) for 24h. Non-polarized MΦ (M0) were incubated with standard medium.

II.2.3.3.2. Standard polarization protocol for human MΦ

The polarization of human MΦ into either M1 or M2 phenotype was performed by selective stimulation. M1 MΦ were stimulated using 100 U/mL human IFN-γ (Peprotech) and 1 µg/mL LPS (Sigma). M2 MΦ were stimulated using 20 ng/mL human IL-4 (Peprotech) for 48 h. Thereafter, the MΦ were ready to be used in functional assays (**Figure 5**).

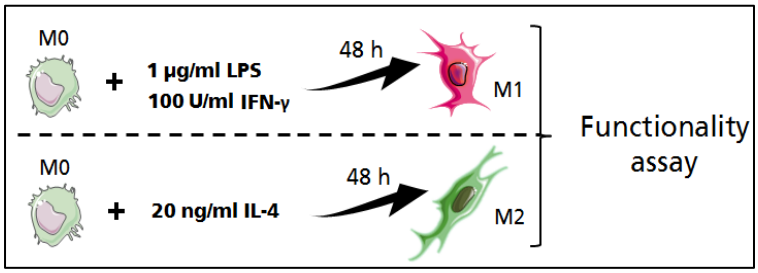

Figure 5: Experimental scheme of polarization of human PBMC-derived MΦ.
Abbreviations: M0, un-polarized, resting MΦ; M1, classically polarized, pro-inflammatory MΦ, M2, alternatively polarized, anti-inflammatory MΦ, LPS, lipopolysaccharides; IL-4, interleukin-4; IFN-γ, interferon-gamma.

II.2.3.3.3. Repolarization of MΦ

To study the plasticity of polarized MΦ, cells were exposed to the reverse stimulus for 24 h. The re-polarizing stimuli (20 ng/mL IL-4 for M1 and 100 U/mL IFN-γ + 1 µg/mL LPS for M2) were added to the medium containing the initial stimulus (**Figure 6**).

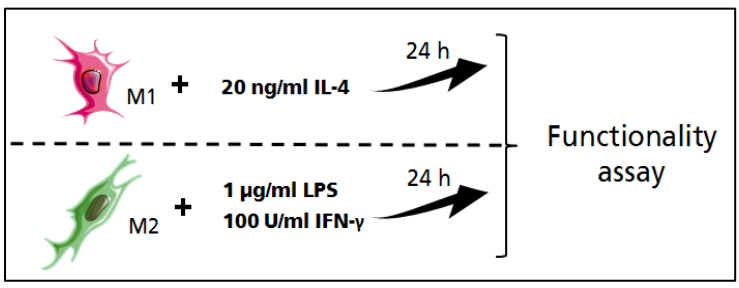

Figure 6: Experimental scheme of repolarization of human PBMC-derived MΦ.
Abbreviations: M1, classically polarized, pro-inflammatory MΦ, M2, alternatively polarized, anti-inflammatory MΦ, LPS, lipopolysaccharides; IL-4, interleukin-4; IFN-γ, interferon-gamma.

II.2.3.4. Immunomodulatory assays

II.2.3.4.1. Immunomodulation using the standard polarization protocol

Isolated MΦ were cultured in 24-well plates and microscopically checked for vitality and adherence. Afterwards, immunomodulatory assays were performed in two different experimental approaches. In the first approach, isolated MΦ being in non-polarized status (M0) were first incubated for a 24 h time period with IM and then polarized following II.2.3.3.2 – noted as **priming**. The corresponding **treatment** approach, in contrary, first started with polarization of MΦ (II.2.3.3.2) to different phenotypes followed by MIMP incubation for 24 h. The final concentration of MIMP used for all experiments was 100 nM. Scheme showing the MIMP assay

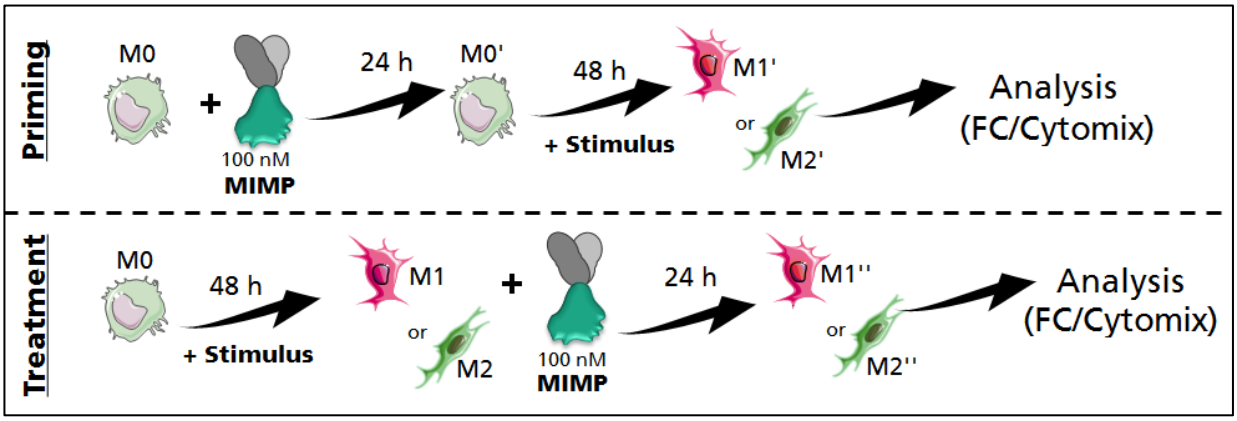

Figure 7: Experimental setup of MIMP assay on standard polarized M1 versus M2
Abbreviations: M0, non-polarized, resting MΦ; MIMP, MΦ immunomodulatory protein; M0', MIMP primed M0; M1' or M2', MIMP primed M1 or M2, polarized to each phenotype; M1" or M2", M0 polarized to M1 or M2 and then treated with MIMP; FC, flow cytometry.

setup is shown in **Figure 7**. The appropriate controls were conducted using either PBS for the vehicle control or the MIMP protein domains separately (e.g. H22(scFv) alone, Trx alone, etc.) instead of fused MIMP. At the end of the immunomodulatory assays 300 µL of the MΦ supernatant were collected, centrifuged at 13200 rpm, 4°C for 5 min and frozen in 150 µl aliquots. The MΦ were detached in the residual medium by incubation on ice for 5-10 min followed by scarpering out. The harvested MΦ were separated in FACS tubes each containing approximately equal amount of cells. The further evaluation was done following chapter II.2.4.1.

II.2.3.4.2. Immunomodulation using sterile exudate from chronic wound

Analogously to II.2.3.4.1, MΦ prepared for functionality assay were first incubated for 24 h time period with MIMPs – noted again as **priming** and then polarized for 48 h using sterile exudate from chronic wounds of diabetic patients (n=3). In contrary, the **treatment** approach first started with polarization of MΦ for 48 h using same exudates followed by MIMP incubation for 24 h. The final concentration of MIMP used for all experiments is 100 nM. The scheme

showing the MIMP assay setup is shown in **Figure 8**. As control was used PBS buffer. The amount of the used chronic exudate was adjusted to final concentration of 200 U/mL IFN-γ. Since an overall high IFN-γ concentration in all chronic wound exudates was estimated (see III.1.1), the volume needed to reach the 200 U/mL IFN-γ was around 5 to 10 µL. At the end of the immunomodulatory assays 300 µL of the MΦ supernatant were collected, centrifuged at 13,200 rpm, 4°C for 5 min and frozen in 150 µL aliquots. The MΦ were detached in the residual medium by incubation on ice for 5-10 min followed by scarping out. The harvested MΦ were separated in FACS tubes each containing approximately equal amount of cells. The further evaluation was done following chapter II.2.4.1.

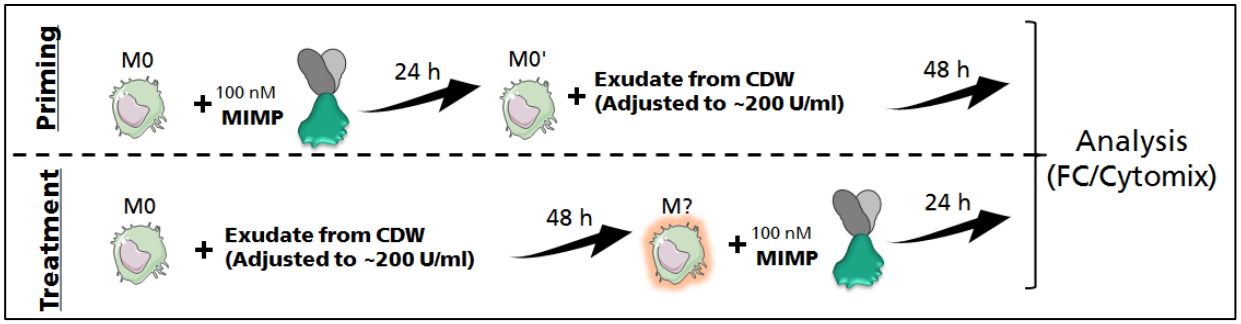

Figure 8: Experimental setup of MIMP assay on MΦ polarized using wound exudate
Abbreviations: M0, non-polarized, resting MΦ; MIMP, MΦ immunomodulatory protein; M0', MIMP primed M0; M?, MΦ incubated with exudate from CDW; FC, flow cytometry; CDW, chronic diabetic wound.

II.2.4. Immunoassays

II.2.4.1. Flow cytometry

II.2.4.1.1. Binding analysis

The binding activity of the recombinant fusion proteins towards mammalian cells and primary MΦ was detected by flow cytometry. Therefore, 1-3 x 10^5 cells with 1 µg recombinant protein in PBS (pH 7.4) containing 2 mM EDTA, 0.5% (w/v) BSA (Sigma) and 1% (v/v) human blocking (HAB) serum (Sigma) for 30 min on ice followed by washing with PBS (pH 7.4). The fluorescence staining with anti-Penta-His AlexaFluor488 antibody (125 ng per sample; Qiagen) for 30 min on ice in the dark was followed by washing twice with PBS (pH 7.4) and subsequent analysis using a FACSCalibur flow cytometer (Becton Dickinson).

II.2.4.1.2. Surface markers analysis

Flow cytometry (FC) was used for multiparametric analysis of the MΦ characteristics. Besides analysis of the shape and size, flow cytometry was used for detection of the surface markers distribution among different experimental groups. Cells were gently detached from well plates by mechanical scraping and after washing steps, they were incubated with a fluorophore-

labeled antibody in PBS (pH 7.4) containing 1% (v/v) human Ab blocking (HAB) serum (Sigma) for 30 min on ice followed by washing twice with PBS (pH 7.4). Prior to FC measurement, tubes were kept on ice. The fluorescence was then analyzed using a FACSCalibur FC (Becton Dickinson) and the results were presented as relative fluorescence intensity. Delta MFI (ΔMFI) was defined by subtraction of the background MFI (i.e. MFI stained only with PBS or isotype control). To calculate relative fluorescence intensities ΔMFI was divided by background MFI, and the acquired values were further evaluated using Graph Pad Prism5 software.

II.2.4.1.3. Quantification of soluble markers

The production of soluble cytokines and chemokines was assessed using Multiplex FlowCytomix™ Multiple Analyte Detection System (eBioscience) according to the manufacturer´s instructions. Samples of human origin were analyzed using Human Inflammation 20plex RTU FlowCytomix Kit allowing quantitative detection of soluble mediators. The sensitivity of the detection kit is indicated in **Table 8**.

Table 8: Sensitivity of FlowCytomix™ Multiple Analyte Detection System

Analyte	Sensitivity (detection limit)
TNF-α	4 pg/mL
IP-10 (CXCL-10)	6 pg/mL
IL-13	4.5 pg/mL
GM-CSF	3.4 pg/mL
ICAM-1	5.3 ng/mL
IFN-α	2.2 pg/mL
IFN-γ	1.6 pg/mL
IL-1α	0.5 pg/mL
IL-1β	4.2 pg/mL
IL-10	2 pg/mL
IL-4	21 pg/mL
LAP (corresponding to TGFβ)	0.7 ng/mL
IL-12p70	2 pg/mL
IL-6	4 pg/mL
IL-8	0.5 pg/mL
IL-17A	2.5 pg/mL
E-selectin	1.2 ng/mL
MIP-1α	1 pg/mL

Analyte	Concentration
MCP-1	2.2 pg/mL
MIP-1β	1 pg/mL

II.2.4.1.4. Cell viability assay

The cytotoxic effect of IT-based fusion proteins was monitored based on the ability of metabolic active cells to reduce the tetrazolium salt XTT (sodium 2,3,-bis(2-methoxy-4-nitro-5-sulfophenyl)-5-[(phenylamino)-carbonyl]-2H-tetrazolium) (Invitrogen) to a water soluble orange formazan dye, as previously described [154]. Briefly, 5×10^5 cells/ml were seeded into a 96-well plate and incubated at standard cell culture conditions. After appropriate stimulation described above, various dilutions of the recombinant protein were added to the wells, and the cells were incubated for additional 72h. The readout was conducted after incubation of the cells for 3-4 h with 50 µl/well of XTT/phenanzine methosulfate (100:1; Sigma Aldrich). The dye absorbance was measured at 450 nm and 630 nm using an Epoch Microplate Spectrophotometer (Biotek). Viability of cells incubated with medium only (untreated) was set to 100% for data normalization. The IT concentration required to achieve 50% reduction of cell metabolism/viability (EC_{50}) related to untreated control cells was calculated using GraphPad Prism v5.0 software. All experiments were carried out in triplicate.

II.2.4.1.5. Apoptosis Assay

To investigate the pro-apoptotic effect of IT on different MΦ phenotypes, double staining using Annexin V in combination with either MΦ markers or propidium iodide (PI) was carried out. Therefore, 5×10^5 cells/mL (II.1.8.2 or II.1.8.3) were seeded in a 24 well plate and polarized to either phenotype as described above. Afterwards IT was added and the cells were incubated for 24 h under standard cell culture conditions. Thereafter, the cells were washed twice with PBS (pH 7.4) and double-stained with AnnexinV-APC (Biolegend) and the appropriate antibody (e.g. anti-human CD14-FITC) in AnnexinV binding buffer containing 1% (v/v) HAB serum for 30 min on ice. Finally, the cells were washed as described above and resuspended in AnnexinV buffer followed by FC-analysis on a FACSCalibur (Becton Dickinson). In case of AnnexinV/PI double staining, 10 µg/mL PI was added to the cells few seconds prior to the measurement.

II.2.4.2. Macrophage functionality assays

II.2.4.2.1. Antibody-independent phagocytosis assay

The phagocytic activity in differently treated MΦ was assessed using uncoated 2-µm fluo-green silica beads (Kisker Biotech) with excitation and emission maximum at 569 and 585 nm, respectively. Briefly, polarized MΦ (3×10^4 cells) were transferred in FACS tubes and incubated for 10 min at RT in R10 medium. For assessment of the phagocytosis level 200 µg silica beads were added for 5 min at RT and the signal of gated MΦ, which have phagocytized fluo-green silica beads, was measured in FL-1 channel of a FACSCalibur system (Becton Dickinson).

II.2.4.2.2. Oxidative stress detection assay

For quantification of the oxidative stress built in differently treated MΦ, the activity of the reactive oxygen species was measured using CellROX® Deep Red Reagent (Thermo Fischer Scientific). The CellROX® Deep Red reagent is a cell-permeant dye with absorption/emission maxima of ~644/665 nm. CellROX® Deep Red reagent is non-fluorescent while in a reduced state and emits fluorescence upon oxidation by ROS with emission maxima of ~665 nm that is measurable in the FL-4 channel of the FACSCalibur device (Becton Dickinson). Briefly, polarized MΦ (3×10^4 cells) were transferred to FACS tubes, washed twice and resuspended in 500 µL PBS. Kinetic measurement of the ROS was initiated by adding 20 µL of the 200µM CellROX® Deep Red reagent to each tube. The kinetic course per tube consists of blank (no dye) measurement and six consecutive measurements (every 1 min).

II.2.4.3. Immunohistochemistry

Biopsy specimens were cut into 8-µm sections on a Cryostat CM 3050 (Leica) and mounted on superfrost slides (Menzel). After silica gel (Roth) assisted drying at RT for at least 72 h, sections were fixed for 7 min with dry acetone and air-dried. Incubation with the primary antibody was carried out at 4°C overnight using 2 µg/mL mouse-anti-human CD14-FITC (eBioscience) in 1% (v/v) normal goat serum in PBS, or mouse-anti-human CD206 (Biolegend), normal goat serum in PBS. Slides were washed three times for 5 min with PBST and incubated with 0.2 µg/mL alkaline phosphatase (AP)-conjugated goat-anti-mouse (Sigma) in 1% (v/v) goat serum in PBS for 1 h. After washing twice in PBST and once in Tris-HCl (0.1 M, pH 8.5), AP activity was detected using naphthol AS-BI phosphate (sodium salt, 50 mg/100 mL; Sigma) as substrate and new fuchsin (10 mg/100 mL; Merck) as the chromogen dissolved in 0.1 M Tris-HCl, pH 8.5, resulting in pink/red staining. Endogenous AP activity was inhibited by adding 0.35 mg/mL levamisole (Sigma) to the reaction mixture. Slides were counterstained with hematoxylin.

II.2.4.1. Microscopy

II.2.4.1.1. Confocal Microscopy

For internalization assay, the CD89(scFv)-SNAP protein was kindly provided by MSc. Stefan Zwirner (Fraunhofer IME). It was coupled to BG-Vista® Green (488nm/524nm) according to the manufacturer's instructions (NEB). Nucleus/cytoplasm were counterstained with DAPI (488nm/500nm). Internalization was verified by incubating 1 x 10^6 promyeloid $CD89^+$ HL-60 cells (1000 U/mL TNF-α) and $CD89^-$ Ramos cells with 50 nM (~2 µg) CD89(scFv)-SNAP-BG-Vista® Green in 100 µL PBS at 4°C or 37°C for 30 min. After washing the cells twice, antigen-dependent internalization was detected using a Leica TCS SP5 high resolution confocal microscope (Leica).

II.2.4.1.2. Light microscopy

Light microscopy was used for analysis of immunohistochemistry. The stained slides were digitalized for quantification analysis in bright field using a Leica DMR microscope supplemented with a Leica DFC320R2 camera (Leica) and Leica N PLAN objectives of 5x and 10× magnification.

II.2.5. Analysis of IHC micrographs

Single micrographs of stained tissue were taken in an overlapping mosaic pattern and stitched into one panorama picture using the auto-merge function from Adobe Photoshop (Photomerge command with the "repositioning"-layout to prohibit transformation of the pictures). All pictures were further processed in Adobe Photoshop to reduce the file to one layer, to add mipmaps, to crop the background and to exclude artifacts from preparation or staining. Final macrographic images were analyzed using HistoCAD software from Fraunhofer MEVIS (Fraunhofer Institute for Medical Image Computing MEVIS, Bremen, Germany). HistoCAD allows analysis of multiple images using identical parameters resulting in uniform staining quantification. Therefore, training of the program was performed diligently on at least three macrographs from each slide. Afterwards, every single slice was checked for sufficient categorizing. The area from stratum corneum to stratum basale (also generally known as epidermis) was excluded since high intrinsic activity of alkaline phosphatases led to unspecific signals. Statistical analysis was performed with GraphPad Prism v5.0.

II.2.6. Statistical analysis

Statistical analysis was performed using GraphPad Prism v5.0 software. Data were expressed as mean ± standard deviation (SD), unless indicated otherwise. Due to the limited samples size (N=5) the statistical comparisons were performed using a non-parametric unpaired Mann-Whitney test using the following pattern: * $p \leq 0.05$, ** $p \leq 0.01$, *** $p \leq 0.001$.

II.2.7. Safety levels

All experiments were carried out according to the S1 (file ID: 64-K-1.51/05 with facility number: 992) or S2 (file ID: 64-K-1.51/05 with facility number: 993) safety level, as required.

III Results

The main objective of the work described in this thesis was to investigate whether MΦ can be manipulated in the context of chronic inflammation, more precisely in a cutaneous model, to explore their plasticity, and to identify the suitability of CD89-directed therapeutic intervention in addition to established strategies targeting CD64. In the first part of the work, cytokine levels were determined in exudates from chronic diabetic wounds (CDWs) and the strong pro-inflammatory environment was confirmed. Furthermore, *ex vivo* analysis demonstrated the potential clinical relevance of MΦ-targeting therapy. This revealed the extraordinary plasticity of MΦ and their suitability for targeted modulation. In the next part of the work, effector proteins involved in inflammation were selected and fused to the well-known CD64-binding antibody fragment H22(scFv), introducing the novel family of MIMPs. Both MIMPs, i.e. H22(scFv)-Trx and H22(scFv)-SOCS2, were expressed, purified and fully characterized in terms of their identity, specific binding and immunomodulatory activities in different assays. The final part of this thesis describes the use of CD89 as a potential target antigen on the MΦ surface. Therefore, the presence of CD89 on different MΦ subsets was investigated and targeting experiments were carried out using a newly-generated IT consisting of a CD89-specific scFv and the well-known toxin ETA'.

III.1. MΦ plasticity and phenotype in disease

III.1.1. Assessment of cytokine profiles in patients with chronic inflammation

To investigate cytokine levels in chronic diseases associated with MΦ proliferation, analysis was carried out on samples of primary material provided by partners in the university hospitals of Aachen and Stuttgart. For chronic skin inflammation, wound exudates from five diabetic patients with CDWs were analyzed. In parallel, sera isolated from five patients diagnosed with chronic myeloid monocytic leukemia (CMML) were also tested. To achieve a better comparison, the background levels of the same cytokines were measured in sera from five healthy blood donors. The experiment was designed to investigate differences in cytokine levels affecting the nature of inflammation in CMML and CDWs. Although unrelated in terms of pathophysiology, one symptom shared by both chronic diseases is the pathological dysregulation of myeloid cells, albeit these are myeloid blasts in CMML and macrophages in CDW.

The samples from healthy blood donors contained only trace amounts of most of the inflammation-associated cytokines (IL-12, IL-6, GM-CSF, TNF-α, IL-1β and IFN-α). Low levels of anti-inflammatory cytokines (IL-10, IL-13, IL-4, and TGFβ) were also detected (**Figure 9**). In contrast, patients with either CMML or CDW produced higher levels of the same cytokines and chemokines, as shown in **Figures 9** and **10**, respectively. Comparable levels of IL-12, IL-6, MIP-1α, MIP-1β, IL-8, CXCL-10 and ICAM-1 were detected in sera from CMML patients and CDW exudates (**Figures 9** and **10**). However, other inflammatory cytokines were significantly more abundant in CDW exudates compared to CMML sera: TNF-α (2-fold↑), GM-CSF (2-fold↑), IL-1α (2-fold↑), IL-1β (2-fold↑), IFN-α (3-fold↑), and IFN-γ was strongly induced (**Figure 9**). The CDW exudates were not completely devoid of anti-inflammatory cytokines, but CMML patient sera contained significantly higher levels of IL-10 (3-fold↑), IL-13 (3-fold↑) and IL-4 (1.5-fold↑) than the CDW exudates. Interestingly, the concentration of LAP (corresponding to TGF-β), which is involved in tissue repair, was two-fold higher in the CDW exudates. Cytokines associated with immunochemotaxis and cell diapedesis are shown in **Figure 10**. The samples from healthy blood donors contained very low levels of all the measured chemokines, except IL-8 (CXCL-8) and E-selectin. The

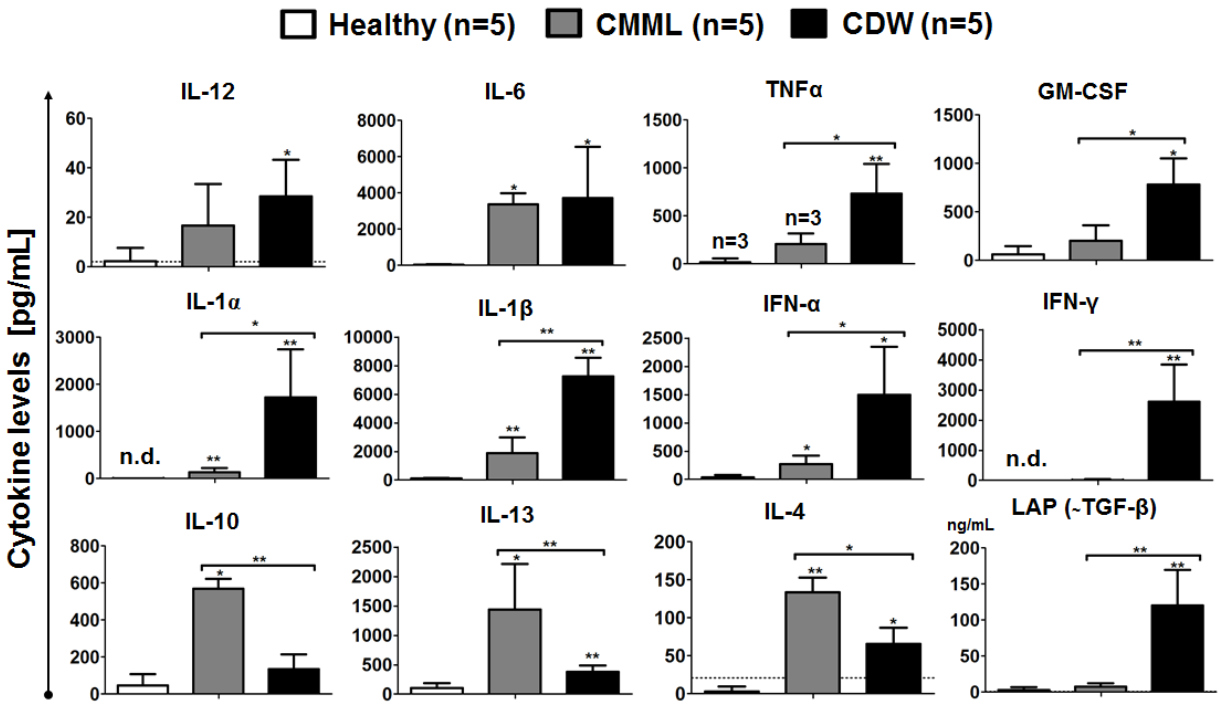

Figure 9: Cytokine profile in exudates obtained from healthy donors and patients with chronic disease. Exudates from diabetic patients with CDWs (n=5) and serum from CMML (n=5) or healthy blood donors (n=5) were analyzed for soluble cytokines using the FlowCytomix™ Multiple Analyte Detection System (eBioscience) as described (II.2.4.1.3). One measurement was carried out per sample. Statistical analysis was carried out using the non-parametric Mann-Whitney U test: *p≤0.05, **p≤0.01. Asterisks above columns indicate comparisons of each patient group versus the healthy controls. Asterisks above the lines indicate comparison between the two patient groups. Dashed lines indicate the detection limit (II.2.4.1.3. Table 8). Abbreviations: n.d., not detectable.

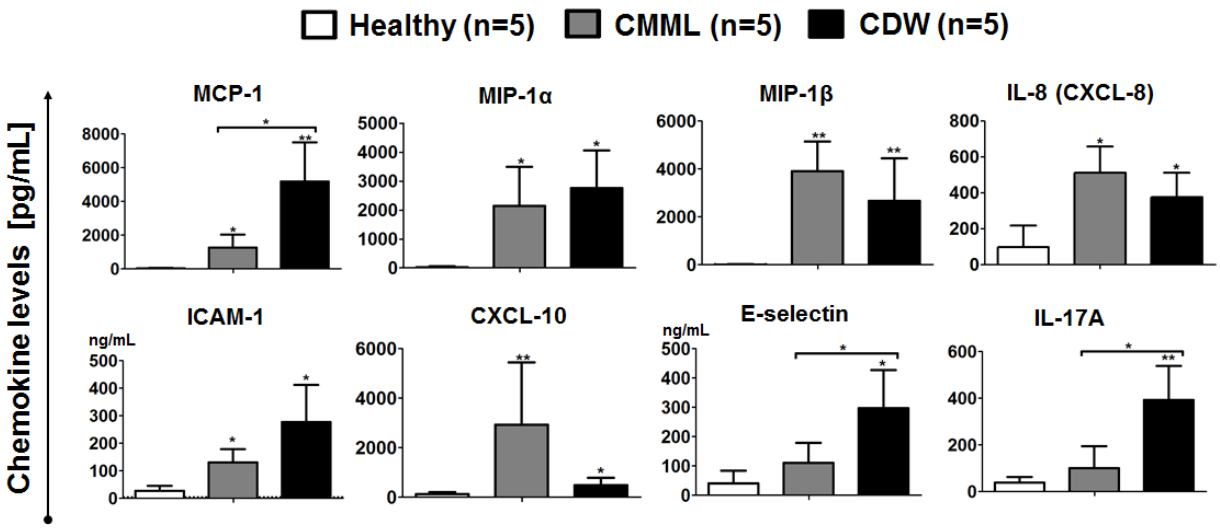

Figure 10: Profiles of chemokines in healthy donors and patients with chronic disease.
Exudates from diabetic patients with CDWs (n=5) or serum from CMML (n=5) or healthy donors (n=5) were analyzed for soluble cytokines using the FlowCytomix™ Multiple Analyte Detection System (eBioscience) as described (II.2.4.1.3). Statistical analysis was carried out using the non-parametric Mann-Whitney U test: *p≤0.05, **p≤0.01. Asterisks above columns indicate comparisons of each patient group versus the healthy controls. Asterisks above the lines indicate comparison between the two patient groups.

concentration of IL-8 was 150 pg/mL in sera from the five healthy donors. Samples from CMML and CDW patients had much higher levels of MCP-1, IL-8, ICAM-1, MIP-1α and MIP-1β. When comparing the two patient groups, only CXCL-10 was substantially more abundant (4-fold↑) in CMML patient sera, whereas MCP-1, IL-17A and E-selectin levels were significantly higher (1.5–2-fold↑) in CDW exudates. **Figure 11** confirms the predominance of the pro-inflammatory cytokine fraction in CDW exudates compared to serum from healthy blood donors. The significantly higher levels of pro-inflammatory cytokines, led by IL-1β, IL-6, IFN-γ, IFN-α, IL-1α, GM-CSF and TNF-α, clearly indicates the failed transition towards

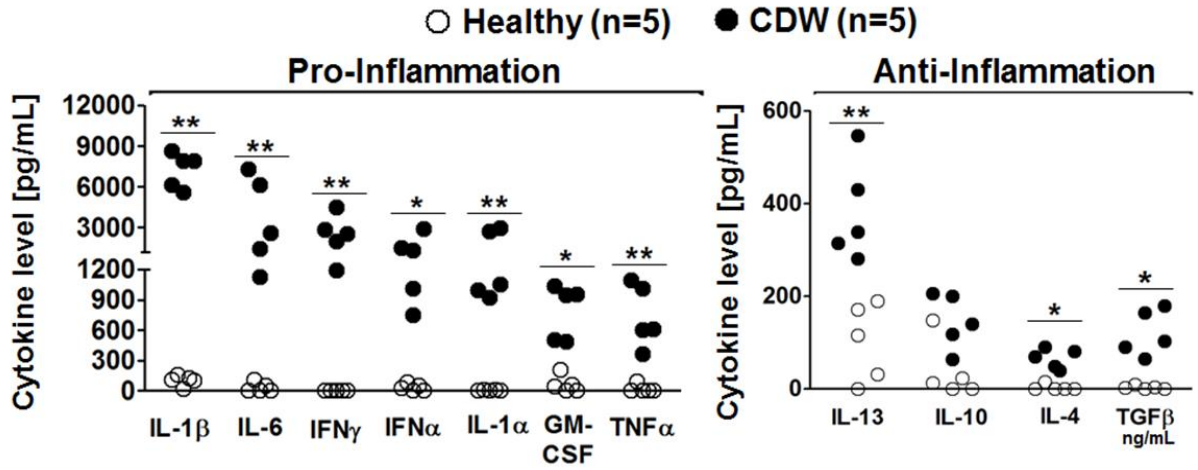

Figure 11: Predominance of pro-inflammatory cytokines in CDW exudates.
Levels of pro-inflammatory versus anti-inflammatory cytokines in serum from healthy blood donors (n=5) and exudates from patients with CDWs (n=5). Samples were analyzed for soluble cytokines using the FlowCytomix™ Multiple Analyte Detection System (eBioscience) as described (II.2.4.1.3). Asterisks indicate comparison of the patient group versus the healthy controls. Statistical analysis was carried out using the non-parametric Mann-Whitney U test: *p≤0.05, **p≤0.01.

the resolution phase of the inflammatory process. The anti-inflammatory cytokines (e.g. IL-13, IL-10) were much less abundant (up to 600 pg/mL) than the pro-inflammatory cytokines. Although higher, the concentration range of anti-inflammatory cytokines in CDW exudates was closer to the concentration detected in sera from healthy donors.

III.1.2. *Ex vivo* elimination and plasticity of MΦ in chronically inflamed skin

Primary skin biopsies from patients with chronic skin inflammation were investigated in addition to the CDW exudates. Clear evidence for the clinical relevance of previous findings concerning the *in vivo* elimination of M1 cells was collected by taking biopsies from the skin lesions of atopic dermatitis patients (n=3) and T2D patients with CDWs (n=2), and treating them *ex vivo* with 1 µM of H22(scFv)-ETA'. IHC staining revealed the depletion of $CD64^+$ and $CD14^+$ M1 cells (**Figure 12A**). The quantification of histological staining for CD14 (M1) and CD206 (M2) using HistoCad image analysis software confirmed that treatment with H22(scFv)-ETA' reduced the number of M1 cells without negatively affecting the M2 population (**Figure 12B**). There was a tendency towards the reduction of M1-related events by 30–90% within the 24–48 h treatment course. Interestingly, the number of $CD206^+$ M2

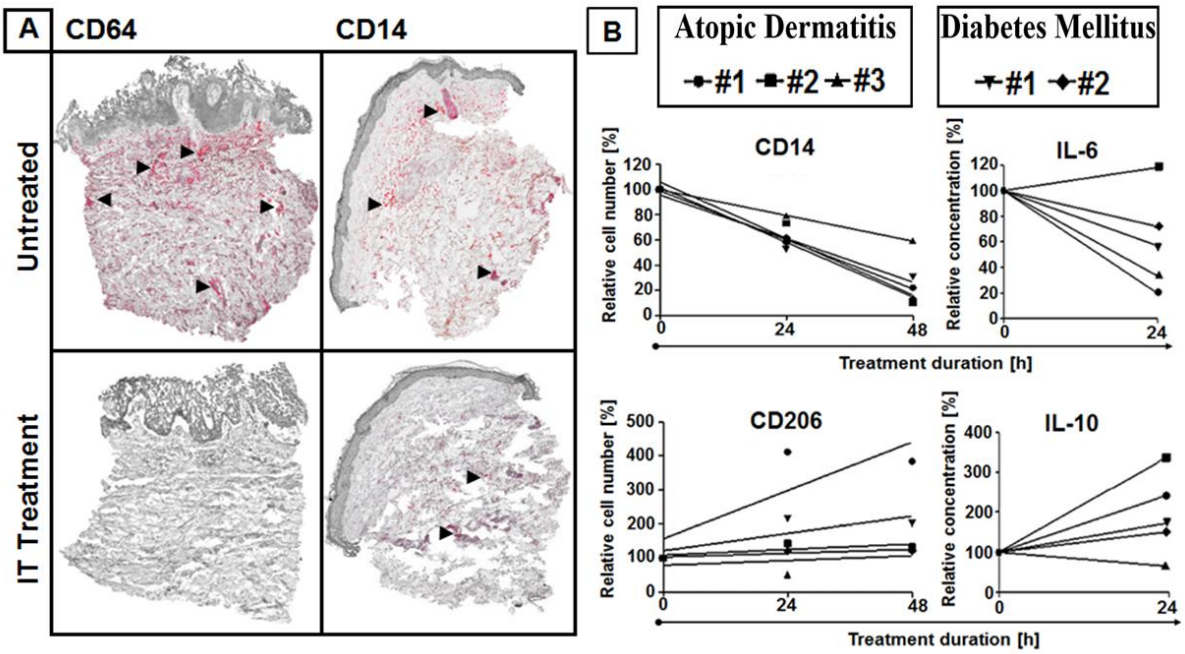

Figure 12: Elimination of M1 cells shifts the microenvironment towards M2 phenotype.
Skin biopsies were taken from patients with atopic dermatitis (n=3) and diabetes type II (n=2). Biopsies were split into equiproportional pieces and treated *ex vivo* with H22(scFv)-ETA' for 24 or 48 h. **(A)** Representative IHC images of untreated and H22(scFv)-ETA' treated skin biopsies from atopic dermatitis patients. Arrows indicate intensively stained M1. **(B)** Quantification of $CD14^+$ and $CD206^+$ cells using HistoCad software. Levels of IL-6 and IL-10 were determined using the FlowCytomix™ Multiple Analyte Detection System (eBioscience) as described (II.2.4.1.3). Each point is the mean value of duplicates. Lines present tendencies of the measured events for each patient.

cells increased slightly. Furthermore, supernatants from the human skin biopsies were analyzed for the presence of relevant cytokines before and after the 24 h treatment. Although the concentrations of IL-12, IFN-γ, TNF-α and IL-4 were below the detection limit, hypothetically due to high dilution in the medium, the pro-inflammatory cytokine IL-6 and the anti-inflammatory cytokine IL-10 were detected. In agreement with the distribution of surface receptors, IL-6 levels showed a clear decline 24 h after treatment with H22(scFv)-ETA', whereas IL-10 levels showed a tendency to increase (**Figure** 12**B**).

III.1.3. *In vitro* heterogeneity of the MΦ population

As shown in **Figure 12**, it is possible to target human M1 cells *ex vivo* without adversely affecting the anti-inflammatory M2 cell population. However, it should be noted that not all M1 cells were eliminated and at least 5–10% remained. This suggested that MΦ unaffected by the IT treatment might actually undergo phenotypic switching in the IT-insensitive M2 direction. To address this hypothesis, *in vitro* IT treatment was carried out and MΦ were then double-stained for Annexin V and the markers CD14 (M1) or CD206 (M2). **Figure 13** shows that the M1 population is heterogeneous in terms of surface marker expression, corresponding to the susceptibility of these subpopulations towards H22(scFv)-ETA'. This confirms that the M1 population also contains M2-like cells that are resistant to H22(scFv)-ETA' (**Figure 13E**

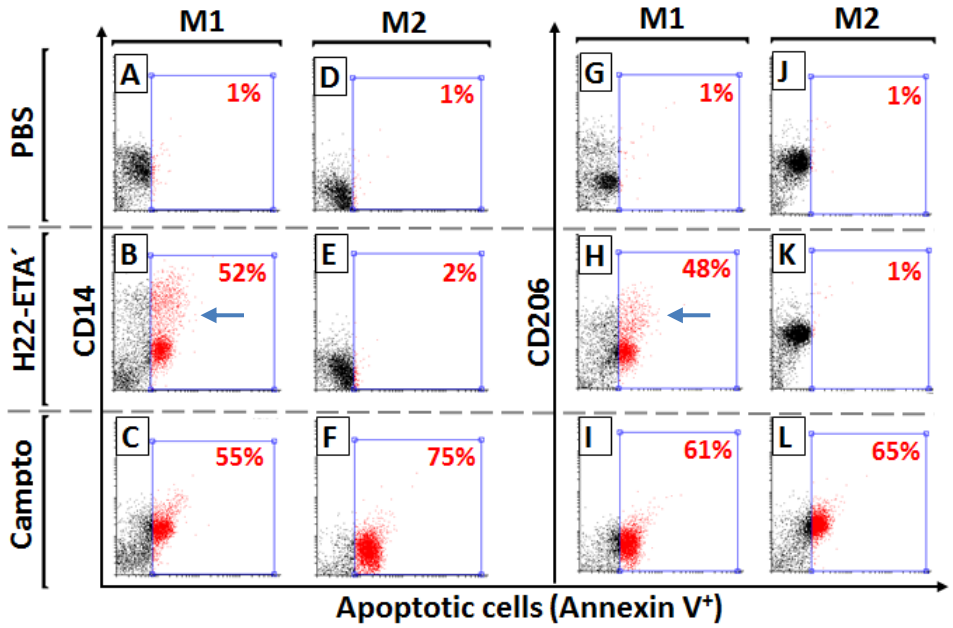

Figure 13: *In vitro* heterogeneity of primary MΦ treated with H22(scFv)-ETA'.
H22(scFv)-ETA' drives M1 MΦ into apoptosis accompanied by phenotype heterogeneity (arrows in images B and H). M1 and M2 were incubated for 24 h with either PBS, or 100 nM H22(scFv)-ETA', or camptothecin as unspecific pro-apoptotic control agent as described (II.2.4.1.5). **(A to F)** Double staining for CD14 and Annexin V of differently treated MΦ. **(G to L)** Double staining for CD206 and Annexin V of differently treated MΦ. Blue arrows indicate heterogeneity within IT-treated M1 population. The dot blots shown are representative data from three repetitions using PBMC-derived MΦ from three different blood donors.

and K). Staining with Annexin V-FITC after incubation with H22(scFv)-ETA' confirmed that the mode of action was the selective induction of apoptosis in M1 cells (**Figure 13B and H**).

III.1.4. *In vitro* functional plasticity of MΦ

To confirm MΦ functional plasticity, cultured murine or human MΦ were re-polarized *in vitro* by reversion of the initial stimuli (IL-4 for M1 and IFN-γ for M2) followed by exposure to H22(scFv)-ETA'. As expected, M1 cells were killed by the IT whereas M2 cells were resistant. However, in addition to the phenotypic plasticity of polarized MΦ shown in **Figure 13**, here their functional plasticity was demonstrated by reversing their sensitivity towards H22(scFv)-ETA'. The stimulation of previously sensitive M1 cells with IL-4 resulted in them becoming resistant to H22(scFv)-ETA', whereas the stimulation of previously resistant M2 cells with IFN-γ resulted in the development of sensitivity towards H22(scFv)-ETA' (**Figure 14, black columns**). MΦ underwent this bidirectional phenotypic switch within 24 h, which indirectly explains the incomplete *ex vivo* killing of these cells in treated skin tissue. These data illustrate that polarized MΦ can still be reverted towards other phenotypes with diverse functions. In this case, the use of IFN-γ or IL-4 provides evidence that the re-polarization of MΦ is a suitable approach for immunomodulation (**Figure 14**).

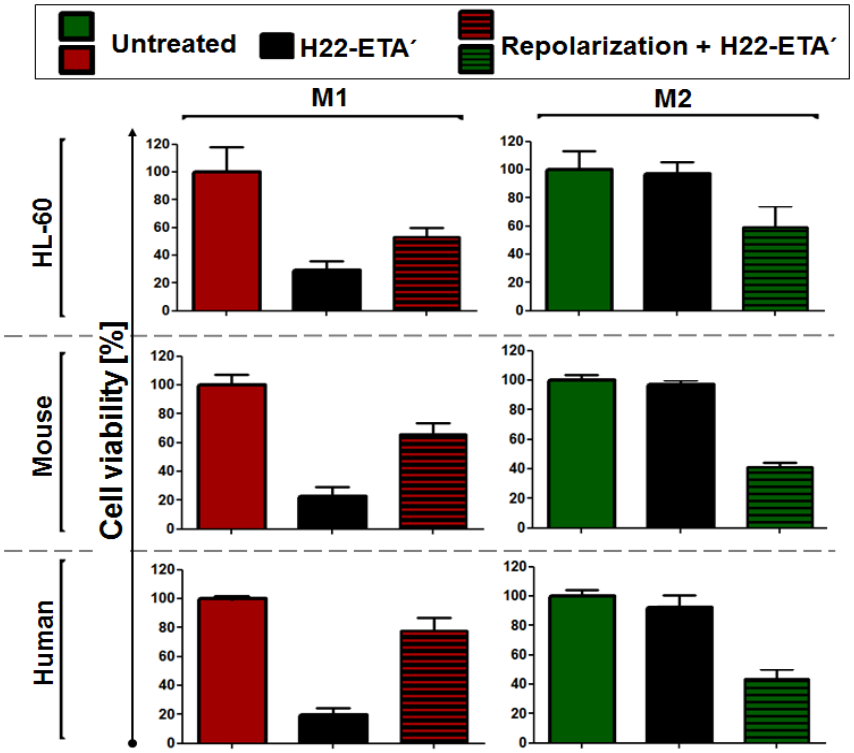

Figure 14: *In vitro* functional plasticity of MΦ.
The re-polarization (24 h IFN-γ for M1 and IL-4 for M2) of polarized MΦ derived from cell line HL-60, mice (tgCD64$^+$) and human patients was carried out as described (II.2.3.3.3). The cells were treated with 100 nM H22(scFv)-ETA' for 24 h. Data are presented as means ± SD of triplicates. The data shown are representative of two repetitions.

III.2. Immunomodulation of MΦ

These previous data show that the *in vitro* M1-M2 subdivision successfully mirrors the immunological events occurring in primary material. Furthermore, the CD64-targeted elimination of pathogenic M1 cells during inflammatory diseases was successful, which in combination with the evidence for MΦ plasticity gives rise to a new therapeutic strategy: CD64-targeted immunomodulation. MIMPs were generated for this strategy comprising the H22(scFv) binding moiety genetically fused to the effector domains Trx-1 and SOCS-2, whose functions are described in section I.8.

III.2.1. Generation of H22(scFv)-Trx-1 and H22(scFv)-SOCS-2

III.2.1.1. Cloning of H22(scFv)-Trx-1 and H22(scFv)-SOCS-2

The generation and characterization of H22(scFv)-Trx-1 is described to some extent in the Master's thesis of Tim Stroisch ("Generation and Evaluation of H22(scFv)-fused Immunomodulatory Proteins") supervised by Radoslav Mladenov in Prof. R. Fischer's laboratory and defended in September 2014 at the RWTH Aachen University [155]. The data presented here have been generated independently of the Master's thesis. Both effector domains (Trx-1 and SOCS-2) were obtained as ready-to-use plasmid DNA (pEX-A2-SOCS-2 and pEX-A2-Trx-1) from MWG-Biotech AG. The Trx-1 (**Figure 15A**) and SOCS-2 (**Figure 15B**) inserts were removed using the restriction enzymes *Not*I and *Blp*I. The pMS vector containing the H22(scFv) sequence was prepared in a linear form for the subsequent ligation procedure (**Figure 15C**) using the same restriction enzymes (II.2.1.5). The presence

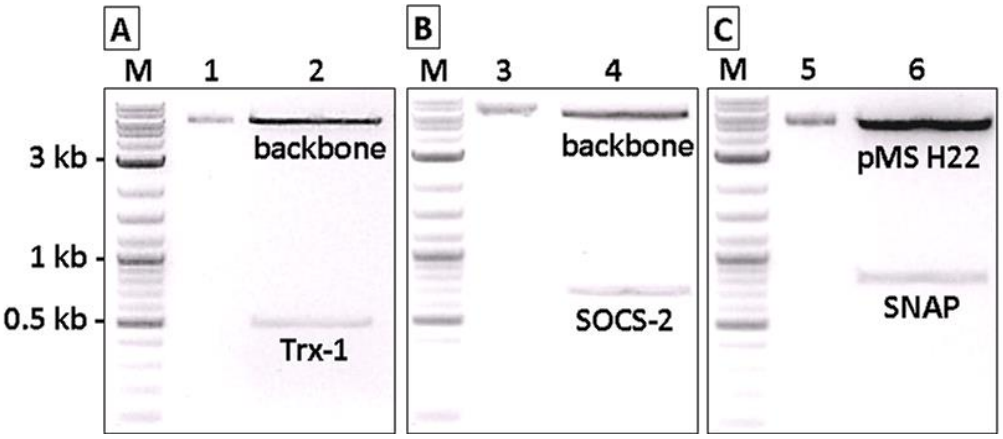

Figure 15: Cloning MIMPs in the H22(scFv) vector.
Preparative DNA digestion of the pMS-H22(scFv) vector, pMS-H22-SOCS1 and pMS-H22-LIP. Plasmid DNA (1µg) was used for preparative digestion. The digest mixture was separated on a 1.2% agarose gel (II.2.1.7). M: 2-log DNA ladder; **(A)** Digestion of pEX-A2-Trx-1. 1: undigested vector, 2: digested vector [*Not*I, *Blp*I]; **(B)** Digestion of pEX-A2-SOCS-2. 3: undigested vector, 4: digested vector [*Not*I, *Blp*I]; **(C)** Digestion of pMS H22(scFv)-SNAP: 5: undigested vector; 6: digested vector [*Not*I, *Blp*I]. Abbreviations: kb, kilobase pairs.

of the intended ligation products was confirmed by a control digest with restriction enzymes cutting uniquely in the desired insert sequence and in addition, selected clones were sequenced (II.2.1.8) using the corresponding primers from **Table 4**.

III.2.1.2. Production of H22(scFv)-Trx-1 and H22(scFv)-SOCS-2

The recombinant MIMPs, i.e. SOCS2 and Trx fused to H22(scFv), were expressed by the liposome-mediated transfection of HEK293T cells (II.2.2.2). Whereas normal serum conditions were required for H22(scFv)-Trx-1 expression, H22(scFv)-SOCS-2 was successfully expressed under serum-free conditions. Previously, H22(scFv)-SOCS-2 was not efficiently expressed and secreted in FCS-supplemented medium and the recombinant protein accumulated in the cytoplasmic space [155]. The supernatant was harvested for enrichment by IMAC using the His_6 tag (II.2.2.3.2) followed by SEC (0). A final yield of 2 mg and 5 mg of purified recombinant protein per liter of cell culture supernatant was achieved for H22(scFv)-SOCS-2 and H22(scFv)-Trx-1, respectively. The purity, concentration and identity of generated MIMPs were confirmed by SDS-PAGE, with Coomassie Brilliant Blue G-250 staining (II.2.2.5.1), Bradford assay (II.2.2.5.3) and western blotting (II.2.2.5.2), respectively. Despite the SEC step, which should separate proteins based on differences in size, the preparation still contained small amounts of impurities as shown in **Figure 16A (lane 3)**. No degradation resulting into free H22(scFv) and Trx-1 was observed as shown by the corresponding commercial free Trx-1 (**lane1**) and in-house H22(scFv) (**lane 2**). The identity

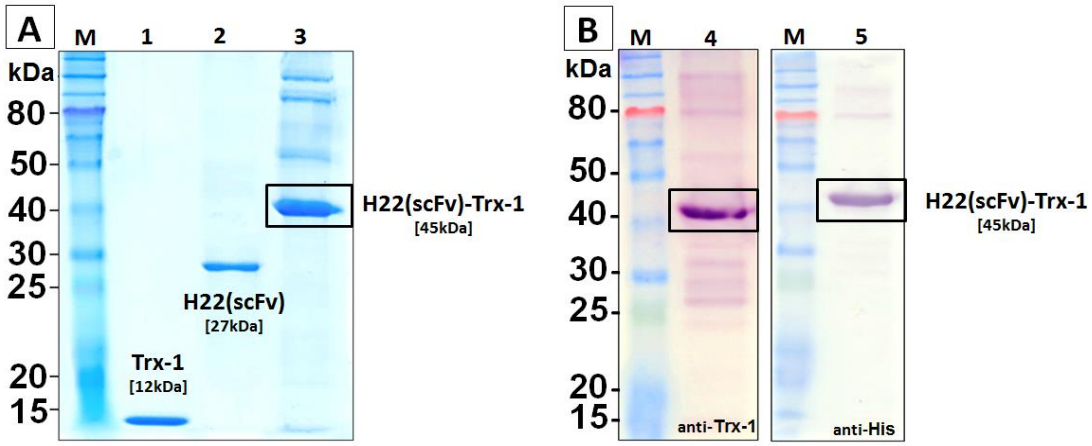

Figure 16: H22(scFv)-Trx-1: SDS-PAGE with Coomassie staining and western blot analysis.
H22(scFv)-Trx-1 (lane3) was expressed in HEK293T cells (II.2.2.2) and purified by IMAC (II.2.2.3) and SEC (0). The purity was assessed by SDS-PAGE (II.2.2.5.1) followed by staining with Coomassie Brilliant Blue G-250 shown in **(A).** The corresponding controls were commercially purchased free Trx-1 (R&D Systems) (lane 1, 500 ng) and in-house H22(scFv) (lane 2, 500 ng). **(B)** Protein identity was verified by western blot using a mouse anti-human Trx-1 mAb (1:5000, AbD Serotec) (lane 4) and mouse anti-His mAb (1:10,000, Qiagen) (lane 5) detected with an alkaline phosphatase-conjugated anti-mouse-IgG mAb (1:5000; Sigma) followed by staining with NBT/BCIP substrate (Thermo Fisher Scientific). M: Pre-stained broad range protein marker (New England BioLabs). Abbreviations: kDa, kiloDalton.

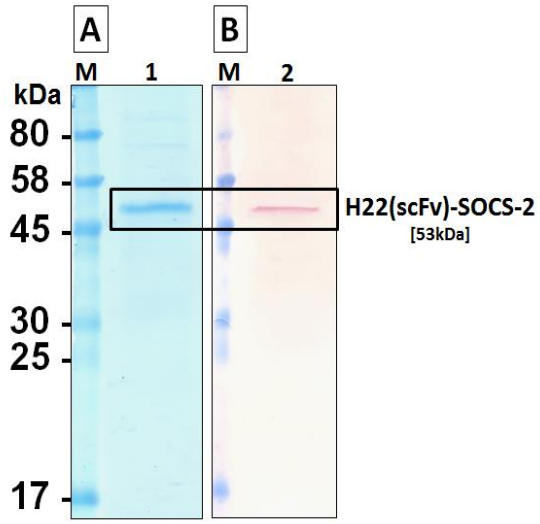

Figure 17: H22(scFv)-SOCS-2: SDS-PAGE with Coomassie staining and western blot analysis. H22(scFv)-SOCS-2 was expressed in HEK293T cells (II.2.2.2) and purified by IMAC (II.2.2.3) and SEC (0). **(A)** The purity was assessed by SDS-PAGE (II.2.2.5.1) followed by staining with Coomassie Brilliant Blue G-250. **(B)** Protein identity was verified by western blot using a rat anti-SOCS-2 mAb (1:5000, BioLegend) detected with an alkaline phosphatase-conjugated anti-rat-IgG mAb (1:5000; Sigma) followed by staining with NBT/BCIP substrate (Thermo Fisher Scientific). M: Pre-stained broad range protein marker (New England BioLabs). Abbreviations: kDa, kiloDalton.

of the product was confirmed by western blotting using anti-His and anti-Trx-1 monoclonal antibodies from AbD Serotec (**lane 4**) and Qiagen (**lane 5**), respectively (**Figure 16B**). However, some minor impurities were detected by both gel staining with Coomassie and western blot suggesting they were product-related. Although unlikely under reducing conditions, dimerization may have yielded the 80 kDa product which is exactly double the size of the 40 kDa H22(scFv)-Trx-1 [156]. Purification of recombinant H22(scFv)-SOCS-2 was conducted successfully using a process analogous to that described for H22(scFv)-Trx-1. Subsequent SDS-PAGE with Coomassie Brilliant Blue G-250 staining (II.2.2.5.1) and western blot analysis (II.2.2.5.2) is shown in **Figure 17A and B**. No impurities were detected in the elution fraction for recombinant H22(scFv)-SOCS-2. The product specifications for both recombinant MIMPs are indicated in **Table 9** (below). All recombinant MIMPs were stored at –20°C in sterile aliquots and for long-term storage at –80°C.

Table 9. Production results of generated MIMPs.

MIMPs	MW[kDa]	Purity [%]	Total yield [mg]	Storage temp.
H22(scFv)-Trx-1	45	>90	10	-20°C/-80°C
H22(scFv)-SOCS-2	53	>95	4	-20°C/-80°C

III.2.1.1. Binding of H22(scFv)-MIMP fusions to target cells

The ability of the recombinant H22(scFv)-Trx-1 and H22(scFv)-SOCS-2 to bind their target cells was tested by flow cytometry (II.2.4.1.1). In the initial *in vitro* experiments, the strong binding activity of both MIMPs was confirmed using human PBMC-derived MΦ, which were polarized to either M1 or M2 phenotypes (**Figure 18A and B**). As expected, both MIMPs bound preferentially to the M1-polarized MΦ. Although human blocking serum was

used to minimize the nonspecific binding of the detection mAb, minimal background binding was nevertheless detected. As expected, there was no detectable binding of either MIMP to the CD64⁻ Ramos cell line (**Figure 18C**). After successfully generating both MIMPs and confirming their specific targeting of human PBMC-derived MΦ, further experiments were conducted to analyze their immunomodulatory activity.

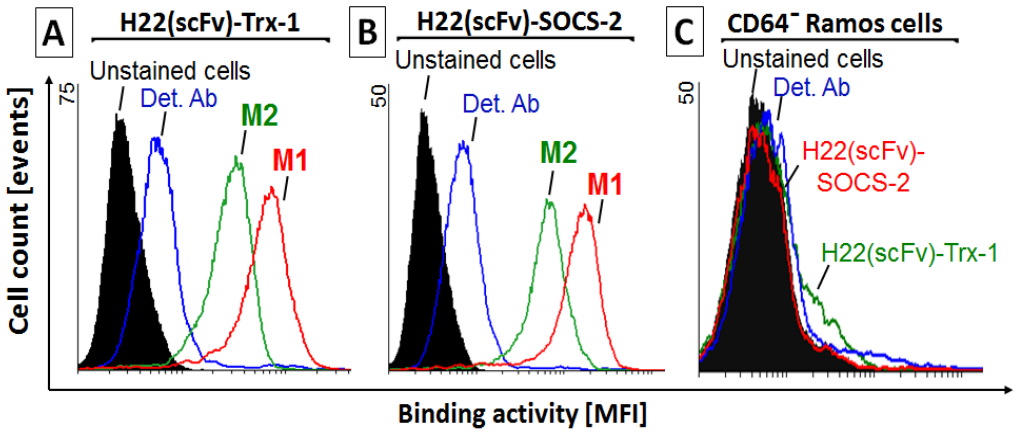

Figure 18: Generated MIMPs successfully bound to MΦ.
Binding analysis of H22(scFv)-based MIMPs towards MΦ and CD64-negative Ramos cells. The binding of purified H22(scFv)-Trx-1 **(A)** and H22(scFv)-SOCS-2 **(B)** was tested by flow cytometry (II.2.4.1.1) to either human M1 and M2 polarized MΦ or CD64-negative Ramos cells **(C)**. Cells were incubated with 1% (v/v) human blocking serum. Abbreviations: Det. Ab: detection antibody (mouse anti-Penta-His AlexaFluor488). The images show representative data from two repetitions. Abbreviations: MFI, mean fluorescence intensity.

III.2.1.2. Cell viability and metabolism after treatment with MIMPs

A prerequisite for the application of MIMPs in humans is their complete lack of toxicity and metabolic disruption of the target cells. To exclude those effects, the metabolism and viability of primary human MΦ treated with increasing concentrations of both recombinant MIMPs was measured *in vitro* using the XTT assay (II.2.4.1.4). In the concentration range 10 pM to 250 nM, neither H22(scFv)-Trx-1 nor H22(scFv)-SOCS-2 induced cytotoxic effects or metabolic disruption in polarized macrophages or non-polarized M0 cells (**Figure 19**). Thus, without adversely affecting the target cells, both MIMPs were tested for immunomodulatory activity using concentration of 100 nM.

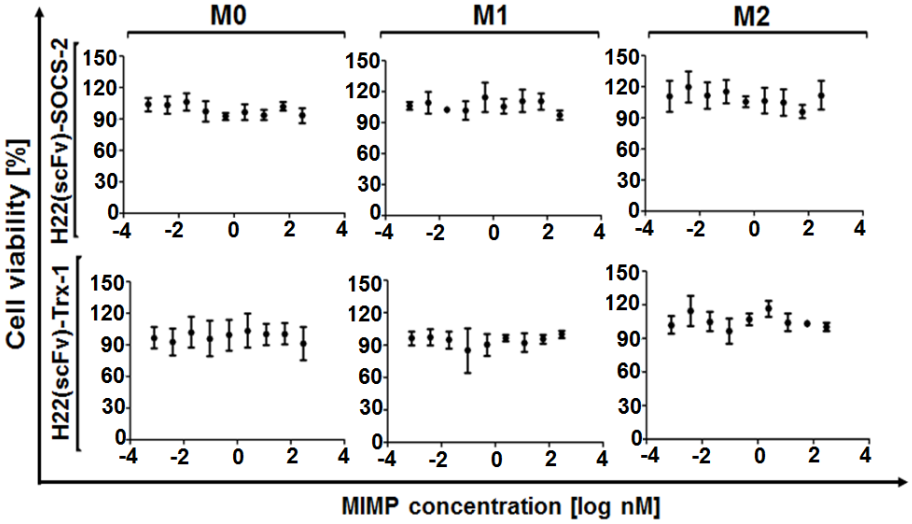

Figure 19: Recombinant MIMPs lack cytotoxic activity against primary MΦ.
Cytotoxicity assays were carried out by incubating PBMC-derived human MΦ (M0, M1 and M2 populations) with different concentration of both MIMPs for 72 h. The highest concentration was 250 nM. Viability was normalized against vehicle control (PBS). Cell viability was measured using an XTT assay (II.2.4.1.4). Data represent mean values of one measurement with SD of triplicates.

III.2.2. Immunomodulation of primary human MΦ

This section shows the immunomodulatory activity of both MIMPs towards primary MΦ. Two different treatment approaches were used to represent two application strategies. Systemic administration of MIMPs will probably reach monocytes and MΦ in the blood, affecting these cells before exposure to the local polarizing environment at the site of inflammation. This can be mimicked *in vitro* by the **priming** approach, in which PBMC-derived MΦ are incubated with the MIMP before polarization. In contrast, a local (e.g. topical) application would introduce the MIMPs to MΦ that have already acquired a distinct phenotype – here called the **treatment** approach. In-house H22(scFv) and commercial carrier-free Trx-1 (R&D Systems) were used as controls. Free SOCS-2 was not generated and is not commercially available, so this control was not included in the experiments. In the MΦ model,

in addition to the classical M1/M2 polarization protocol (II.2.3.4.1), the phenotype of MΦ exposed to sterile CDW exudates was also investigated (II.2.3.4.2). The readout involved the analysis of 16 surface and soluble markers associated with chemotaxis, pro-inflammatory and anti-inflammatory events.

III.2.2.1. Modulation by H22(scFv)-SOCS-2 in the MΦ model

Recombinant H22(scFv)-SOCS-2 was used in the classical MΦ model as described in section II.2.3.4.1. To study the influence of the recombinant MIMP on polarized MΦ, the expression of surface (**Figure 20**) and soluble (**Figure 21**, **Figure** 22 and **Figure** 23) markers was assessed as described in section II.2.4.1. As expected, surface CD64 decreased significantly upon priming and also following treatment with the CD64-targeting H22(scFv) fusion protein (**Figure 20**). Surface CD14 remained unaffected by the MIMP in all MΦ phenotypes. Both M2 markers, CD206 and CD301, remained unchanged in the M0 and M1 populations during both treatment approaches with H22(scFv)-SOCS-2. In contrast, M2-polarized MΦ primed with the MIMP showed a tendency towards the increased surface expression of CD206 and CD301. Interestingly, this effect was not observed when already polarized M2 cells were treated with the MIMP. H22(scFv)-SOCS-2 had a much stronger impact on the secretion of pro-inflammatory cytokines (**Figure 21**). The suppression of cytokine signaling in the primed M1 population caused a significant reduction in the levels of IL-12 (2–3-fold↓). There was also a tendency towards lower levels of IL-6 (2-fold↓) and TNF-

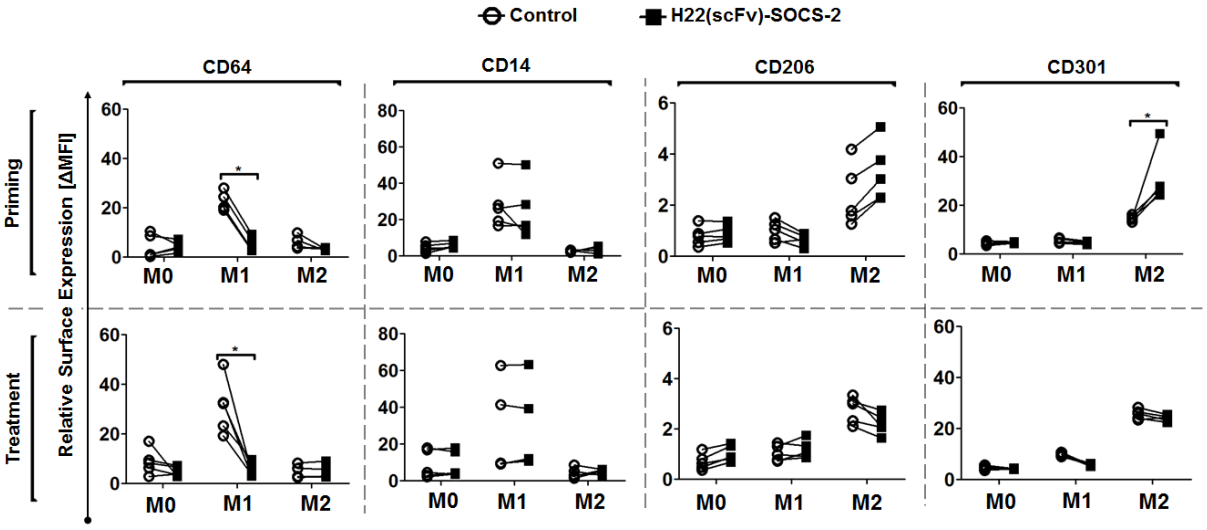

Figure 20: H22(scFv)-SOCS-2 reduced surface CD64.
PBMC-derived MΦ were either primed or treated with 100 nM H22(scFv)-SOCS-2 for 24 h as described in II.2.3.4. Cells of triplicates were merged to comprise one point for each measurement. The expression of surface markers of MΦ was carried out using flow cytometry as described in chapter II.2.4.1.2. Control group represents the PBS vehicle control. The values represent the normalized fold expression levels presented as symbols connected with and without treatment (n=5 different PBMC donors). Statistical analysis was carried out using non-parametric Mann-Whitney U test: *p≤0.05. Abbreviations: ΔMFI, delta mean fluorescence intensity.

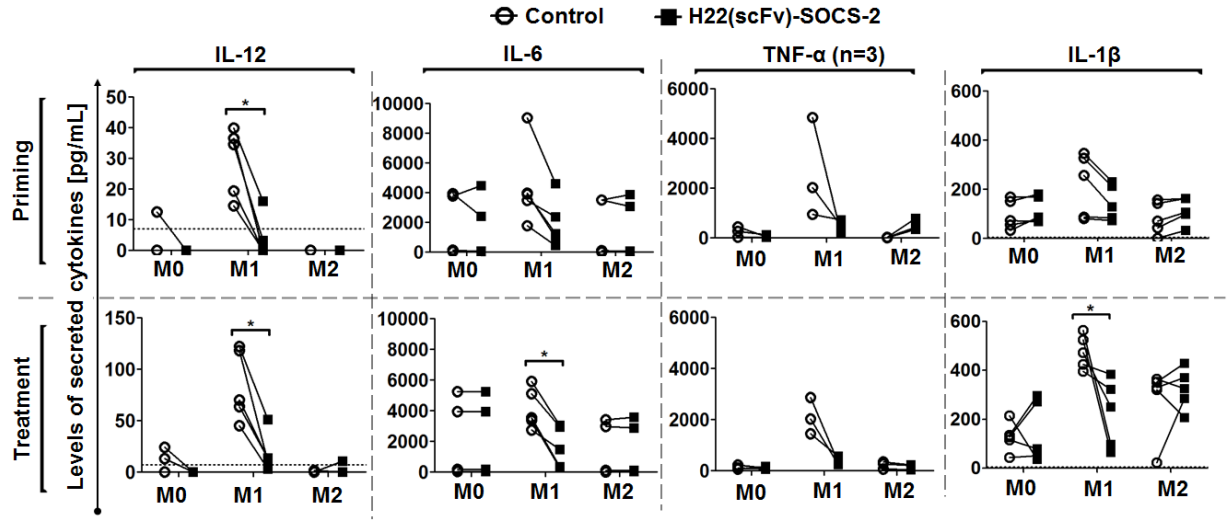

Figure 21: H22(scFv)-SOCS-2 reduces the abundance of surface CD64.
PBMC-derived MΦ were either primed or treated with 100 nM H22(scFv)-SOCS-2 for 24 h as described in section II.2.3.4. Cells of triplicate samples were merged to yield one point for each measurement. The expression of MΦ surface markers was measured by flow cytometry as described in section II.2.4.1.2. The control group is the PBS vehicle control. The values represent the normalized fold expression levels presented as symbols connected with and without treatment (n=5 different PBMC donors). Statistical analysis was carried out using the non-parametric Mann-Whitney U test: *p≤0.05. Abbreviations: ΔMFI, delta mean

α (2-fold↓) in M1 cells. M0 and M2 cells secreted these cytokines at very low levels and the MIMP had no effect. When polarized M1 cells were treated with H22(scFv)-SOCS-2, there were significant declines in the levels of IL-12 (2-fold↓), IL-1β (1.5–3-fold↓) and IL-6 (2-fold↓). The concentration of TNF-α was slightly reduced. **Figure 22** shows the distribution of anti-inflammatory cytokines following incubation with H22(scFv)-SOCS-2. When MΦ were primed with MIMP and subsequently polarized, M1 cells showed a tendency towards the

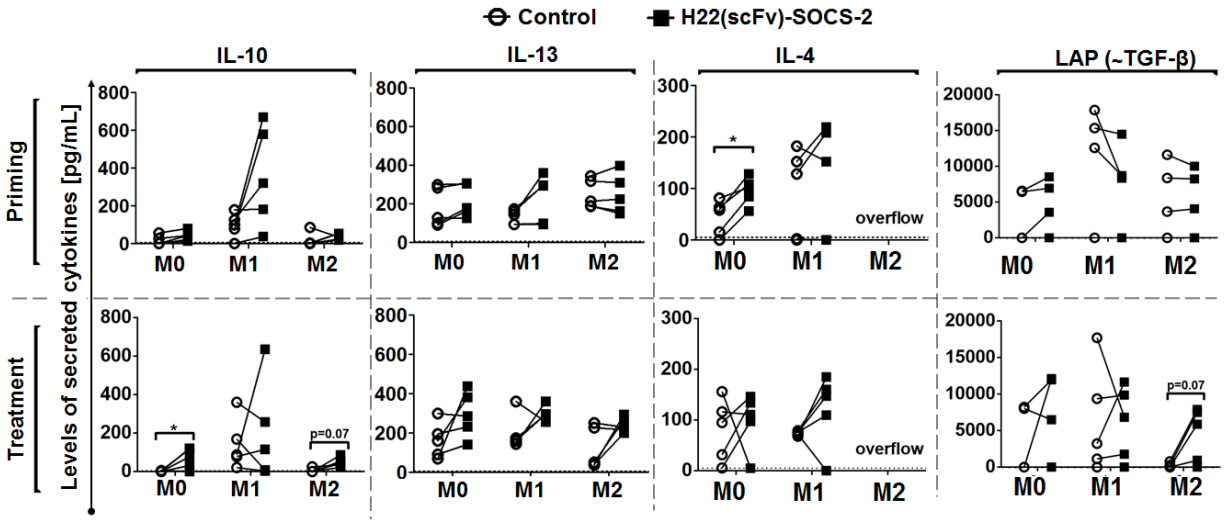

Figure 22: H22(scFv)-SOCS-2 triggers the production of anti-inflammatory cytokines.
PBMC-derived MΦ were either primed or treated with 100 nM H22(scFv)-SOCS-2 for 24 h as described in section II.2.3.4. MΦ supernatants from triplicate samples were merged to yield one point for each measurement. Cytokine levels were measured by Multiplex analysis as described in section II.2.4.1.2. The control group is the PBS vehicle control. Values are presented as symbols connected with and without treatment (n=5 different PBMC donors). Statistical analysis was carried out using the non-parametric Mann-Whitney U test: *p≤0.05. Small dashed lines indicate the detection limit.

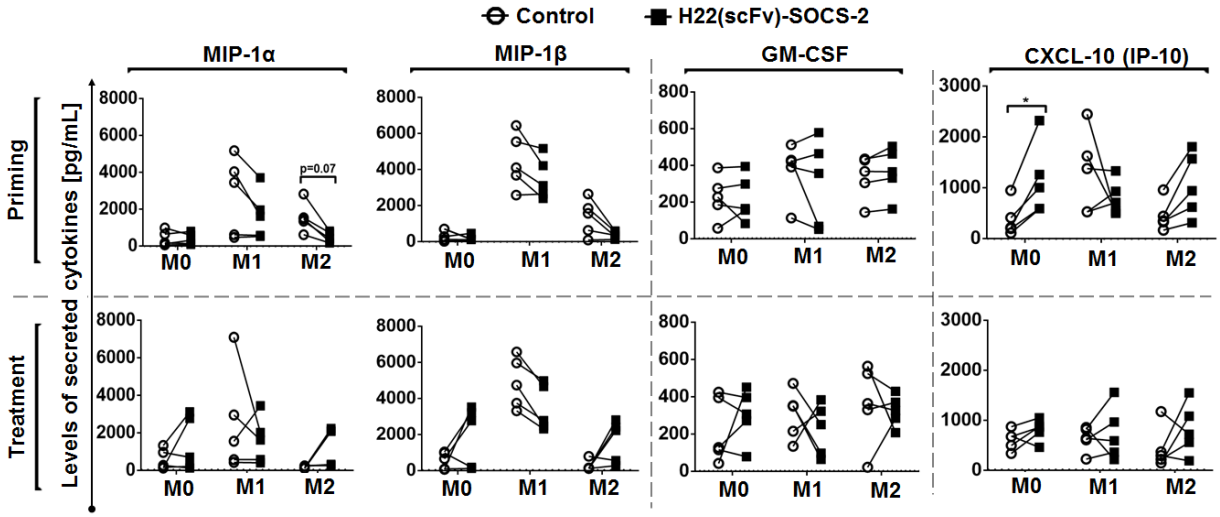

Figure 23: The impact of H22(scFv)-SOCS-2 on the chemokine fraction.
PBMC-derived MΦ were either primed or treated with 100 nM H22(scFv)-SOCS-2 for 24 h as described in section II.2.3.4. MΦ supernatants from triplicate samples were merged to yield one point for each measurement. Cytokine levels were measured by Multiplex analysis as described in section II.2.4.1.23. The control group is the PBS vehicle control. Values are presented as symbols connected with and without treatment (n=5 different PBMC donors). Statistical analysis was carried out using the non-parametric Mann-Whitney U test: *p≤0.05. Small dashed lines indicate the detection limit.

stronger secretion of IL-10, whereas priming M0 cells with H22(scFv)-SOCS-2 significantly induced IL-4. Both IL-13 and TGF-β showed no difference in expression profile when primed or treated with the MIMP. Interestingly, IL-10 levels increased significantly in M0 and M2 cells during the treatment experiment. Because IL-4 was used for M2 polarization, an overflowing signal was detected for M2 cells (**Figure 22**). In addition to the standard panel of pro-inflammatory and anti-inflammatory cytokines, the levels of some important chemokines were determined (e.g. MIP-1α, MIP-1β and CXCL-10), as well as GM-CSF, which is chemotactic for M0 cells but also a growth/proliferation factor. As shown in **Figure 23**, priming with H22(scFv)-SOCS-2 had an impact on both the M1 and M2 populations, resulting in substantially lower levels of MIP-1α and MIP-1β secretion. M0 and M2 cells primed with the MIMP produced more CXCL-10 than the medium control, aligning them to the levels detected in M1 cells. No difference was found in the levels of GM-CSF. In summary, the observed effects on M1 cells were complemented by observations indicating that the $CD64^{low}$ M2 population is slightly sensitive to CD64-targeted immunomodulation, unlike previous experimental observations of ITs *in vitro* and *ex vivo*.

III.2.2.2. H22(scFv)-Trx-1 mediated modulation in MΦ model

Preliminary data concerning the immunomodulatory activity of H22(scFv)-Trx-1 is also provided in the Master's thesis of Tim Stroisch („Generation and Evaluation of H22(scFv)-fused Immunomodulatory Proteins") performed under R. Mladenov´s technical supervision at Prof. R. Fischer´s laboratory and defended in September 2014 at RWTH Aachen University in collaboration with Fraunhofer IME in Aachen. The preliminary findings concerning H22(scFv)-Trx-1 are extended and validated herein through experiments on human MΦ. Recombinant H22(scFv)-Trx-1 was analyzed for its targeted immunomodulatory activity in the same way as H22(scFv)-SOCS-2 above, using the MΦ model as described in section II.2.3.4. To determine the specific activity of the fusion protein, the medium control group was complemented with controls comprising each of the unfused components, i.e. H22(scFv) and the Trx-1 effector domain. CD64-directed targeting with H22(scFv) and H22(scFv)-Trx-1 was confirmed by the loss of CD64 on the cell surface. The Trx-1 effector protein alone had no effect on any of the surface markers. Furthermore, CD64 was expressed in greater amounts on M0 cells than M2 cells, but in both cases much lower than the level detected on M1 cells (**Figure 24).** A similar pattern was observed for CD14. No significant difference in the surface abundance of CD301 and CD206 was observed when MΦ were either primed or treated with the MIMP (**Figure 24**). Neither the Trx-1 nor the H22(scFv) control affected the levels of any

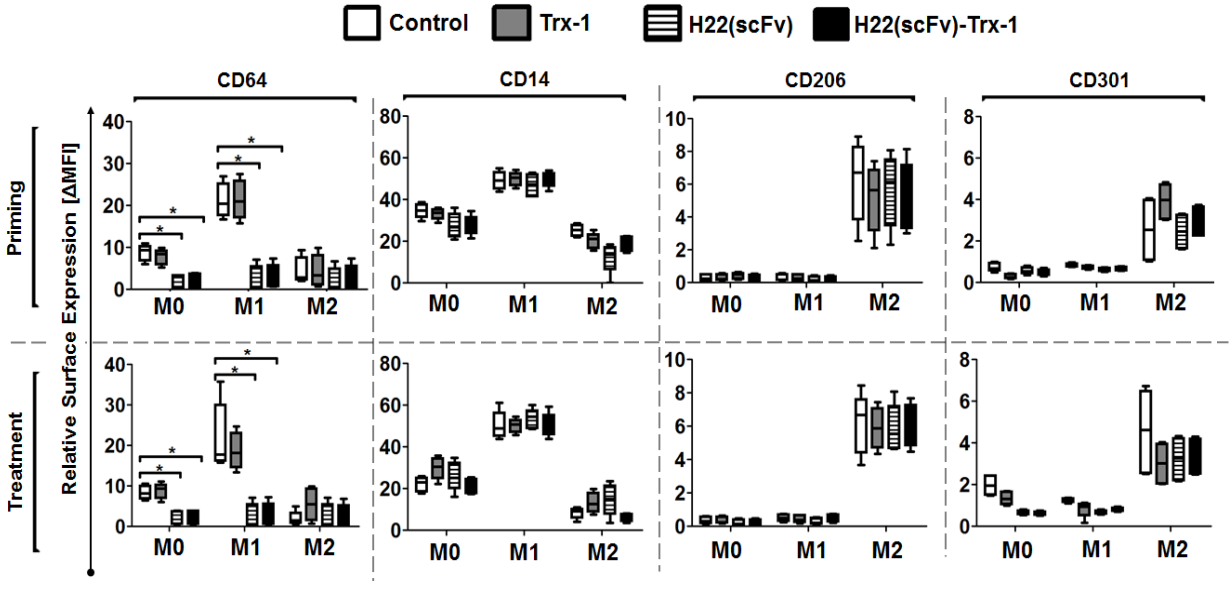

Figure 24: H22(scFv)-Trx-1 and H22(scFv) reduce the abundance of surface CD64.
PBMC-derived MΦ were either primed or treated with 100 nM H22(scFv)-Trx-1, H22(scFv) or Trx-1 for 24 h as described in II.2.3.4. Triplicate samples were merged to yield one point for each measurement. The expression of MΦ surface markers was measured flow cytometry as described in section II.2.4.1.2. The control group is the PBS vehicle control. Values are presented as box and whiskers with interquartile range and min and max values indicated by error bars (n=5 different PBMC donors). Statistical analysis was carried out using the non-parametric Mann-Whitney U test: *p≤0.05. Abbreviations: ΔMFI, delta mean fluorescence intensity.

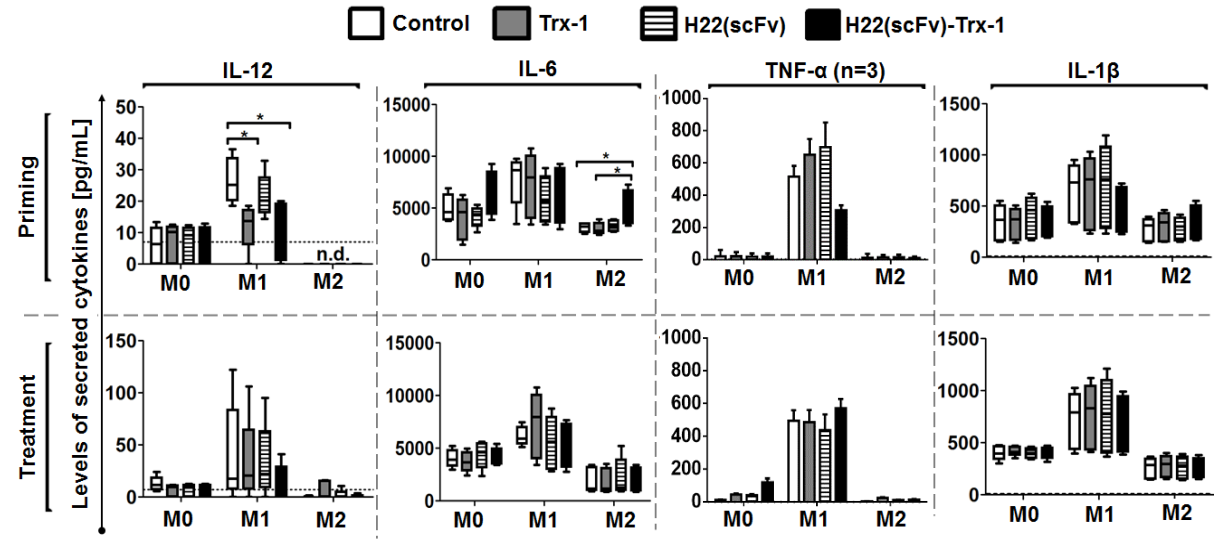

Figure 25: H22(scFv)-Trx-1 effect on pro-inflammatory cytokines
PBMC-derived MΦ were either primed or treated with 100 nM H22(scFv)-Trx-1, H22(scFv) or Trx-1 for 24 h as described in II.2.3.4. MΦ supernatants of triplicates were merged to comprise one point for each measurement. Cytokine levels were obtained using Multiplex analysis according to II.2.4.1.2. Control group represents the PBS vehicle control. Values are presented as box and whiskers with interquartile range and min and max values indicated by error bars (n= 5 different PBMC donors). Values of TNF-α concentration (n=3) are presented as bars with standard deviation (SD). Statistical analysis was carried out using non-parametric Mann-Whitney U test: *p≤0.05. Small dashed lines in figures indicate the detectable limit.

soluble markers, with the exception of IL-12 (**Figures 25** and **Figure** 26). The priming experiment with free Trx-1 and H22(scFv)-Trx-1 resulted in a significant loss of IL-12 in the M1 population. Interestingly, in the same experimental approach, the secretion of IL-6 by M0 and M2 cells was triggered by H22(scFv)-Trx-1, reaching approximately the levels observed in the M1 population. When MΦ were primed with the MIMP before polarization, TNF-α and

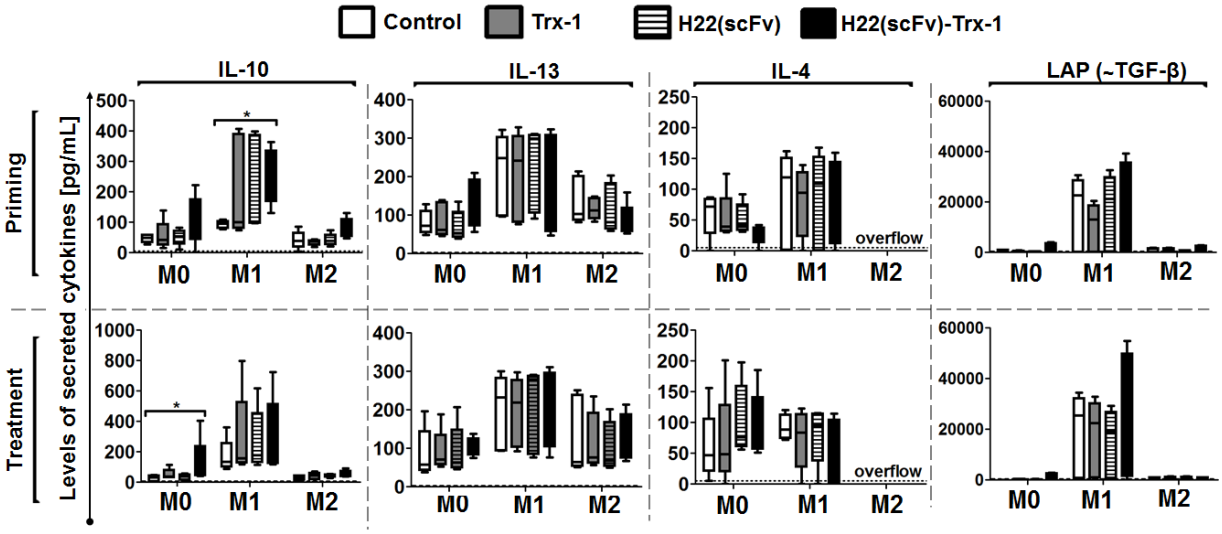

Figure 26: Effects of H22(scFv)-Trx-1 on anti-inflammatory cytokine production.
PBMC-derived MΦ were either primed or treated with 100 nM H22(scFv)-Trx-1, H22(scFv) or Trx-1 for 24 h as described in II.2.3.4 MΦ supernatants of triplicates were merged to comprise one point for each measurement. Cytokine levels were obtained using Multiplex analysis according to II.2.4.1.2. Control group represents the PBS vehicle control. Values are presented as box and whiskers with interquartile range and min and max values indicated by error bars (n= 5 different PBMC donors). Statistical analysis was carried out using non-parametric Mann-Whitney U test: *p≤0.05. Small dashed lines in figures indicate the detectable limit.

IL-1β levels tended to decline in the M1 population. The treatment of polarized MΦ with H22(scFv)-Trx-1 had no significant effect on pro-inflammatory cytokines, but the levels of IL-12 tended to decline in M1 cells. Free H22(scFv) had no significant effect on the production of pro-inflammatory cytokines (**Figure 25**). **Figure 26** depicts the measured levels of anti-inflammatory cytokines. In the priming approach, the levels of secreted IL-10 were significantly higher in M1 cells incubated with H22(scFv)-Trx-1 (2-fold↑). However, this observation could not be confirmed using the treatment approach. In comparison to the controls, M0 cells showed a strong tendency to produce more IL-10 when incubated with H22(scFv)-Trx-1, whereas the levels of IL-4 and IL-13 remained unchanged in both the priming and treatment approaches. Neither the H22(scFv) nor Trx-1 controls affected the levels of anti-inflammatory cytokines. In this experiment, TGF-β levels showed a high standard deviation and no substantial difference was observed. The levels of different chemokines were also investigated (**Figure 27**). H22(scFv)-Trx-1 doubled the levels of MIP-1α and MIP-1β in M0 cells following both the priming and treatment approaches, whereas the free H22(scFv) and Trx-1 controls had no such effect. Interestingly, the induction of both forms of MIP-1α was also observed in the M2 population when primed or treated with H22(scFv)-Trx-1. The controls lacked this effect and the recorded values were in the same range of the PBS control. Immunomodulation did not influence the levels of CXCL-10. The treatment of M1 cells with H22(scFv)-Trx-1 resulted in a significant reduction in the

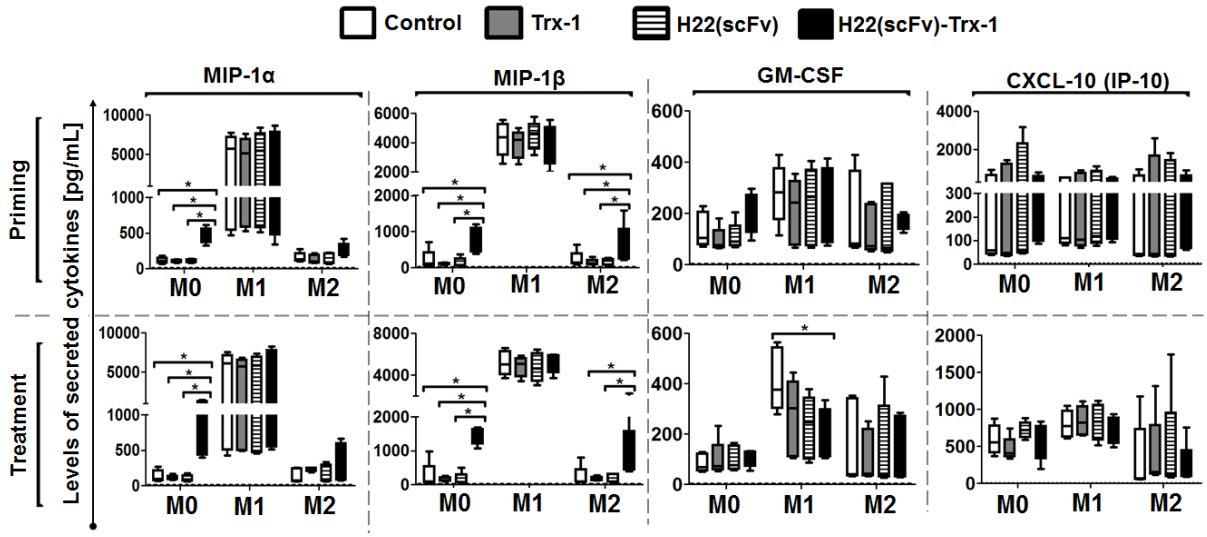

Figure 27: Chemokine levels of H22(scFv)- Trx-1 treated primary human MΦ
PBMC-derived MΦ were either primed or treated with 100 nM H22(scFv)-Trx-1, Trx-1 or H22(scFv) for 24 h as described in II.2.3.4. MΦ supernatants of triplicates were merged to comprise one point for each measurement. Chemokine levels were obtained using Multiplex analysis according to II.2.4.1.2. Control group represents the PBS vehicle control. Values are presented as box and whiskers with interquartile range and min and max values indicated by error bars (n=5 different PBMC donors). Statistical analysis was carried out using non-parametric Mann-Whitney U test: *p≤0.05. Small dashed lines in figures indicate the detectable limit.

concentration of GM-CSF, but only in comparison to the PBS control. This effect was not observed in the priming experiment.

III.2.2.3. Comparison of CD64-directed immunomodulation using both MIMPs

The responses of MΦ treated with different MIMPs yields a complex picture, so a better overview of MIMP-specific immunomodulatory activity was achieved by summarizing the measured cytokines in a table based on their pro/anti-inflammatory or chemotactic properties. The secretion levels were evaluated relative to the appropriate controls, and the corresponding values were plotted as shown in **Figure 28**. Thereby, the summary of the cytokine levels demonstrates the different mode of action of both H22(scFv)-fused proteins towards different MΦ subtypes. H22(scFv)-SOCS-2 had a clear inhibitory effect on the secretion of pro-

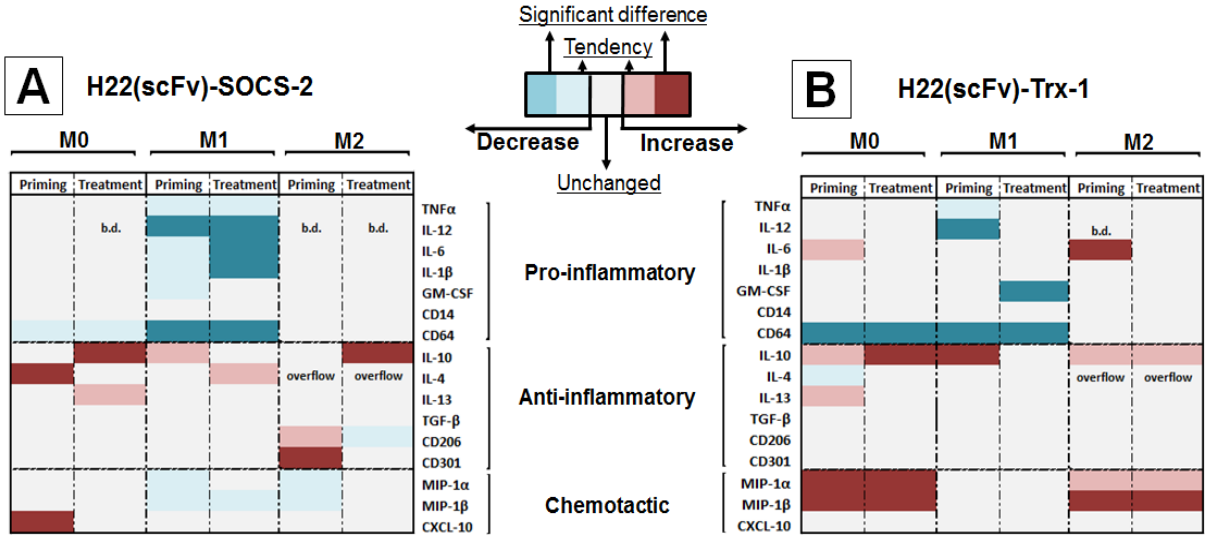

Figure 28: Overview of cytokine profiles upon priming or treatment with both MIMPs
Multiplex analysis of surface receptors and cytokine levels (II.2.4.1.2) of primary MΦ (n=5) treated with 100 nM MIMP. **(A)** Summary of H22(scFv)-SOCS-2 effect. **(B)** Summary of H22(scFv)-Trx-1 effect. A specific effect of both MIMPs is defined by a significant difference in values (dark color) or a tendency (light color) in expression of particular marker in comparison to the appropriate control(s) (n=5). Tendency is interpreted by a non-significant inclination towards an increase or decrease. Cytokines are sorted according to general properties: pro-/anti-inflammatory and chemotaxis.

inflammatory cytokines (e.g. IL-12, IL-6 and TNF-α) in M1 and also a slight induction of IL-10 (**Figure 28A**). This summary of cytokine levels demonstrates the different modes of action of each MIMP towards different MΦ subtypes. H22(scFv)-SOCS-2 clearly inhibited the secretion of pro-inflammatory cytokines in M1 cells (e.g. IL-12, IL-6 and TNF-α), slightly induced the secretion of IL-10, and showed a tendency to reduce the levels of MIP-1α and MIP-1β (**Figure 28A**). The induction of IL-10 by H22(scFv)-SOCS-2 was also detected in M0 and M2 cells. This is a particularly interesting finding because M0 and M2 cells have low CD64 expression profiles. In contrast to H22(scFv)-SOCS-2, H22(scFv)-Trx-1 had much less impact on MΦ when considering the modulation of cytokine profiles. Priming M1 cells with

H22(scFv)-Trx-1 caused significant anti-inflammatory activity (IL-10↑, IL-12↓ and TNF-α↓), but this was absent in the treatment approach (**Figure 28B**). As noted for H22(scFv)-SOCS-2, M0 and M2 cells also responded when incubated with H22(scFv)-Trx-1. Most prominent was the significant upregulation of MIP-1α and MIP-1β, but there was also a tendency for increased levels of IL-10. Overall, H22(scFv)-SOCS-2 provoked stronger cytokine responses than H22(scFv)-Trx-1 in different MΦ populations. However, further analy1sis of the functional properties of immunomodulated MΦ should be carried out.

III.2.2.1. Oxidative stress in MΦ treated *in vitro*

Macrophages produce reactive oxygen species (ROS) such as O_2^-, H_2O_2 and *OH, all of which are critical components of the antimicrobial repertoire of MΦ used to damage and kill pathogens in phagosomes. However, ROS also contribute to the pathogenesis of inflammatory diseases. The commercially available CellROX® Deep Red reagent was used to

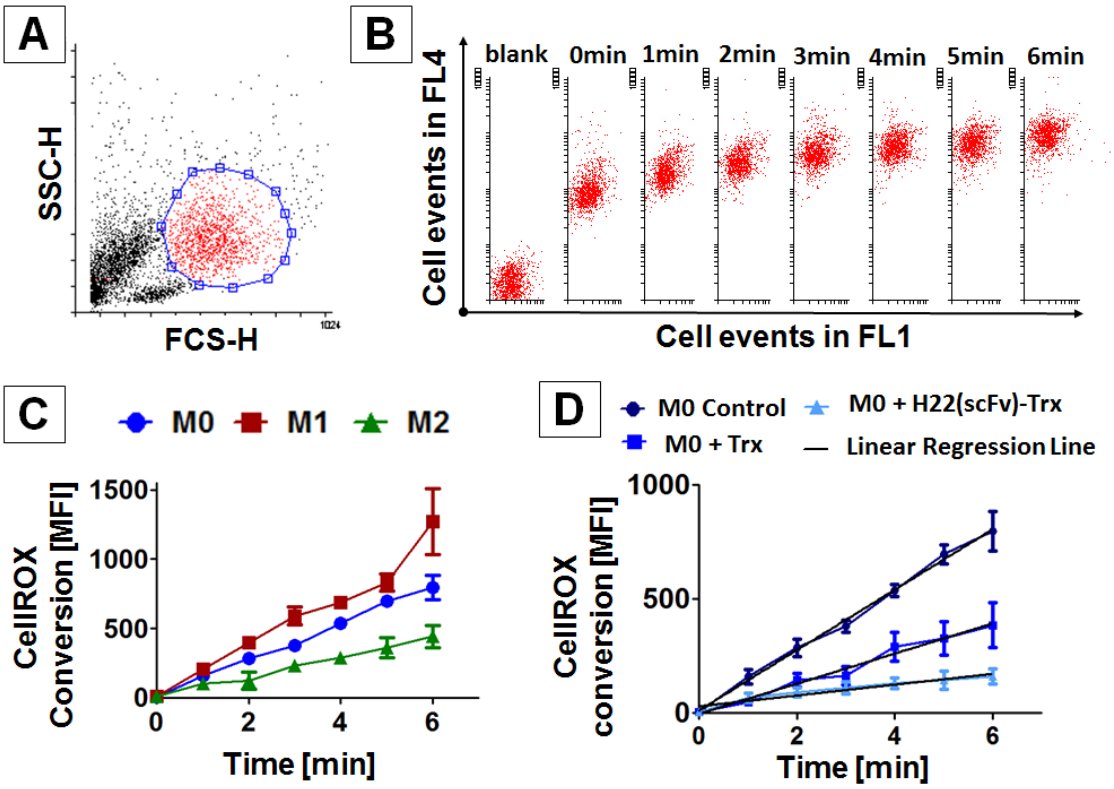

Figure 29: ROS profiles of different MΦ phenotypes.
MΦ were prepared for the analysis of ROS kinetics as described in section II.2.4.2.2. **(A)** The MΦ population was identified and gated for further analysis of ROS activity. **(B)** Gated MΦ convert CellROX® Deep Red reagent over time, which results in a shift in the FL-4H channel. **(C)** MFI values of the conversion kinetics in (B) were plotted against time (n=3 different PBMC donors). **(D)** Estimation of ROS activity in differently treated M0 cells. MΦ were polarized and primed with 100 nM Trx-1 or H22(scFv)-Trx-1 as described in section II.2.3.4. The slope of the linear regression lines was calculated using GraphPad Prism v5 to determine the ROS activity for each approach. Data represent three independent experiments (n=3 different PBMC donors) and values are presented as means ± SD. Abbreviations: SSC, side scatter; FCS, forward scatter; MFI, mean fluorescence intensity.

investigate ROS levels in different MΦ populations, and ultimately to identify changes in ROS profiles following MIMP treatment. The advantage of CellROX® is its suitability for FACS-based analysis, which allows cell populations of interest to be gated for the measurement of intracellular ROS activity. The gating of MΦ populations is shown in **Figure 29A**. ROS kinetics was measured for 6 min until the converted CellROX® reagent reached signal saturation (**Figure 29B**). The conversion was most efficient in the presence of M1 cells followed by M0 and finally M2 (**Figure 29C**). As shown in **Figure 29D**, the ROS activity of MΦ treated with Trx-1 was estimated by the slope of the linear regression lines overlaid on the curves representing CellROX® conversion. This experiment demonstrated the redox ability of free Trx-1 and H22(scFv)-Trx-1. In contrast to the control group of untreated M0 cells, incubation with 100 nM Trx-1 or H22(scFv)-Trx-1 attenuated the ROS activity, and M0 cells treated with H22(scFv)-Trx-1 showed the lowest ROS levels (**Figure 29D**). The CellROX® conversion kinetics of human MΦ under different treatment regiments were measured and

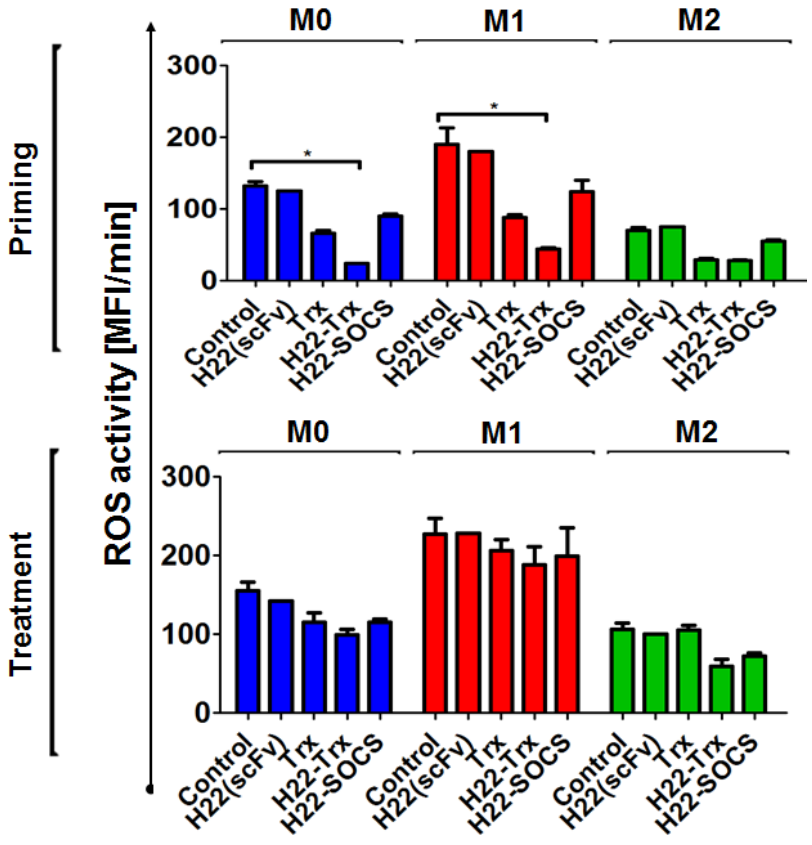

Figure 30: ROS activity of differently treated human MΦ
MΦ were polarized and treated with 100 nM H22(scFv), Trx-1 or H22(scFv)-Trx-1 as described in section II.2.3.4. The control group is the PBS vehicle control. The MΦ population was gated and the kinetics of CellROX® conversion was measured as described in section 0. The slope of the linear regression lines was calculated using GraphPad Prism v5 to determine the ROS activity for each approach. Data represent three independent experiments (n=3 different PBMC donors) with the exception of MΦ treated with H22(scFv) (n=1 PBMC donors). Values are presented as means ± SD. Statistical analysis was carried out using the non-parametric Mann-Whitney U test: *p≤0.05. Abbreviations: MFI, mean fluorescence intensity.

used to estimate ROS activity. This experiment demonstrated the dominance of M1 cells in terms of ROS production, achieving the highest activity among the three MΦ phenotypes. Non-polarized M0 cells showed lower ROS activity than M1 cells, but were more active than M2 cells (**Figure 30, controls)**. In a single experiment (n=1), the H22(scFv) control showed no effect on ROS activity in any of the MΦ phenotypes in either priming or treatment approaches. As shown in **Figure 29D**, Trx-1 and H22(scFv)-Trx-1 significantly reduced CellROX® conversion in M0 and M1 cells, which translated to reduced ROS activity. A similar tendency was observed in M2 cells. Interestingly, this effect was strongest in the priming approach. Whenever already polarized MΦ were treated with Trx-1 or H22(scFv)-Trx-1, the ROS activity tended to be slightly lower for M0 cells and unchanged for M1 and M2 cells. Furthermore, although not statistically significant, H22(scFv)-Trx-1 showed a tendency to attenuate ROS activity more strongly in M0 and M1 cells than the free Trx-1 control, which supports the conclusion that H22(scFv)-Trx-1 achieves more efficient targeting and intracellular distribution. H22(scFv)-SOCS-2 also showed a tendency towards reduced ROS activity in primed M0 and M1 cells, but failed to inhibit ROS activity to the degree achieved by H22(scFv)-Trx-1.

III.2.2.2. Phagocytic activity of immunomodulated MΦ

Phagocytosis is one of the key features of MΦ and there are two general types: antibody-dependent and antibody-independent. The immunomodulation strategy described herein targets CD64, one of the Fc receptors most strongly involved in antibody-dependent phagocytosis, and thus clearly blocks its functions. Therefore, the effect of immunomodulation on phagocytosis was evaluated using 2-µm fluo-green silica beads (Kisker Biotech), which are engulfed by MΦ in an antibody-independent manner. The MΦ population was gated (**Figure 31A**) and the frequency of phagocytosis determined by end-point measurement after 5 min, which represents the number of fluorescent MΦ (**Figure 31B**). Preliminary data (n=3 PBMC donors) demonstrated no significant difference in antibody-independent phagocytosis among the different regimens. In the priming approach, phagocytosis measurements in the control group, Trx-1, H22(scFv)-Trx-1 and H22(scFv)-SOCS-2 regimens were in the range 35–40% for all MΦ phenotypes (**Figure 31C**). However, in the treatment approach, there was a tendency towards slightly more frequent phagocytosis in M1 and M2 cells compared to M0, but no effect caused by the MIMP itself (**Figure 31D**). The clear effect of priming with MIMPs before MΦ polarization versus the treatment of polarized MΦ with MIMPs seen in earlier experiments based on ROS activity and cytokine levels were not observed in the antibody-independent phagocytosis assay.

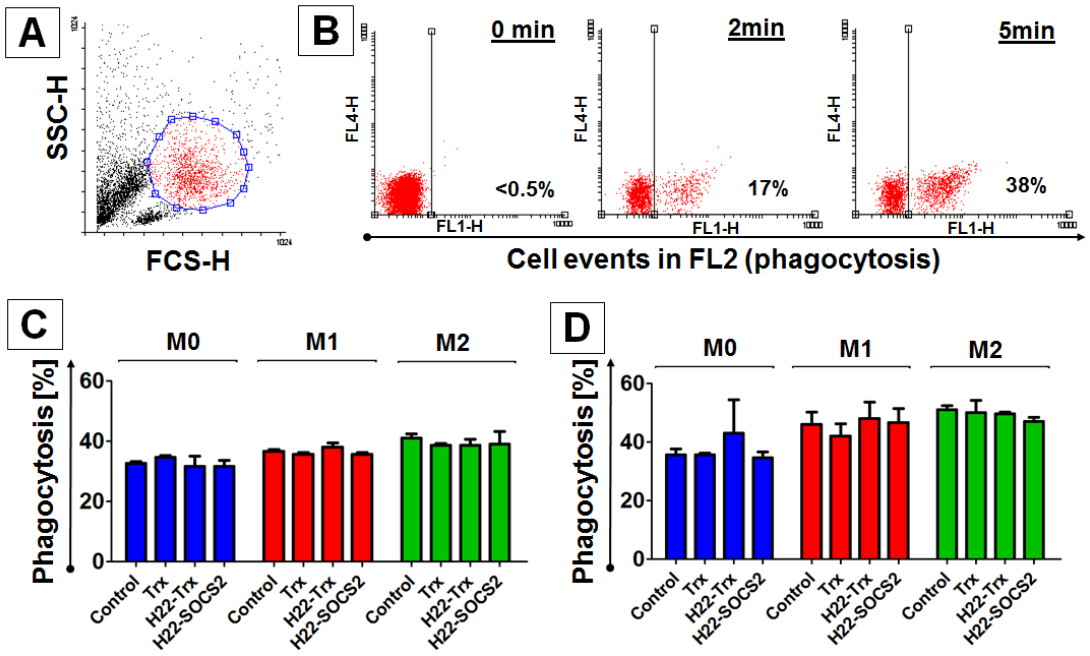

Figure 31: Phagocytosis profile of different MΦ phenotypes.
MΦ were prepared for the assessment of phagocytosis levels as described in section II.2.4.2.1. **(A)** The MΦ population was identified and gated for further analysis. **(B)** Gated MΦ (M0) take up fluo-green silica beads by phagocytosis over time, causing a shift in the FL-1H channel. **(C)** Percentage of green fluorescent human MΦ **primed** with Trx-1, H22(scFv)-Trx-1 or H22(scFv)-SOCS-2 after 5 min of phagocytosis. **(D)** Percentage of green fluorescent human MΦ **treated** with Trx-1, H22(scFv)-Trx-1 or H22(scFv)-SOCS-2 after 5 min of phagocytosis. Data represent three independent experiments (n=3 different PBMC donors) and values are presented as means ± SD. Abbreviations: SSC, side scatter; FCS, forward scatter.

III.2.2.3. Immunomodulation of human MΦ exposed to chronic inflammation

The *in vitro* immunomodulation of MΦ under chronic inflammatory conditions was achieved by incubating PBMC-derived MΦ from healthy donors with sterile exudate material from CDWs. To achieve a better comparison, the final dose of IFN-γ was adjusted to 200 U/mL in all exudates. MΦ representing different healthy donors responded similarly towards CDW exudates, i.e. there was a strong induction of surface CD64 expression combined with the slight upregulation of CD14. In line with previous observations, priming or treatment with H22(scFv)-SOCS-2 and H22(scFv)-Trx-1 reduced the levels of surface CD64, confirming the efficient targeting of the receptor. Although both MIMPs reduced the abundance of CD64, only H22(scFv)-SOCS-2 caused the slight induction of CD14 (**Figure 32A**). CD206 was weakly upregulated in response to the exudates, whereas CD301 surface expression was unaffected (**Figure 32B**). Unlike Trx-1, the SOCS-2 priming approach slightly induced

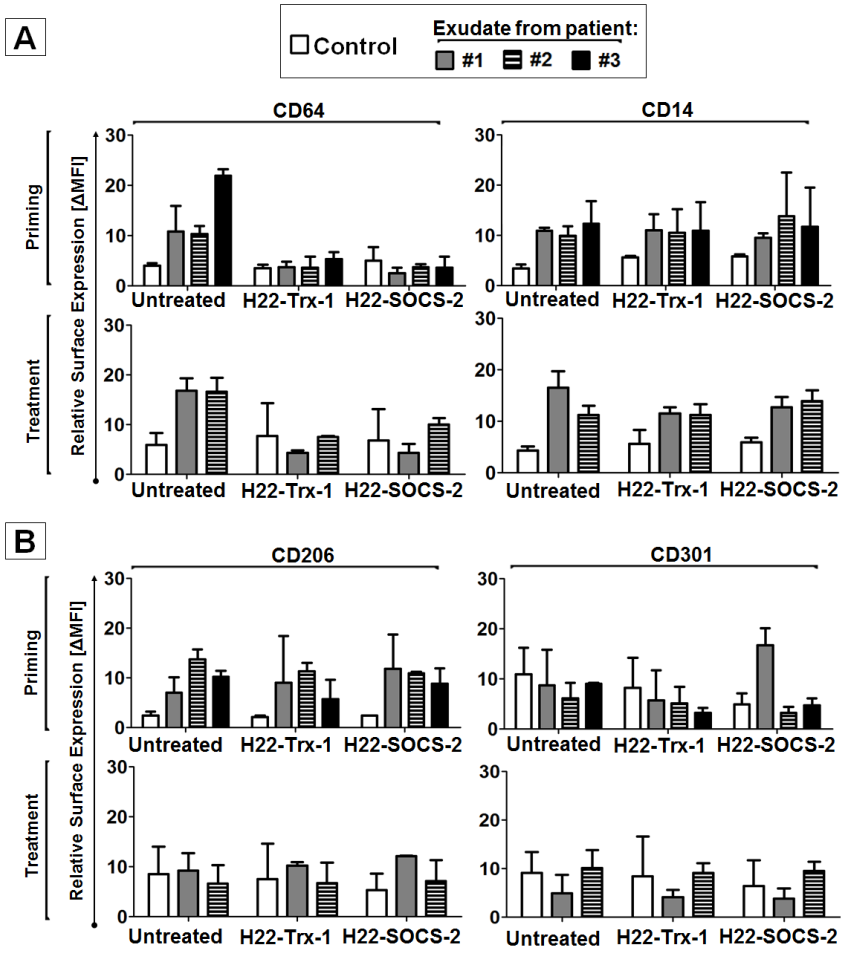

Figure 32: CDW exudates induce CD64, CD14 and CD206 on MΦ.
Flow cytometry (II.2.4.1.2) was used to analyze surface markers on PBMC-derived MΦ incubated with 100 nM of H22(scFv)-SOCS-2 or H22(scFv)-Trx-1 as described in section II.2.3.4.2. **(A)** Levels of the M1-associated surface markers CD14 and CD64. **(B)** Levels of the M2-associated surface markers CD301 and CD206. The control group is the PBS vehicle control. Priming approach: n=3 exudates. Treatment approach: n=2 exudates due to limited availability. The values represent the normalized fold expression related to treated MΦ without exudates (mean ± SD of n=2 PBMC donors). Abbreviations: ΔMFI, delta mean fluorescence intensity.

CD206 expression, which was not the case in the treatment approach, whereas surface CD301 levels remained unchanged in response to both the priming and treatment approaches. To evaluate the humoral effect of the immunomodulatory treatment, the cytokine fraction was investigated as described above. The cytokine levels in the exudate-polarized MΦ were related to the levels of the corresponding MΦ controls incubated with medium only, following priming or treatment with MIMPs. The exudate-polarized MΦ showed a tendency towards increased levels of all pro- inflammatory cytokines, which were then assigned an arbitrary level of 1 (**Figure 33A**, **control groups – white columns**). Most prominent was the induction of IL-6 by 60–100-fold and the induction of TNF-α and IL-1β by 30-fold. The production of IL-12 increased almost 3-fold (**Figure 33A, priming**). Priming with H22(scFv)-Trx-1 or H22(scFv)-SOCS-2 tended to have the strongest protective effect on MΦ polarization under

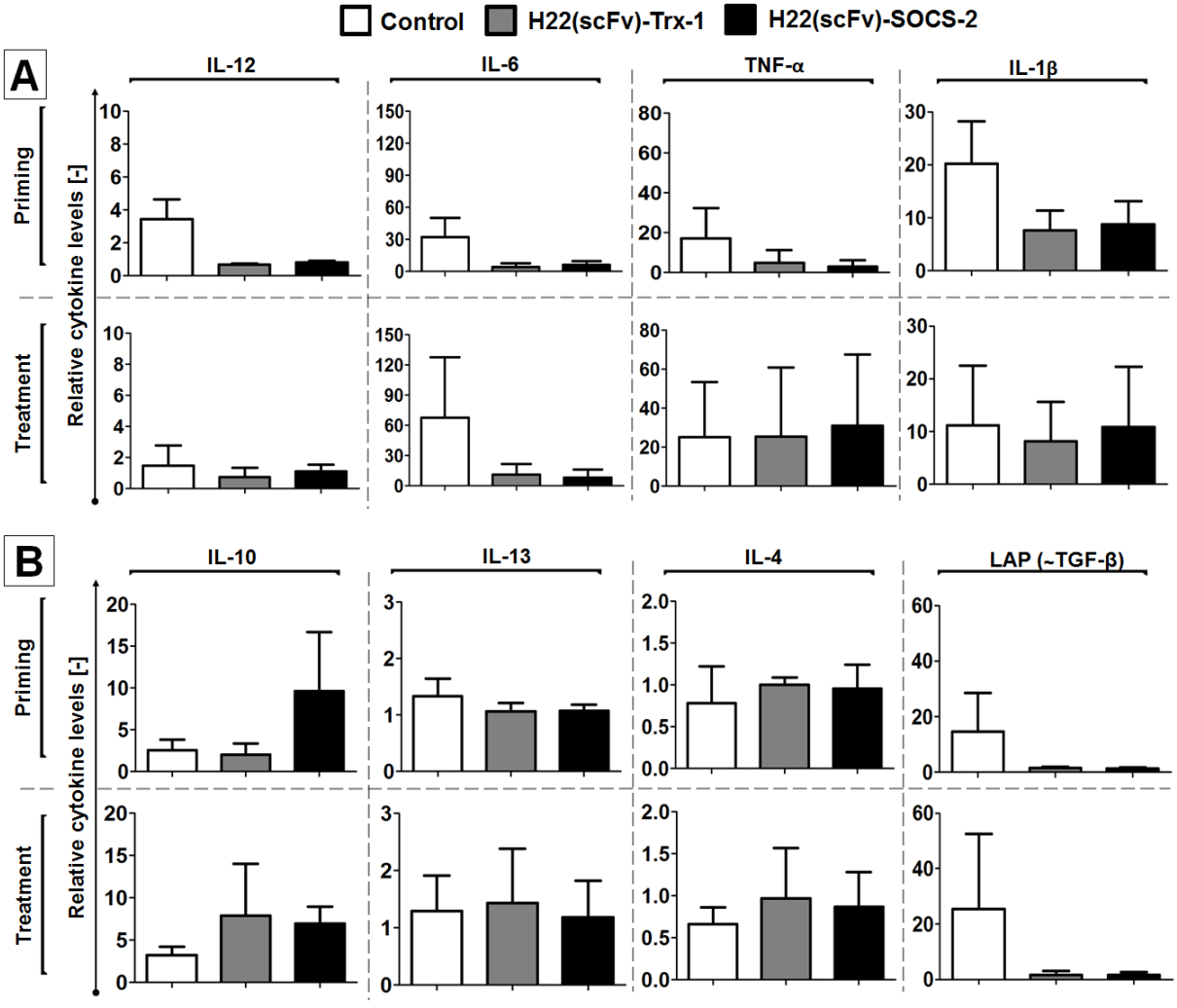

Figure 33: Priming with both MIMPs inhibits M1 cytokines.
Multiplex analysis of cytokine levels (II.2.4.1.2) in primary MΦ treated with 100 nM of H22(scFv)-Trx-1 or H22(scFv)-SOCS-2 as described in section II.2.3.4.2. The levels of pro-inflammatory **(A)** and anti-inflammatory cytokines **(B)** are presented relative to untreated (resting) MΦ (medium only) set arbitrarily to 1.0. The control group is the PBS vehicle group. Priming approach: n=3 exudates. Treatment approach: n=2 exudates due to limited availability. The presented values are relative to treated MΦ without exudates (mean ± SD of n=2 PBMC donors).

chronic inflammatory conditions. The recombinant MIMPs blocked the production of IL-6, TNF-α, IL-1β and IL-12 by at least 50% compared to the control group. Interestingly, once the MΦ developed their pro-inflammatory phenotype under the stimuli present in the cytokine cocktail of exudates, treatment with MIMPs appeared unable to reverse or attenuate the MΦ phenotype (**Figure 33A, treatment**). However, whereas the levels of IL-13 and IL-4 remained unaffected during priming or treatment, secretion of the anti-inflammatory cytokine IL-10 was induced by H22(scFv)-SOCS-2 in both approaches (**Figure 33B**). In contrast, H22(scFv)-Trx-1 did not substantially induce IL-10. TGF-β secretion was suppressed when priming MΦ with both MIMPs, but this was not the case in the treatment approach. The chemokine response to CDW exudates was also investigated, revealing that all measured chemokines were induced compared to the resting MΦ. In line with previous observations, MΦ priming with both MIMPs reduced the levels of MIP-1α, MIP-1β and GM-CSF by 50% (**Figure 34**). Interestingly, when MΦ were primed with H22(scFv)-Trx-1, the level of CXCL-10 declined sharply compared to control MΦ and those primed with H22(scFv)-SOCS-2.

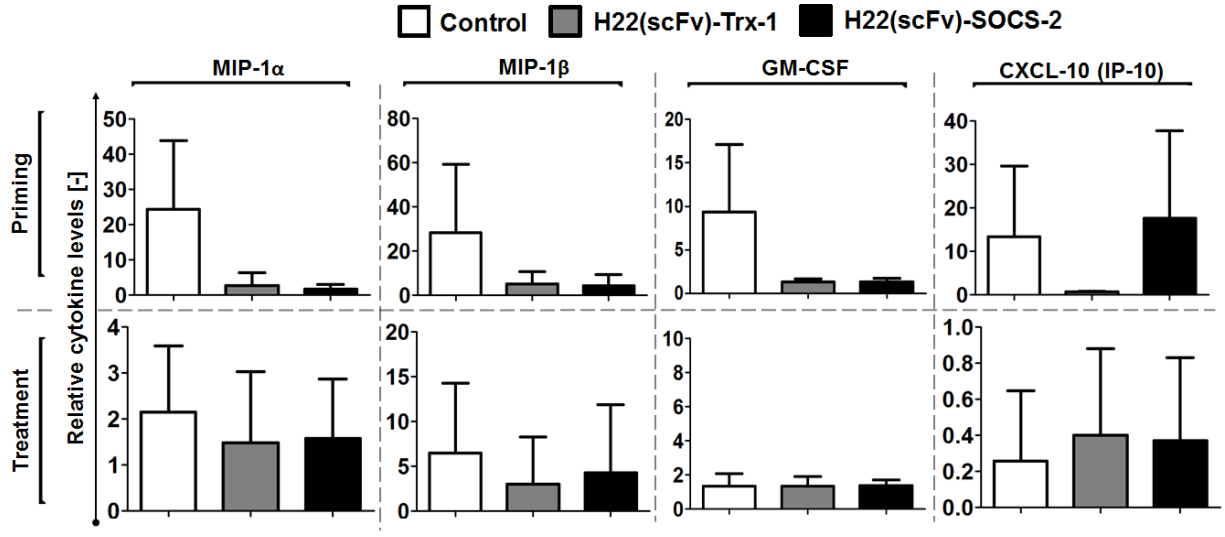

Figure 34: Priming with MIMPs reduces the release of chemokines
Multiplex analysis of cytokine levels (II.2.4.1.2) in primary MΦ treated with 100 nM of H22(scFv)-Trx-1 or H22(scFv)-SOCS-2 as described in section II.2.3.4.2. The fraction of chemokines related to untreated control MΦ with the chemokine level arbitrarily set to 1.0. The control group represents the PBS vehicle control. Priming approach: n=3 exudates. Treatment approach: n=2 exudates due to limited availability. The values are presented relative to treated MΦ without exudates (mean ± SD of n=2 PBMC donors).

III.3. FcαRI (CD89) directed targeting of MΦ

The last part of this work considers the suitability of FcαRI as an alternative target antigen for direct MΦ immunotherapy. The FcγRI-targeting component H22(scFv) was therefore replaced with the FcαRI-targeting component CD89(scFv), derived from the full size mAb clone A77 [157]. The resulting CD89(scFv)-ETA' construct was expressed as a recombinant protein in *E. coli* and evaluated *in vitro* for its cytotoxicity towards human primary MΦ and differently-conditioned MΦ derived from cultivated cell lines.

III.3.1. Confirmation of CD89 expression on human MΦ

The expression of CD89 and CD64 was compared using the Qifikit® showing that both receptors were clearly present in sufficient amounts on human PBMC-derived MΦ. M1 cells tended to express more CD89 molecules than M2 cells, i.e. ~60,000 vs ~45,000 (**Figure 35**). The density of CD89 on M1 cells was ~50% that of CD64 (>130,000). M2 cells expressed fewer copies of both Fc receptors, i.e. ~65,000 copies of CD64 and ~45,000 of CD89. In addition, the receptor density was determined on cultured myeloid monocytic cells (HL-60, THP-1, MonoMac-1 and U937) and these data have been published [158].

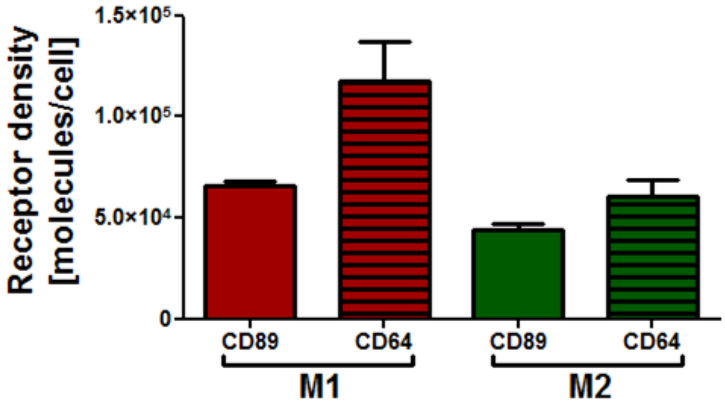

Figure 35: CD89 and CD64 expression on polarized MΦ. PBMCs were polarized to either the M1 or M2 phenotype as described in section II.2.3.4.1 and stained with PE-labeled detection antibodies in PBS with 1% (v/v) blocking human serum. The receptor density was determined using the Qifikit® according to the manufacturer's protocol. Flow cytometry was carried out using antibodies specific for CD64 or CD89 (**Table 3**), and a PE-labeled goat anti-mouse IgG1 mAb was used as an isotype control. The values represent the mean ± SD of n=3 blood donors.

III.3.2. Production and characterization of CD89(scFv) fusion proteins

Having determined the CD89 expression profile in differently-polarized MΦ, a CD89-specific IT was generated by combining the CD89-specific scFv [157] with ETA'. The recombinant IT was expressed in bacteria and purified by affinity chromatography targeting the His_{10} tag. A yield of 3 mg/L culture supernatant was achieved with >90% purity as determined by SDS-PAGE followed by staining with Coomassie Brilliant Blue G250. The identity of the recombinant protein was confirmed by western blot using an ETA'-specific

mAb. Under denaturing conditions, SDS-PAGE revealed a band with the expected molecular weight of approximately 70 kDa (**Figure 36A**). For the subsequent internalization assays, Stefan Zwirner and Lea Schenke (Fraunhofer IME) kindly provided a CD89(scFv)-SNAP protein, which was efficiently coupled to the BG-Vista® Green fluorophore (**Figure 36A, lanes 3 and 4**). The ability of purified CD89(scFv)-ETA' to bind target cells was tested by flow cytometry. In the initial *in vitro* experiments, the human CD89^{+} AML M2 cell line HL-60 was tested, with the CD89^{-} Burkitt lymphoma cell line Ramos as a control. This confirmed the specific binding of CD89(scFv)-ETA' to HL-60 cells, with the highest binding activity observed when the cells were stimulated with TNF-α (**Figure 36D**). CD89(scFv)-ETA' also bound to the differently-conditioned MΦ (M0, M1 and M2) (**Figure 36C**). Efficient CD89-specific internalization into HL60 cells was demonstrated using CD89(scFv)-SNAP-BG-Vista® Green, revealing the intracellular accumulation of the labeled protein after incubation for 30 min at 37°C. As expected, no internalization was detected at 4°C. Neither binding nor internalization was observed when testing the CD89^{-} Ramos cells (**Figure 36B**).

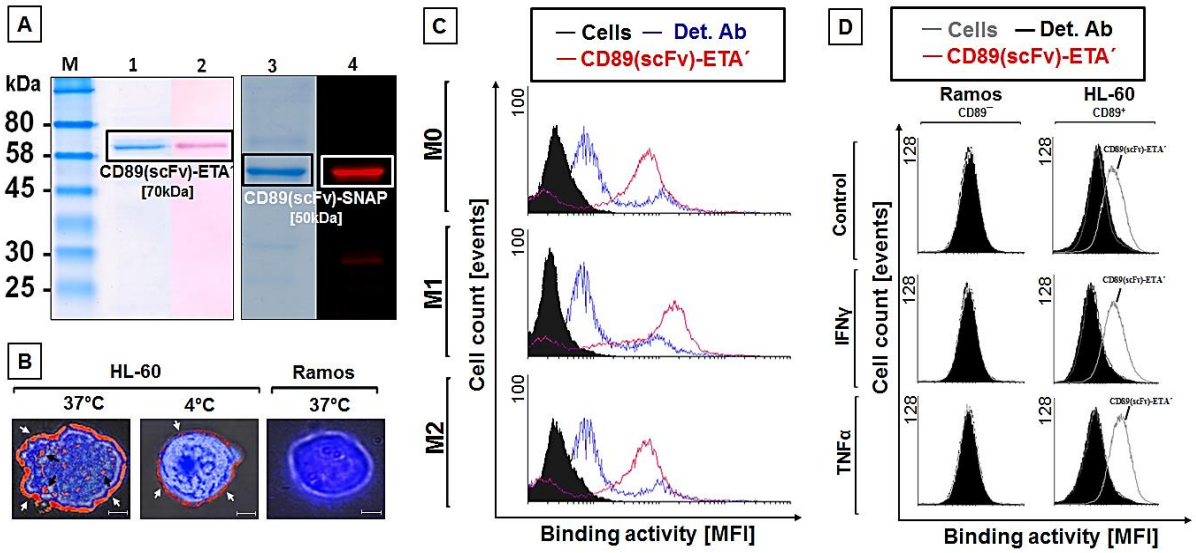

Figure 36: Generation and characterization of CD89(scFv)- ETA'
(A) CD89(scFv)-ETA' was eluted from a Ni/NTA matrix followed by SEC and buffer exchange to PBS (II.2.2). Lane 1 shows an SDS-PAGE gel stained with Coomassie Brilliant Blue G250. Lane 2 shows the corresponding western blot probed with a mouse anti-ETA' primary mAb (TC1) and an AP-conjugated goat anti-mouse secondary mAb. Purified CD89(scFv)-SNAP (lane 3) was coupled to BG-Vista® Green and the coupling efficiency was verified by SDS-PAGE (lane 4, red band). **(B)** Confocal microscopy of stimulated HL-60 cells (1000 U/mL TNF-α) following incubation with 50 nM CD89(scFv)-SNAP-BG-Vista® Green at 37°C and 4°C. CD89^{-} Ramos cells were used as a negative control. Internalization was analyzed after 30 min incubation. Nucleus was counterstained with DAPI. White and black arrows indicate surface binding and internalization, respectively. Bar = 1 µm. **(C)** Specific binding of the IT to non-polarized MΦ (M0), M1 and M2 demonstrated by flow cytometry using an Alexa488-coupled mouse anti-polyhistidine mAb. Black, background fluorescence of the cells; red, CD89(scFv)-ETA' and blue, detection mAb. The data are representative of three repetitions. **(D)** Specific binding of the IT to unstimulated CD89^{+} HL-60 and CD89^{-} Ramos cells, and the same cells stimulated with 100 U/mL IFN-γ or 1000 U/mL TNF-α, analyzed by flow cytometry with an Alexa488 coupled mouse anti-polyhistidine mAb as described in section (II.2.4.1.1). Black, background fluorescence of the cells; gray, CD89(scFv)-ETA' and detection mAb. The data are representative of three repetitions. Abbreviations: MFI, mean fluorescence intensity.

III.3.3. Toxicity of CD89(scFv)-ETA'

Cytotoxic effector proteins should preferably induce apoptosis rather than necrosis or pyroptosis because the former does not cause undesirable inflammatory responses.

III.3.3.1. CD89-directed toxicity towards MΦ derived from cultures cell lines

The ability of CD89(scFv)-ETA' to induce apoptosis in promonocytic cell lines was tested by double staining with Annexin V and PI after treatment for 72 h. Accordingly, CD89(scFv)-ETA' triggered apoptosis in HL-60 cells regardless of the presence or nature of stimulation but did not affect CD89⁻ Ramos cells (**Figure 37A and B**). Quantitative experiments confirmed a dose-dependent relationship, i.e. greater concentrations of CD89(scFv)-ETA' incrementally increased the efficacy of apoptosis in HL-60 cells regardless of the presence or nature of stimulation (**Figure 37B**). The cytotoxic activity of CD89(scFv)-ETA' was similar to that previously described for H22(scFv)-ETA' under comparable conditions [159]. The EC_{50} value of CD89(scFv)-ETA' towards HL-60 cells was stimulus-dependent: it was higher than 1 µM in the absence of stimuli, i.e. only medium, ~0.2 nM in the presence of 100 U/mL IFN-γ, and ~3 nM in the presence of 1000 U/mL TNF-α (**Figure 37C**). The rate of IT-mediated cell death in other promonocytic cell lines was also investigated (THP-1, Mono-Mac-1 and U937) (**Figure 38A**). THP-1 and Mono-Mac-1 cells showed

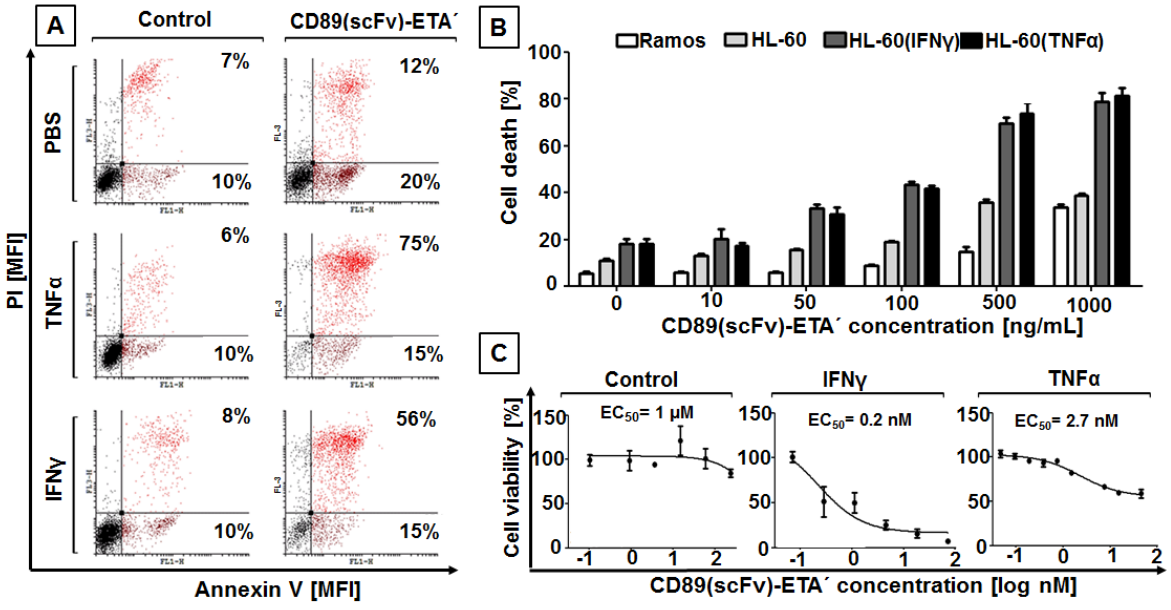

Figure 37: Cytotoxicity of CD89(scFv)-ETA' towards HL-60 cells.
Cytotoxicity assays (II.2.4.1.4 and II.2.4.1.5) were carried out by incubating CD89(scFv)-ETA' with unstimulated HL-60 cells or the same cells stimulated with 100 U/mL IFN-γ or 1000 U/mL TNF-α. **(A)** Dot blots of Annexin V/PI stained HL-60 cells after incubation with either PBS as a control or 15 nM (~1 µg/mL) CD89(scFv)-ETA'. **(B)** Quantitative analysis of dot blots representing death cells in response to increasing IT concentrations. Cell death is shown as the sum of early and late apoptotic/necrotic cells measured by Annexin V/PI staining. **(C)** Cytotoxicity of CD89(scFv)-ETA' towards differently-conditioned HL-60 cells determined using an XTT assay. Data represent mean values of one measurement with SD of triplicates. Abbreviations: MFI, mean fluorescence intensity; nM, nanomolar.

similar responses to CD89(scFv)-ETA' whereas U937 cells showed a minimal response. Antigen-dependent CD89(scFv)-ETA' cytotoxicity was confirmed using a competition assay on TNF-α-stimulated HL-60 cells. A clear reduction in cytotoxicity was demonstrated in the presence of a 50-fold molar excess of the competing CD89(scFv) fused to the non-toxic SNAP protein [160]. Neither CD89(scFv) nor H22(scFv) fused to non-toxic SNAP showed evidence of cytotoxicity against these cell lines (**Figure 38B**).

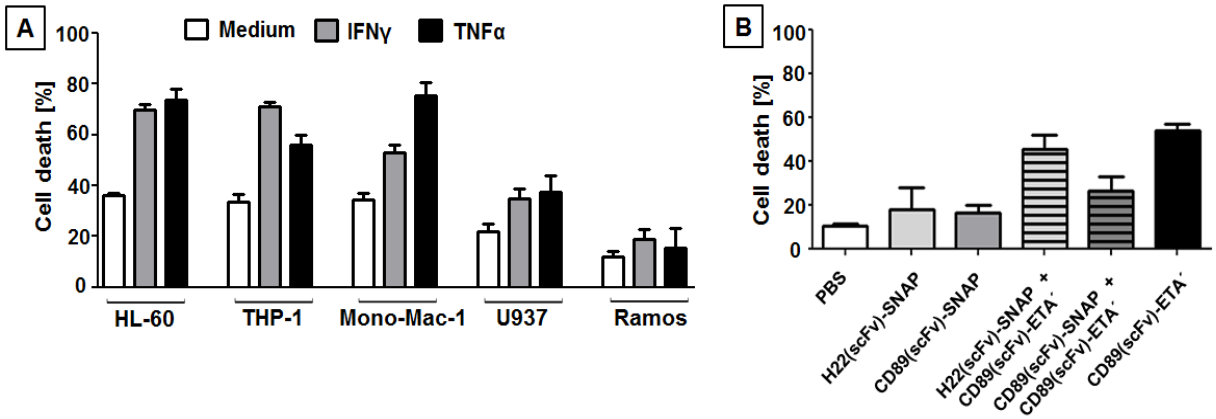

Figure 38: The cytotoxicity of CD89(scFv)-ETA' is antigen-specific.
Cell death is shown as the sum of early and late apoptotic/necrotic cells measured by Annexin V/PI staining as described in section (II.2.4.1.5). (A) An apoptosis assay was carried out using 10 nM (~700 ng/mLl) CD89(scFv)-ETA' to treat unstimulated cancer cells and the same cells stimulated with 100 U/mLl IFN-γ or 1000 U/mLl TNF-α. The number of dead cells was determined after 72 h of exposure to the IT. (B) Induction of apoptosis by 10 nM CD89(scFv)-ETA' in TNF-α-stimulated HL-60 cells (1000 U/mlmL) was only blocked by the addition of a 50-fold molar excess of CD89(scFv)-SNAP and not with the control H22(scFv)-SNAP. Data represent mean values of one experiment with SD of triplicates.

III.3.3.2. CD89-directed toxicity towards primary MΦ

Having determined the mode of killing and cytotoxicity ranges for monocytic cell lines, the potency of CD89(scFv)-ETA' was tested against human PBMC-derived MΦ. In addition to the XTT assay, which was used to detect changes in metabolism and proliferation, the exact proportion of pro-apoptotic cells was determined by Annexin V/PI staining. Whereas the viability of M1 and M2 cells decreased slightly at high IT concentrations (>300 nM), the viability of M0 cells was affected in the presence of 100 nM CD89(scFv)-ETA' (**Figure 39A**). However, the recombinant IT showed a minor dose-dependent cytotoxic effect towards M1 and M2 cells. To determine the exact proportion of pro-apoptotic cells, primary MΦ acquiring

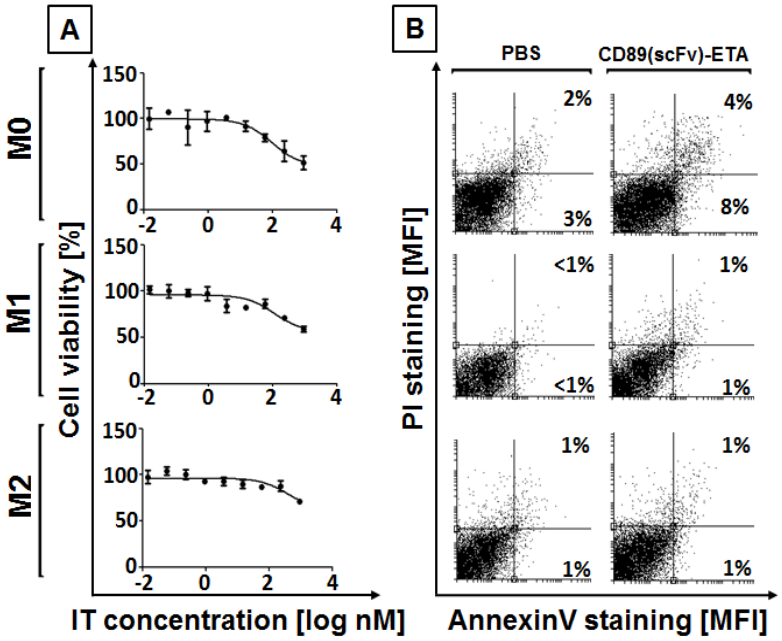

Figure 39: Primary human MΦ are resistant to CD89(scFv)-ETA′
(A) Cytotoxicity of CD89(scFv)-ETA' towards differently-polarized MΦ determined using an XTT assay as described in section (II.2.4.1.4). Values are normalized to the untreated vehicle control (100% viability) and Zeocin-treated control (0% viability). **(B)** Representative dot plots of Annexin V/PI staining in differently-polarized MΦ after 24 h incubation with either PBS as the vehicle control or 100 nM (~7 µg/mL) CD89(scFv)-ETA'. The percentage of early and late apoptotic/necrotic cells measured by Annexin V/PI staining is indicated. In each case, the data represent mean values with SD of triplicates and the experiment was carried out twice. Abbreviations: MFI, mean fluorescence intensity, nM, nanomolar

different phenotypes were treated with 100 nM CD89(scFv)-ETA' for 24 h followed by Annexin V/PI double staining (**Figure 39B**). In agreement with the viability assays, the M1 and M2 populations were completely resistant to the CD89-specific IT. However, a slightly greater proportion (~12%) of M0 cells were susceptible to the IT treatment compared to the PBS vehicle control (**Figure 39B**), supporting the XTT assay data. Taken together, CD89(scFv)-ETA' does not appear to be toxic towards human MΦ, which is beneficial for therapeutic interventions targeting other $CD89^+$ subsets of immune cells associated with different types of pathogenesis (e.g. leukemia or neutrophilia).

IV Discussion

Chronic inflammatory diseases have increasing abundance in modern society and cause an exacerbation in the health care system worldwide. Recent studies attribute the imbalance in MΦ populations to induce and augment the pathology of chronic inflammatory diseases. In general, MΦ are able to adapt to micro-environmental changes and to acquire distinct phenotypes coined M1 (pro-inflammatory) and M2 (anti-inflammatory). The M1 contribute to onset of inflammation, whereas the M2 orchestrate resolution and repair, whereby failure to switch from predominantly M1 to M2 reinforces a pro-inflammatory environment and chronic inflammation. The aim of this doctoral thesis is to investigate a new approach for therapeutic intervention in M1-dominated chronic inflammation. First, the plasticity and heterogeneity of MΦ population was studied *in vitro* and *ex vivo* on skin biopsies from patients with atopic dermatitis or chronic diabetic wounds. Having determined the enormous MΦ plasticity, these findings are here translated into a novel therapeutic concept - the CD64-directed immunomodulation. Therefore, new constructs composed of H22(scFv) and an effector molecule (Trx-1 or SOCS-2) were developed and characterized *in vitro*. Moreover, to expand the arsenal of MΦ targeting moieties, this work also investigated the CD89 expression profile on polarized MΦ and its suitability for direct immunotherapy.

IV.1. Heterogeneity of MΦ and their contribution to IMIDs

IMIDs are defined by middle- to long-term inflammatory processes directed at a particular antigen. Thus, there is a considerable overlap with autoimmune inflammatory conditions such as MS and type 1 diabetes (T1D). However, the definition of IMIDs can also be extended to cover a range of other conditions that are not classified as ‘autoimmune’ but rather as chronic inflammatory diseases, such as inflammatory bowel disease (IBD), chronic diabetic wounds (CDWs), idiopathic pulmonary fibrosis, atherosclerosis, etc. [161]. Typically for IMIDs, the immune system undergoes an excessive activation involving the cellular and the humoral part. As major part thereof, MO and MΦ are involved in the inappropriate immunological response and contribute to the general pathophysiology. In the last decade, numerous studies revealed the enormous heterogeneity and plasticity of the myeloid deriving MO/MΦ population, previously known as rather static [16]. Based on recent findings on this topic, the pathogenesis of IMIDs can now be better classified in regards to the polarization state of the MΦ. Being described as a multispectral continuum, the MΦ polarization scheme draws two opposing extremes - M1 and M2. While M2 are widely termed in the current literature as

inflammation resolving, wound healing, tissue repairing, and trophic or regulatory MΦ, the most important aspect is the consideration of M2 as the benign opposites of the M1 activated MΦ [162]. Having a close interplay with the Th-1 response, the classically activated M1 are central for overcoming viral or bacterial infections; however, there is also evidence that they crucially cause, participate and augment a variety of IMIDs [163, 164].

For instance, M1-directed polarization in intestinal tissues directly contributes to disruption of the epithelial barrier. Under influence of M1 population the tight junction proteins are deregulation, which partially induces apoptosis of epithelial cell and thus driving intestinal inflammation in IBD [29]. Similar contribution of M1-like MΦ has been observed in renal pathology, whereas the inflammation during ischemia-reperfusion could be suppressed by inducing M2 polarization [30, 165]. In a more recent therapeutic approach, the reduction of oxidative stress after ischemia-reperfusion injury using M1-depleting IT ameliorated renal damage [112]. Many studies using different models of acute pancreatitis confirmed an intense M1 activation of peritoneal MΦ, reflected in the high expression of pro-inflammatory cytokines such as TNF-α, IL-1β, IL-6 and enzymes such as induced nitric oxide synthase (iNOS) [30, 166]. These MΦ-derived mediators contribute to the toxicity of ascites fluid, which has a negative effect during acute pancreatitis and thereby, promotes a transition to the chronic phase [34, 167]. Abnormal ascites fluid dominated by pro-inflammatory cytokines causes liver damage.

Cells of the MO-MΦ lineage such as the liver-resident Kupffer cells (KC) are key components of the homeostatic functions of the liver and play a major role in the metabolic adaptation of hepatocytes. Similar to MΦ, KCs undergo polarized inflammatory programs [168]. M1-associated KC phenotype play a central role in the pathogenesis of alcoholic liver disease, by expressing high levels of pro-inflammatory cytokines (e.g., TNF-α). In contrary, cannabinoid-2 receptor agonists and adiponectin were shown to shift KC polarization to the M2 phenotype preventing the progression of nonalcoholic steatohepatitis [169-171]. As close relatives to other MΦ types, KCs regulate the oxidation of fatty acids in liver. This process can be altered in response to the common inflammatory cytokines (e.g., TNF-α, IL-6, and IL-1β) and thereby, an increased lipid storage in hepatocytes during obesity can be triggered, which ultimately results in hepatic insulin resistance [172]. Therefore, a beneficial role for alternatively M2-activated KCs is strongly suggested in metabolic syndrome and T2D [173, 174].

In the central nervous system, immune cells sharing certain characteristics with MΦ are the microglial cells, which contribute to immune-surveillance, immunoregulation and

homeostasis. Analogous to MΦ, the microglial cells can undergo M1/M2 polarization and, thereby, influence the CNS activity. M1 polarized microglia is capable of producing pro-inflammatory cytokines, reactive oxygen species (ROS) and reactive nitric species (RNS), suggesting that these contribute to dysfunction of neural network in the CNS, whereas M2 polarized microglia express cytokines and receptors that are involved in inhibiting inflammation and restoring homeostasis [175]. It was recently proposed that M1/M2 polarization plays an important role in relapse and remission of psychiatric disorders and diseases. During the last decade, multiple sclerosis (MS) appeared among the most abundant IMIDs in CNS [176, 177]. The mechanistic cause of the MS-pathogenesis is still under intensive investigation, but the main characteristics of MS have been clarified. Among lesions in CNS and destruction of myelin sheaths of neurons, the associated vast inflammation has emerged as major trigger of the disease [178]. The specific elements that start this inflammation are still unknown. Among other cell types, activated MΦ and other APCs play an important role in the primary inflammatory phase of MS. In a recent study, Vogel *et al.* observed increased presence of MΦ overexpressing CD40, CD86, CD64 and CD32 in lesion of MS patients in comparison to white matter of healthy human brain [33]. Concomitant to previous findings, CD64 is a strong M1 marker suggesting prevalence of M1 in the human MS lesions. Moreover in same study, diminished presence of the mannose receptor (MR, CD206) and CD163 expressing MΦ, both distinct M2 markers, was observed in patient tissue [33]. In line with these observations, an earlier study revealed that an imbalance towards M1 promotes relapsing experimental autoimmune encephalomyelitis (EAE) in rats. The impaired M2 expression tends to be a key factor in development of relapses, since adoptive transfer of *ex vivo* activated M2 both suppressed ongoing severe EAE and increased immunomodulatory expression patterns in lesions confirming the M2 role in the induction of recovery [179]. Among well-established therapeutics for MS is glatiramer acetate [180]. It shows sufficient efficacy in well controlled clinical trials in patients with relapsing-remitting MS (RRMS). The substance reduced relapse rate and decreased MRI-assessed disease activity and burden [181]. Although the exact mechanism of action in humans is not yet clear [182], treatment with glatiramer acetate in a mouse model promoted development of M2 [183]. Moreover, this anti-inflammatory cytokine shift was associated with high concentration of IL-10 and TGF-β and reduction of IL-12, TNF-α and STAT-1 signaling. In the same study, M2 facilitated development of T_{reg} cells and inhibited Th17 differentiation in a MHCII-dependent manner. Notably, the adoptive transfer of M2-induced regulatory T-cells alone also reversed EAE. This is therefore a great demonstration of how targeted type II polarization (M2, Th2, Treg) is a promising therapeutic strategy [183].

In the aspect of the cardiovascular system, MO/MΦ are involved, next to general immune defense, also in the homeostasis and neovascularization of blood vessels and the heart. MO migrate into the bloodstream from the bone marrow, deriving from precursor cells called monoblasts that differentiated from hematopoietic stem cells. The heterogeneity and plasticity sign can be evidently observed at the intermediate stage being able to distinguish between three subtypes of MO, which is based on the expression levels of CD14 and CD16 [184]. The further explorations of the role and functionality of the three subsets of MO are rather fragmented. However, there is evidence that the subsets differ in their response to environmental stimuli and therefore, the exact distribution numbers are hard to quantify. For instance, as a response to bacteria the $CD14^{high}$ $CD16^{high}$ MO produce much stronger pro-inflammatory cytokines (e.g. IL-12, TNF-α) as compared to $CD14^{high}CD16^{neg}$ MO, which showed a rather attenuated phenotype. Interestingly, the composition of blood MO behaves highly plastic, as for example the dominating MO population in septicemia patients is identified as $CD14^{high}$ $CD16^{high}$ $IL\text{-}6^{high}$, whereas it might shift to another phenotype during the sunset of infection [185]. In different pathological conditions like heart failure or atherosclerosis, the MO undergo a step forward in the differentiation pattern to become MΦ, whose tenure might last months. As the predifferential stage of the MO in circulation might differ, so the MΦ phenotypes also have a high variety. In a simplified scheme, Nahrendorf *et al.* showed that during heart infarction the early M1 arise from $CD14^{high}$ $Ly\text{-}6C^{high}$ MO to later transit into the healing M2 phenotype. However, M2 can be directly promoted by $CD14^{high}$ $Ly\text{-}6C^{low}$ MO and since in the steady-state, $Ly\text{-}6C^{low}$ MO can derive from $Ly\text{-}6C^{high}$ MO, it is not clear whether the conversion path involves intermediate stages [186]. Thus far, it is clear that M2 phenotype and its accompanying functions are essential for heart recovery, because M2 but not M1 promote angiogenesis [187, 188].

In contrast to the acute heart infarction, the atherosclerosis is a chronic inflammatory disease that arises from an imbalance in lipid metabolism. MΦ play a pivotal role therein, whereas the balance of MΦ in the atherosclerotic plaque is dynamic and thus, MΦ numbers and phenotype influence plaque fate [25]. Interestingly, the classical M1 phenotype is induced in the plaque by excessing the degradation capacity of the lysosome, lipolysis and lipophagy machinery after massive phagocytosis or macropinocytosis of aggregated LDL leading to cholesterol crystals-mediated activation of the inflammasome. Next to the excess of free intracellular cholesterol, the oxidized LDL activates the CD36 receptor, which in combination with TLR4-6 signaling driven by cholesterol-rich lipid grafts promotes a massive Nf-κB activation and subsequent cytokine/chemokine production [189, 190]. The results are

detrimental for plaque formation, growth and rupture. Next to the M1/M2 dichotomy, a unique Mox phenotype has been described in the context of atherosclerosis, which is characterized by increased expression of nuclear respiratory factor 2 (NRF2)-dependent genes and ROS [191]. Numerous *in vivo* studies have suggested that reducing the ROS pressure at the plaque site can stabilize the arterial plaques, avoiding rupture and thereby, improve disease outcome [192].

Oxidative stress is crucial for disease development of RA. It is proposed that ROS set the threshold for activation of the immune cells and thereby, the IMIDs like RA can be regulated [193]. In the pathogenesis of RA phagocytes and in particular, MΦ play a central role. Identically to other IMIDs, an imbalance of pro-inflammatory over anti-inflammatory MΦ in the RA synovium results in high levels of inflammatory cytokines and factors, but also pro-apoptotic signals like death receptor 5 (DR5), Fas, and others. In synovial liquid of RA patients, like also in sera of MS patients, excessive levels of TNF-α, IL-1, IL-6 and GM-CSF were measured, similar to the ones obtained in exudates of CDWs in the present work [32, 194, 195]. Although the complex pathological picture behind RA has not been fully uncovered, many clinical, preclinical, and animal studies have provided substantial insights into the role of MΦ polarization and heterogeneity. Hence, as Li *et al*. recently reckoned, an effective therapeutic approach for RA and other autoimmune diseases like AS will be the reestablishment of MΦ equilibrium by inhibiting the development and/or eliminating of the pro-inflammatory MΦ [24, 35]. In line with the compelling evidence of cytokine imbalance in IMIDs, the results of this thesis confirmed the strong dominance of the pro-inflammatory (IL-1β, IL-6, TNF-α, GM-CSF and IFN-γ) cytokines over the fraction of anti-inflammatory ones (IL-10, IL-4, IL-13 and TGF-β) in exudates of CDWs (**Figure 11).** Interestingly, although present in more than just trace levels, the anti-inflammatory cytokines seemed to be unsuccessful in promoting wound resolution. Similar observation was obtained by Gohel *et al.* concluding that the increasing concentration of TGF-β in wound fluid mirrored the healing of chronic venous ulcers in a study with 80 patients [196]. Although IL-4 and IL-13 has been broadly investigated in the last decade, their significant wound repairing effect still needs to be proven in translational studies to humans [197]. In recent years, it has emerged that IL-10 is indisputably essential in re-establishing tissue integrity and the subsequent healing process. In two preclinical studies and a phase II randomized control study the implication of recombinant human IL-10 improved wound healing and reduced scarring by suppression of inflammation [198]. Taken together, the manipulation of cytokines seems to be a promising therapeutic strategy for treating IMIDs.

IV.2. Targets for Ab-based therapy in IMIDs

As key elements of the IS´s communication network, cytokines and chemokines regulate the recruitment, survival, expansion, effector function, and contraction of different immune cells in IMIDs [199]. Thus, the profile and kinetics of certain cytokines indicates the disease course, as for example incrementing concentrations of TGF-β are associated with wound healing [196]. Furthermore, elevated levels of IL-6, TNF-α and IL-1 associated with rheumatoid arthritis are also critical for development of atherosclerosis and high risk of cardio-vascular diseases [200-202]. In this work, the collected data provided solid evidence for strong predominance of the pro-inflammatory cytokine fraction in contrast to the trace amounts of anti-inflammatory cytokines in exudates from CDW. Concomitant with the growing knowledge on etiology and pathophysiology of IMIDs, it becomes obvious that the distortion of the cytokine balance draws the disease pattern and inevitably worsens its course. Therefore, monoclonal therapeutic antibodies capable of neutralization of inflammatory cytokines such as Canakinumab (Ilaris®) against IL-1ß, Adalimumab (Humira®) and Infliximab (Remicade®) against TNF-α, and Tocilizumab (Actemra®) against IL-6 are effectively employed in a range of chronic inflammatory conditions and currently count to the standard of care in RA, systemic juvenile idiopathic arthritis, cryopyrin-associated periodic syndromes and other IMIDs [203]. Many more are the antibody therapeutics in phase III clinical studies [204]. For instance, Janssen´s Sirukumab and Regeneron´s Sarilumab show improved IL-6 neutralization at lower dosage than Tocilizumab [204] in a trial with RA patients. Novartis´ Secukinumab (Cosentyx) targeting IL-17A has recently been approved by the FDA for treatment of moderate-to-severe plaque psoriasis [205]. Another antibody inhibiting the IL-17A signal path is the Amgen´s Brodalumab, which was recently approved by FDA [206]. Blocking the IL-12p40/23p19-mediated activation of T-cells seems to be a promising strategy for fighting plaque psoriasis as shown in phase III trials of Janssen´s Guselkumab and Sun Pharmaceutical´s Tildrakizumab. Being able to blocks the activity of the both cytokines IL-12 and IL-23, Abbvie´s Briakinumab and Janssen´s Ustekinumab show promising results in completed phase III clinical trials for plaque psoriasis [207, 208]. However, the same two antibodies failed to show any specific effect in phase II trials for MS demonstrating that anti-IL-12/23 therapy is generally an ineffective treatment for MS [209, 210]. As a matter of fact, unlike the subcutaneous application mode in psoriasis, in those studies and in another phase II study for Crohn´s disease the intravenous administration of the therapeutic anti-IL-12/23 antibody either lacked the desired effect or caused a strong side-effect resulting in termination of the trial (e.g. Briakinumab) [211, 212].

Not only pro-inflammatory cytokines have been a target for development of antibody therapies. Regeneron´s Dupilumab is designed to block the subunit-α of IL-4 receptor and consequently, it modulates signaling of both the IL-4 and IL-13 pathway. Thereby, Dupilumab is implicated in the pathophysiology of allergic disease such as asthma, but also inflammatory skin diseases e.g. atopic dermatitis. Results from clinical trials phase III on atopic dermatitis have been recently announced. Analogous to phase II trials it could be demonstrated that monotherapy with dupilumab significantly improved measures of overall disease severity and quality of life [213, 214]. A summarized list of monoclonal antibody in clinics for treatment of IMIDs is shown in VII.3 (p. 106).

Intriguingly, the most potent producers of the above-mentioned inflammatory mediators are activated MΦ, which could also provide a good target for the development of next generation ADCs, ITs or MIMPs, aiming at resolving chronic inflammatory conditions. In a previous study, our group demonstrated that the M1/M2 ratio in chronic cutaneous inflammation is increased and this seems to contribute to inhibition of wound healing processes, which are marked by a M2 prevalence in order to induce the tissue repair stage [113]. The inappropriate persistence of M1 and dominance of pro-inflammatory cytokines are directly associated with the development and perpetuation of many other chronic inflammatory and autoimmune diseases [215-217]. Therefore, besides the conventional cytokine-neutralizing therapies, a strategy for directly targeting M1 is a promising and much more efficient way to shift the M1/M2 ratio and subsequently the cytokine imbalance towards the resolution process. Thepen *et al.* first demonstrated that depletion of $CD64^+$ MΦ (later identified as M1) using a Ricin-based IT was accompanied by the clearance of other inflammatory cells, including T-cells and DCs, which ultimately promoted *in vivo* resolution of chronic cutaneous inflammation [218]. Herein, this finding was confirmed by treating *ex vivo* biopsies from patients with atopic dermatitis and CDWs using bacterial H22(scFv)-ETA' ITs and thereby, the M1-restricted elimination revealed a shift in M2 direction. This indicates that depletion of M1 cells changes the microenvironment in a way that favors M2 polarization. This could affect newly infiltrating MO *in vivo* [18], but also push remaining MΦ to develop *in situ* a M2 phenotype as shown in this work with *ex vivo* treated biopsies (**Figure 12**). It is suggested that the increased presence of M2 cells gives rise to resolution by enhanced phagocytosis of debris and apoptotic NΘ, and by secretion of anti-inflammatory mediators including cytokines (e.g. IL-10, IL-1 RA, IL-1 type II decoy receptor) and lipid-based SPMs (e.g. lipoxins, resolvins, protectins) [295]. This tendency was indicated in the present work by upregulated IL-10 levels with simultaneous

reduction of IL-6 (**Figure 12B**), which again underlined the extraordinary MΦ plasticity when specifically targeted.

IV.3. MΦ plasticity and M1 susceptibility

Diversity and plasticity are hallmarks of cells of the MΦ lineage. In response to IFNs, Toll-like receptor engagement, or IL-4/IL-13 signaling, MΦ undergo M1 or M2 activation. The resulting M1/M2 dogma is a simplification showing just two extremes among many other phenotypes and polarization states within the MO/MΦ family [118]. In tissue, phenotypic and functional plasticity is a key feature of polarized MΦ and the pathological inability of MΦ to switch phenotype from M1 to M2 can lead to chronic inflammation [219]. In the analyzed human skin explants, there was a tendency towards an increase in M2 after selective elimination of M1 (**Figure 12**). Taking into consideration the fact that the skin explants represent an isolated system without infiltration by new MΦ from the circulation, this observation could be explained by local proliferation of M2 cells and/or M2-directed repolarization of remaining differently polarized MΦ in the tissue. Thus, the pro-inflammatory pressure ruled by M1 seems to be the major inhibition block for the failed induction of M2. To confirm this phenotypic transition *in vitro*, human and murine MΦ were repolarized by reversion of the initial stimuli (IL-4 for M1 and IFN-γ for M2), and IT treatment was applied. Thereby, the functional plasticity was demonstrated underlining that despite the expression of CD64 on both (M1 and M2) MΦ subsets, ultimately only M1 MΦ (IFN-γ polarized) are susceptible to the CD64-directed IT H22(scFv)-ETA'. However, it should be noted that the subdivision in M1 and M2 does not appear to be absolute (**Figure 13**), meaning that MΦ heterogeneity is also present *in vitro*. In light of the fact, this finding might be the missing explanation why IT-mediated elimination of M1 never reaches the absolute 0% viability when measuring the cell metabolism/proliferation in XTT assays (**Figure 14**). Therefore, it is hypothesized that the selective sensitivity of M1 MΦ must be determined by other factors, for instance, alternative routing and processing after internalization. One potential mechanism for this M1-restricted selectivity could be a difference in endosomal protease activity, which is indeed – in accordance with the literature - significantly lower in M1 compared to M2 cells [220, 221]. The lower protease activity in the endosomes of M1 cells may allow internalized toxin molecules to escape proteolysis and subsequently leak into the cytosol in order to exert their pro-apoptotic effect. This mechanism for M1-selectivity is also in line with the distinct functions M1 and M2 fulfill during various phases of the immune response. Upon activation, for example by infection, the primary function of M1 cells is to fight the pathogen and to initiate an immune response [222]. The phagocytosed

material is therefore not completely degraded, but rather processed in a size that is appropriate for presentation of conserved antigenic epitopes. This is accompanied by increased expression of MHC molecules on M1 supporting this role in antigen presentation during inflammation [223]. In contrast, M2 require a higher level of protease activity in accordance with their role in scavenging, tissue remodeling and repair [224]. It is however noteworthy that the observed effect of polarization on endosomal protease activity is influenced by the nature of the activation, e.g., viral vs. autoimmune-based. Further identification of the exact mechanisms associated with MΦ plasticity and polarized activation provides a basis for MΦ-centered therapeutic strategies. As such, in this study, the M1-specific targeting concept was further expanded and the targeted immunomodulatory strategy using fully human constructs was introduced in detail. For that purpose, in this work the CD64-binding Ab fragment H22(scFv) was fused to SOCS-2 or Trx-1, which resulted in the first in its kind MIMP.

IV.4. The route of CD64/H22(scFv)-fusion complex and cytosol delivery of fused cargo

Thus far, the routing path of the engulfed CD64/H22(scFv)-fusion complex is not completely understood. In flow cytometry experiments, the specific and preferential binding to M1 was confirmed, whereas the low expression of CD64 in M2 was detected (**Figure 18**). Examination of internalization profile was not performed due to numerous previous studies demonstrating a rapid CD64 intake and intracellular processing of bound H22(scFv)-fusion proteins [225]. In order to perform its modulating activity, the internalized MIMP requires trafficking into the cytosol. This is considered the most essential part for the efficiency of the CD64-directed therapy. In his study on the same binding molecule Guyre *et al.* highlighted that internalized H22(scFv)-eGFP was not localized entirely in early endosomes, recycling vesicles, or lysosomes. Intriguingly, it was found to colocalize with intracellular MHC class I suggesting cytosolic escape of the CD64-targeted antigens and ultimately assembling upon a class I processing pathway [226]. Such a mechanism is consistent with an early cytosolic model of Ag processing described by Rock *et al.*, in which exogenous Ag escapes the endocytic pathway and enters the cytosol for proteosomal degradation [227]. The latter laid the fundaments of many studies focusing on the mechanisms of cross-presentation by DCs and MΦs. The cross-presentation is a feature of certain antigen-presenting cells to take up, process and present extracellular antigens not exclusively on MHC II, but also on MHC class I molecules, which target a response via $CD8^+$ T-cell axis (cytotoxic T cells, CTL) [228]. Furthermore, Fcγ receptors (CD16, CD32 and CD64) targeting through immune complexes has been suggested to allow more efficient cross-presentation compared to soluble antigen, which are ingested via

endocytosis/scavenger receptors [229]. In this respect, the CD64-directed intake of fused cargo in case of MIMPs is likely to follow the suggested path for cross-presentation and this will ultimately provide access of the effector proteins to the cytosol. To portray the H22(scFv)-mediated delivery system in context of immunotherapy and more precisely, immunomodulation, a hypothetical model is proposed here based on the research of Guyre *et al.* and Rock *et al.* (**Figure 40**). In a first stage, the H22(scFv)-fused protein binds specifically the extracellular portion of the CD64 molecule and eventually competes out the occupying IgG antibody. It is generally accepted that this process triggers receptor-mediated internalization of the whole complex followed by formation of early endosomes (**stage 2**) [225]. An important stage for the final efficacy of the targeted therapy is **stage 3** denoted by cytosolic release of MIMPs or parts thereof prior to maturation of the early-to-late endosome and later fusion with the lysosome. The formation of endolysosome is considered to be the ultimate dead end for the endosomal content in terms of protein structure, folding and integrity [2]. Being able to escape the endolysosome processing, unknown numbers of effector molecules are transferred into cytoplasmic space, where they should become a target for cross-presentation [230]. At this

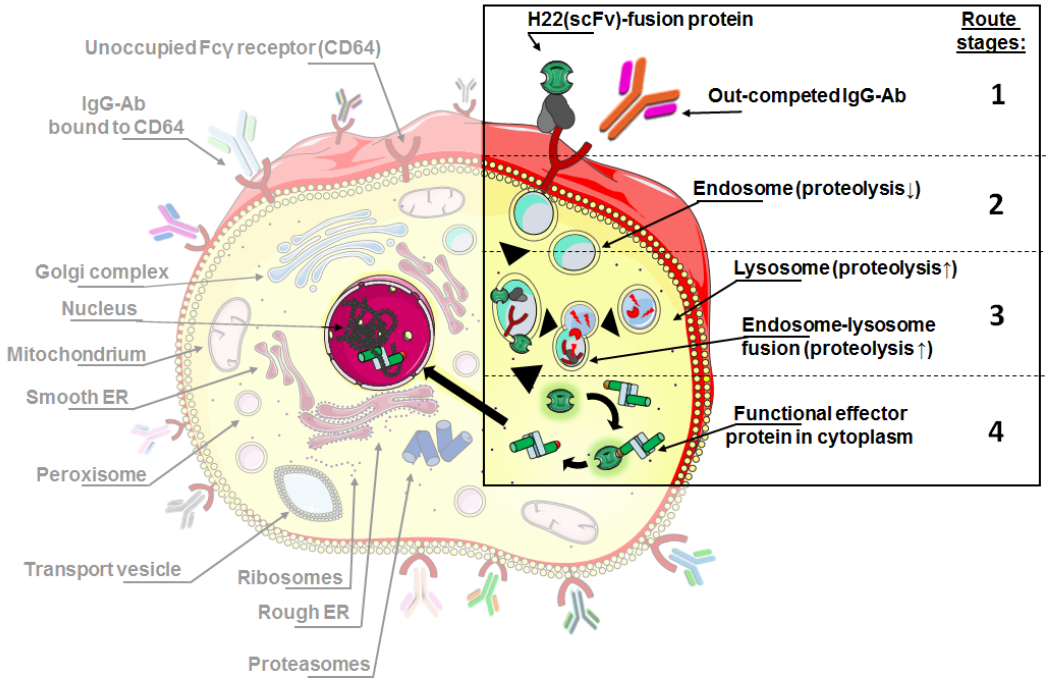

Figure 40: Hypothetical model for cytosolic release of H22(scFv)-delivered protein cargo
The route of internalized complex of CD64 and MIMP is summarized in four stages: **1**, H22(scFv)-fusion protein binds to CD64 and out-competes the bound (captured) IgG Ab due to higher binding affinity [1]; **2**, The complex of receptor and fusion protein undergoes internalization and forms early-to-late endosome with low proteolytic activity [2]; **3**, Endosome consisting of the internalized receptor-MIMP complex is leaky and, under not completely understood mechanisms free effector molecules are released into the cytosol; **4**, Free functional effector proteins can exert their immunomodulatory activity in cytosol and trigger upstream and/or downstream signaling. This image uses some elements provided by Servier Medical Art powerpoint image bank. Conceptual design is by Radoslav Mladenov. Abbreviations: ER, endoplasmic reticulum; IgG, immunoglobulin isotype class G.

point, the effector proteins are able to exert their modulatory activity, which depending on the nature of the effector protein might lead to an upstream and/or downstream signal transduction (**Figure 40, stage 4**). Therefore, the read-out system is focused on modification of MΦ phenotype in terms of surface markers, cytokine secretion, ROS activity and phagocytosis as result of the active immunomodulatory protein (Trx-1 or SOCS-2) when compared to the control groups. In case of cytotoxic molecules, such as bacterial ETA' or human MAP, the successful delivery and thus, toxic activity can be estimated easily through observations on cell metabolism and viability [116].

IV.5. SOCS-2 downregulates pro-inflammatory phenotype of MΦ towards resolution

Being able to express the recombinant H22(scFv)-SOCS-2 protein in mammalian cells a total yield of 4 mg was achieved, which is similar to the reported yields of other fusion proteins (**Figure 17**) [231]. Since there are no literature evidence of any SOCS protein exerting its activity in other but cytosolic environment [40], controls using only effector domain were not obtained. Thus far, SOCS-2 has been reported to have an important role in the immune response to various infections, since SOCS-2 knock-out mice exhibit stronger presence and activation of MΦ and NΘ during infection Furthermore, the expression of pro-inflammatory cytokines (e.g. IFN-γ, IL-12 and TNF-α) was significantly increased in SOCS-2 deficient mice upon *Toxoplasma gondii* infection. Moreover, the same model revealed that SOCS-2 is required for endogenous lipoxin (A_4) and aspirin-triggered anti-inflammatory actions [129]. Additionally, an early *in vitro* study showed that overexpression of SOCS-2 inhibits IL-6 sensitivity of the M1 monocytic cell line [232]. In line with those fragmented observation, the results in this work point out the rather protective role of exogenous SOCS-2 in human MΦ during pro-inflammatory conditions. The recombinant MIMP successfully prevented polarization towards M1 in both – priming and treatment approach using the standard M1/M2 polarization protocol. H22(scFv)-SOCS-2 resulted in substantially reduced levels of IL-12, IL-6, TNF-α and IL-1β (**Figure 21** and **Figure 22**). Furthermore, the same effect was detected when priming MΦ with H22(scFv)-SOCS-2 prior to exposure to chronic inflammatory conditions of CDWs exudates **(Figure 33**). Hence, it seems that once MΦ have acquired the chronic pro-inflammatory phenotype, the treatment with H22(scFv)-SOCS-2 was not efficient enough to adequately reverse the process within 24 hours. Similar observations are reported in context of tumor-associated macrophages (TAM), which tend to be hardly reprogrammed into a tumor rejection phenotype [233]. It is therefore suggested that understanding the mechanisms and kinetics of MΦ reprogramming will definitely aid the identification and selection of new therapeutic

targets for correction of impaired immunity [234]. Being able to substantially inhibit the production of IL-12, IL-6, TNF-α and IL-1β, and simultaneously induce expression of IL-10, the SOCS-2-based immunomodulation would be a highly beneficial intervention in the strict inflammatory phase of IMIDs and thus, normalization of the imbalance towards disease resolution is expected (**Figure 33**). In addition to the cytokine analysis, the fraction of chemokines was analyzed, which interestingly revealed effect of H22-mediated MIMP activity on M2 and also resting M0. Unlike the IT approach, MIMP treatment appeared to be active on all examined MΦ phenotypes. Nevertheless, this approach is still considered to be CD64-restricted.

A class of steroid hormones with a similar potential but highly unspecific effect has been reported for glucocorticoids, which currently count to the "off-the-shelf" anti-inflammatory medications [235]. Interestingly, a rat hepatocyte study showed that glucorticoids upregulate SOCS-1 and SOCS-2 but block SOCS-3 transcript levels under growth hormone stimulation suggesting a possible connection in the patterns [236]. An explanation for that might be the finding by Spence *et al.* in a knock-out study on the role of SOCS-2 and SOCS-3 in MΦ polarization. It was shown that SOCS-2-deficient murine MΦ were biased towards the M1 subset, whereas SOCS-3-deficient MΦ had a stable M2 profile. Moreover, compared with controls, SOCS-2 deficiency resulted in higher levels of phosphorylated STAT1 (signal transducer and activator of transcription 1) following stimulation with IFN-γ, and SOCS-3 deficiency had impact on more active STAT6 in response to IL-4 [128]. This fact provides a substantial explanation for our observations about SOCS-2 mediated prevention of M1-directed polarization when exposed to exudate of CDWs (**Figure 33**). Thus, it is hypothesized that SOCS-2 and SOCS-3 might control MΦ polarization by regulating cytokine–STAT signaling. Next to activity within growth hormone signal transduction [237], SOCS-2 has been also intensively linked to maturation of human MO derived-DCs regulating TLR signaling via the MyD88-dependent and -independent signaling pathways [238]. However, unlike SOCS-1 and SOCS-3, no links between SOCS-2 presence and Nf-κB regulation or Fas-induced apoptosis in lymphocytes were found in previous investigations [239, 240]. Taken together, it can be concluded that SOCS-2 is an important effector protein involved in a variety of regulatory pathways and it represents an excellent target for therapy of IMIDs.

IV.6. Trx-1 fine-tunes MΦ phenotype and ROS activity

Thioredoxin-1 (Trx), NADPH and thioredoxin reductase are the major components of the thioredoxin system, which is basically ubiquitous from Archea to man [241]. The Trx system

has functions in thiol-dependent thiol-disulfide exchange reactions, which are crucial for controlling the reduced intracellular redox environment, defense against oxidative stress, cellular growth or control of apoptosis. Furthermore, the Trx system has multifaceted roles in mammalian cells including implications in inflammation and cancer [242]. It plays a pivotal role in redox homeostasis in mammalian cells by keeping the redox balance of all cellular proteins and also protecting the DNA from ROS damage [243]. Moreover, under oxidative stress to preserve their integrity the mammalian cells upregulate the activity of the antioxidant responsive elements including the Trx system. By higher expression of Trx-1 the cellular redox system can be accelerated [244]. Interestingly, up-regulation of Trx-1 increases the expression of a hypoxia-inducible factor 1-alpha protein leading to increased vascular endothelial growth factor production and enhanced tumor angiogenesis. This fact has brought Trx-1 under the spotlight of tumorigenic targets for therapy [245]. However, in aspect of pro-active inflammation associated with excessive oxidative stress, Trx-1 together with Trx machinery is evidenced to play a protective and prevalent anti-inflammatory role. For instance, application of human Trx-1 in COPD mice protects against chronic neutrophilic inflammation in the lungs [246]. In addition to the inhibition of NΘ chemotaxis, the suppression of prolonged GM-CSF release by Trx-1 is involved in the resolution of late disease phase. Next to this finding, the potential of human Trx-1 as a novel therapeutic agent for exacerbation of chronic inflammation has been shown in a mouse model for smoke-induced lung inflammation. In the same study, human Trx-1 transgenic mice had significantly less inflammation, oxidative damage, and apoptosis, but also decreased levels of matrix metalloprotease-12 mRNA and serum TNF-α [247]. In line with this observation, the *in vitro* approach in the present work showed less TNF-α secretion of the H22(scFv)-Trx-1 treated M1 (**Figure 25**). This effect was however at lower extend than described in the *in vivo* study, which can be explained by the unspecific and systemic delivery/secretion of the Trx-1 protein and therefore, the resulting activity thereof can affect not only MO/MΦ but also NΘ and other cells. In aspect of cardiovascular disorders, systemically administered human Trx-1 promotes $CD206^{+}$ M2 and thereby, antagonizes atherosclerosis in ApoE2.Ki mice. The Trx-1 treatment significantly reduced the LPS-induced polarization towards M1, as indicated by the decreased expression of the M1 cytokines including TNF-α and also MCP-1 [139].

Importantly, human Trx-1 acts in both scenarios - extra- and intracellularly. Components of the Trx system are present in fresh healthy blood donor plasma, but also in specimens in aspect of inflammation and tumor progression. Many reports reveal extracellular Trx-1 to have chemoattractant and antioxidant properties, but it can also supplement cytokine activities [248].

In a recent study, Trx-1 outside the cell was even shown to act as growth factor promoting cell growth and thereby, it is likely to be implicated in tumorigenesis. On top of that, Trx stimulates cancer cell survival, promotes angiogenesis, and inhibits drug-induced apoptosis. Therefore, it is believed that Trx-1 is a promising therapeutic target for cancer prevention and intervention [249, 250]. Nonetheless, Trx-1 is one of hundreds of bioactive molecules that can be detected in elevated amounts during neoplastic development. In the context of IMIDs, these anti-inflammatory functions of Trx-1 would be highly beneficial for restoring the balance and tissue homeostasis. Inside the cell, Trx-1 alleviates oxidative stress by scavenging ROS and thereby, regulates a variety of redox-sensitive signaling pathways as well as ROS-independent genes. Thus, it is known that Trx-1 exerts potent cytoprotective effects [250]. Moreover, due to the functions of Trx-1 as a redox operator in the cell, it is reported that upregulation of Trx-1 can also regulate the activation of Nf-κB [251, 252]. As shown in this work, the H22(scFv)-Trx-1 demonstrated great potency in attenuation of ROS, which was produced dominantly by M1 but also in lower portions by M0 and M2 (**Figure 30**). The antioxidant activity of the H22-fused Trx-1 will be highly beneficial for alteration of oxidative stress in a variety of inflammatory conditions (e.g. atherosclerosis, MS and RA) [253]. In general, the ability to regulate the ROS levels during inflammation turns to be a key factor how to control the severity of some IMIDs such as RA [193]. Next to the redox potential, there is evidence of Trx-1-mediated secretion of IL-10 in sufficient levels for induction of $CD206^+$ M2 [139]. This observation lines up partially with our *in vitro* finding (**Figure 26**). Unlike H22(scFv)-SOCS-2, in this study H22(scFv)-Trx-1 failed to strongly reduce the pro-inflammatory cytokines, when tested in the classical MΦ model. However, in terms of protective function, H22(scFv)-Trx-1 proved successful in preventing M1-polarization when exposed to wound fluid. The effect is almost identical to the SOCS-2 based MIMP, which hints to either similar mode of action or an H22-dependent cascade exerting protective response. The second hypothesis is however unlikely, since in all previous experiments within this work and also in other studies, the CD64-binding moiety showed no impact on MΦ viability, polarization status or functionality (**Figure 25- 30, H22(scFv) control groups**) [1, 113].

Interestingly, the truncated version - Trx80 promotes the M1 phenotype and enhances atherosclerosis [142]. It induces the secretion of IL-12 in PBMC-derived MO and thereby, directs the immune response into Th-1 pathway [254]. Hypothetically, both Trx versions counteract in their cellular activity and thus, regulate the balance of Trx system. A powerful molecule combining the biological action of both is presented by migration inhibitory factor (MIF) [255]. Currently, the interplay between Trx-1 and MIF is under intensive investigation

and there is a suggestion that the anti-inflammatory mechanisms of TRX could be mediated partially by downregulation of MIF [256]. In regard to Trx-1 function in T-lymphocytes, Sido *et al.* showed in the context of intestinal lamina propria the potentiation of cytokine mRNA levels (IL-1a, IL-2, IL-6, IL-8, TNF-α and IL-10) as response to recombinant human Trx-1 [257]. It is therefore likely that Trx-1 acts differently in lymphoid- versus myeloid-deriving cells. This fact, in turn, underlines the necessity of the directed targeting of the Trx-1 molecule to the M1 population, which in case of this work is greatly performed by the H22(scFv).

The CD64-directed delivery system has so far proven successful in distributing a variety of different protein payloads such as bacterial ETA', human angiogenin and granzymes, and now also a human modulatory effector molecule. A potential combinatory therapy including a local application of M1-eliminating agent in face of CD64-directed IT and a systemic application of the MIMP would eventually assemble a highly promising therapeutic tool. Not to be neglected is the much higher potency of the MIMP due to its direct mode of action. In theory, the IT-driven M1 depletion will desolate the inflammation battle to be undertaken by the low initial M2 population, which would require time for *in situ* expansion. In contrast, the supremacy of the MIMP is considered in saving biological time, since it is likely to recruit the same numbers of M1 towards the M2 pool in order to directly increment it. A MIMP/IT combinational approach might however face some limitations because both strategies depend on one target molecule – CD64. Therefore, alternative targets are preferable for more efficient combinatory therapy. For that purpose, in the present thesis the suitability of CD89 as a CD64-alternative immunotherapy towards cells deriving from myeloid lineage was identified.

IV.7. Immunotherapy targeting CD89

FcαRI (CD89) is constitutively expressed on MO/MΦ, eosinophilic and neutrophilic granulocytes and DCs, but importantly not on non-effector cell populations (such as fibroblasts, keratinocytes, endothelial cells, hepatocytes, etc.) [258]. However, tissue specific MΦ such as Kupffer cells can be circumstantially positive for CD89 [259]. CD89 binds efficiently all forms of IgA (monomeric IgA, polymeric IgA and secretory IgA) and by mediating ADCC, direct phagocytosis or just routine Ig recycling it plays a key role in immune protection [260]. Furthermore, CD89 associates with the FcRγ-chain signaling molecule through a unique charge-based mechanism and thus, it is connected to the ITAM signaling machinery located within the cytoplasmic part of FcRγ-chain [261]. Interestingly, CD89 is not uniform in its activation form, but its response differs depending on the binding ligand. For example, monovalent targeting of CD89, by anti-FcαRI Fab or scFv, or monomeric IgA, triggers potent

inhibitory ITAM (ITAMi) signaling through the associated FcRγ chain, which results in low-intensity signaling cascade and ultimately inhibition of cell response. In contrast, multimeric ligands lead to cross-linking of CD89 resulting in massive induction of tyrosine kinase Syk and finally, to fully activate immune cells. Consequently, CD89 is capable to mediate both pro- and anti-inflammatory response in ligand-dependent manner [260]. This regulatory function might be used for CD89-targeted inhibitory therapy during pro-inflammatory response. In mouse models, CD89-mediated inhibitory function was able to suppress several inflammatory diseases including asthma and glomerulonephritis. Thus, intravenously applied mIgA and anti-CD89 monovalent antibodies and fragments, thereof, represent promising tools for immunotherapy [262].

CD89 has been proposed earlier as a potential immunotherapeutic target but has mainly been used as the effector component of bispecific conjugates alongside with single-chain antibody fragments [258]. Thereby, the effector functions of CD89 itself and cells bearing it have been investigated in detail more recently [263]. In this context, studies have focused on generation of CD89-directed bispecific Abs or IgA antibodies targeting cancer cells or pathogens. A recombinant bispecific scFv (bsscFv) directed towards CD89 and MHC class II mediated efficient recruitment of polymorphonuclear leukocytes (PMN) as effector cells for target specific killing of malignant lymphoid B-cells overexpressing MHC-II. Furthermore, primary tumor cell isolates were also exclusively lysed in the presence of the bsscFv [157]. On the other hand, the application of full-sized recombinant IgA antibodies against epidermal growth factor receptor (EGFR) also triggered an efficient ADCC against tumor cells contributed by PMNs and mononuclear cells [264]. Despite its potential role as an effector molecule in antibody-based therapies, little is currently known about the presence, expression level and modulation of CD89 throughout the different stages of myeloid cells in humans. In a recent publication, the CD89 and CD64 density in myeloid cell cultures (e.g. HL-60, THP-1, MonoMac-1 and U937) was obtained. Moreover, the inducibility of surface CD89 was clearly identified when cells were exposed to different stimuli (e.g. TNF-α or IFN-γ) [158]. Here, the expression profiles of CD64 and CD89 on M1 and M2 was found to be 10- to 20-fold higher than published data for the monocytic cell cultures (**Figure 35**) [158]. Since CD64-directed elimination of M1 using IT but also hCFPs proved successful with comparable cytotoxicity for different effector molecules like ETA', granzyme B and angiogenin, there is an urge to investigate the suitability of CD89 for the same therapy approach [100, 115].

Having determined the preferential expression of CD89 on M1, an immunotoxic construct comprising a CD89-specific scFv derived from the humanized full-size anti-human CD89 mAb

A77 [157] and the truncated ETA' was generated. The achieved final yield of 3 mg of highly pure CD89(scFv)-ETA' per liter of bacterial culture was similar to the reported yields of other ITs [107]. The specific binding of CD89(scFv)-ETA' preferentially to M1 but also to lower extend on M2 and M0, and monocytic cell lines was confirmed in flow cytometry experiments (**Figure 36**). Furthermore, the efficient and antigen-specific killing of monocytic cell lines was demonstrated *in vitro*. The cytotoxic efficacy of CD89(scFv)-ETA' was promising, with EC_{50} values ranging from 0.2 to 3 nM. Nevertheless, the control IT based on H22(scFv) achieved a significantly lower EC_{50} value of 0.04 nM [108], which can be explained by the 2- to 3-fold higher density of CD64 on the surface of the same cells, allowing more ITs to be internalized (**Figure 37**). There was also only a distant correlation between the number of apoptotic cells and the cell viability, which probably reflects the number of early-apoptotic cells and metabolically active cells. The cytotoxicity of CD89(scFv)-ETA' in the presence of TNF-α stimulus is explained by the upregulation of CD89 caused by TNF-α stimulation. In contrast, the cytotoxic effect of CD89(scFv)-ETA' appears to be independent of the abundance of CD89 when the cells are stimulated with IFN-γ. In previous studies, IFN-γ was shown to augment the CD64 expression thus promoting the cytotoxicity of CD64-targeted ITs [97]. Even so, IFN-γ was able to influence the efficacy of CD89(scFv)-ETA' in a receptor-independent manner. This finding is in line with the hypothesis that IFN-γ stimulation modulates the post-internalization trafficking of the receptor-binding complex, which gradually, as already discussed above, seems to be the reason for higher sensitivity of IFN-stimulated myeloid cell lines. In a strong contrast, the primary PBMC-derived MΦ from healthy blood donors showed strong resistance against the CD89-directed IT (**Figure 39**). While cell metabolism of M1 and M2 remained completely unaffected, the IT-treatment slightly decreased the proliferation rate of the M0 measured in XTT assay. Nevertheless, the Annexin V/PI-assisted investigation of the treated MΦ revealed no substantial pro-apoptotic activity of the CD89(scFv)-ETA'. This observation is conform to our recent study showing resistance of freshly isolated primary non-polarized PBMCs to the CD89(scFv)-ETA' therapy [158]. Nonetheless, the same study showed that the IT was able to target and kill primary leukemia cells freshly derived from peripheral blood samples of AML and AMML patients. On top of that the primary leukemic cells were not pre-stimulated with IFN-γ or TNF-α as done in similar approaches, where however slightly higher cytotoxicity of H22(scFv)-based hCFP was observed [225, 265]. Interestingly, in same studies the non-polarized leukemia cells revealed stronger resistance to the applied IT. A reason for that might be a differential (progenitor) stage of the blasts. Furthermore, the activation status and ultimately the triggered cell program upon polarization seem to be crucial. As identified in

sera from CMML patients, there is a dominance of anti-inflammatory cytokines (IL-10, IL-4 and IL-13) while the pro-inflammatory fraction (IL-12, IFN-γ, etc.) had low concentrations (**Figures 9 and 10**). In the context of leukemia and many solid tumor types, all these anti-inflammatory biomarkers are linked to TAMs or also myeloid-derived suppressor cells (MDSC), which are an opposite phenotype of M1 and also different than M2a or referred here as M2 [266]. As CD89 seems not to be a promising target for depletion of monocytic cells in IMIDs, it might be highly important in therapy of myeloid-deriving malignancies. Targeting and killing of only the malignant cells, while the healthy circulating myeloid cells remain unaffected regardless of polarization status, will definitely result in a highly beneficial immunotherapy.

IV.8. Summary and Outlook

The work described in this thesis demonstrates the dominance of pro-inflammatory cytokines in chronic diabetic wounds mirroring the prevalence of M1 type of macrophages. Moreover, these findings were confirmed *ex vivo* using skin biopsies of AD and CDWs patients. Next to confirming previous finding in regard of IT-mediated M1 depletion resulting in enhanced M2 presence, the application of recombinant MIMPs targeting CD64 and thereby, influencing primarily the M1 population was herein introduced for the very first time . Although the preliminary data (N=5) should be further expanded, the constructs showed so far promising efficacy *in vitro* and proved successful in exerting an anti-inflammatory activity. An improvement of their efficacy might be achieved by optimization of the receptor-mediated delivery system. The path of the intracellular routing and translocation is so far poorly understood. Improved translocation efficiency might enhance the immunotherapeutic potential of the MIMPs to make them even more suitable for clinical applications. Therefore, research has focused on strategies to promote the release of the cargo from early endosomes [267, 268] in face of carrier systems (e. g. liposomes, cationic polymers and nanoparticles) or linker, which induce membrane translocation [268-270]. Another strategy is to use a multifunctional adapter fused genetically between binding and effector domain of the MIMPs [271].

In regard of the extended future application of the MIMPs, the economic and up-scaled production of active Trx-1 and SOCS-2 has to be considered. Therefore, expression in *E. coli* or yeast cells is likely to increase protein yield with lower expenses unless the lack of post-translational modifications alters the protein functionality. The serum stability is also an important point to be addressed prior to preclinical studies.

The present work provides “proof of concept” for the efficient CD64-directed delivery of functional protein payload. The fusion and application of other effector domains to H22(scFv) will likely uncover their biological function in the context of the particular disease model. Promising candidates are for instance SOCS-1 or DUSP-1 (dual specificity phosphatase 1), since both are documented to be important regulators in the innate immune system [272, 273]. Furthermore, a combinatorial treatment using MIMPs with different effector domains (e.g. SOCS, DUSP, etc.) might result in a more efficient re-polarization, which will stronger support the wound healing. For the future, next to broadening the spectrum of inflammatory signal transducers, one might also challenge only a single peptide target instead of the whole complex cytokine network. Moreover, a therapeutic approach combining IT and MIMPs treatment would be of immense interest. Hypothetically, the strictly M1-polarized cells will be rapidly depleted by the IT application, which would provide better working conditions for the MIMP treatment. Thereby, the immunomodulatory therapy might be much more efficient, ultimately resulting in more potent M2-directed rebalance of the inflammatory environment.

Henceforth, to test this therapeutic approach *in vivo* using human CD64-transgenic animals one should consider switching to the murine effector protein, since in previous work in our group a species-dependent functionality of the human fusion proteins was observed in mice [115]. Regardless of the *in vivo* results the question remains open whether human and animal effector molecules such as SOCS-2 or Trx-1 converge in their mode of action. Furthermore, despite the fully-human nature of the constructs, such fusion proteins might generate unique neotopes, which are recognized by the overactive immune system in patients with IMIDs and eventually become immunogenic.

In addition to the well-characterized CD64 immunotherapeutic biomarker, the suitability of CD89 for targeted therapy was investigated in the present work. Although overexpressed on M1 and M2, a CD89-directed ETA' IT was inefficient in eliminating primary MΦ *in vitro.* However, the generated IT will have future impact on therapeutic interventions in aspect of myeloid leukemia and thereby, CD89 will serve as novel diagnostic and therapeutic target for neoplasia. To show the utility of this potential agent, an animal model will be necessary to back up the *in vitro* data. This crucial step includes the establishment of a disseminated tumor model using one of the tested AML cell lines. For the future, CD89(scFv)-ETA` immunotherapy might be applied in diseases associated with prevalence of the $CD89^{high}$ neutrophilic population such as neutrophilia, chronic neutrophilic leukemia, and others.

V References

1. Hristodorov, D., R. Mladenov, H. Brehm, R. Fischer, S. Barth, and T. Thepen, Recombinant H22(scFv) blocks CD64 and prevents the capture of anti-TNF monoclonal antibody: A potential strategy to enhance anti-TNF therapy. mAbs, 2014. **6**(12): p. 11.
2. Vaithilingam, A., N.Y. Lai, E. Duong, J. Boucau, Y. Xu, M. Shimada, M. Gandhi, and S. Le Gall, A simple methodology to assess endolysosomal protease activity involved in antigen processing in human primary cells. BMC Cell Biol, 2013. **14**: p. 35.
3. CDC, Center for Disease Control and Prevention US CDC-Report: http://www.cdc.gov/chronicdisease/about/prevention.htm. 2014.
4. Heap, G.A. and D.A. van Heel, The genetics of chronic inflammatory diseases. Hum Mol Genet, 2009. **18**(R1): p. R101-6.
5. Rodriguez, E., K. Eyerich, and S. Weidinger, [Genetics of common chronic inflammatory skin diseases : An update on atopic dermatitis and psoriasis]. Hautarzt, 2011. **62**(2): p. 107-18.
6. Miller, A.H., V. Maletic, and C.L. Raison, Inflammation and its discontents: the role of cytokines in the pathophysiology of major depression. Biol Psychiatry, 2009. **65**(9): p. 732-41.
7. Serhan, C.N. and N. Chiang, Novel endogenous small molecules as the checkpoint controllers in inflammation and resolution: entree for resoleomics. Rheum Dis Clin North Am, 2004. **30**(1): p. 69-95.
8. Basil, M.C. and B.D. Levy, Specialized pro-resolving mediators: endogenous regulators of infection and inflammation. Nat Rev Immunol, 2016. **16**(1): p. 51-67.
9. Serhan, C.N., Pro-resolving lipid mediators are leads for resolution physiology. Nature, 2014. **510**(7503): p. 92-101.
10. Serhan, C.N. and J. Savill, Resolution of inflammation: the beginning programs the end. Nat Immunol, 2005. **6**(12): p. 1191-7.
11. Buckley, C.D., D.W. Gilroy, and C.N. Serhan, Proresolving lipid mediators and mechanisms in the resolution of acute inflammation. Immunity, 2014. **40**(3): p. 315-27.
12. Bosma-den Boer, M.M., M.L. van Wetten, and L. Pruimboom, Chronic inflammatory diseases are stimulated by current lifestyle: how diet, stress levels and medication prevent our body from recovering. Nutr Metab (Lond), 2012. **9**(1): p. 32.
13. Ernst, J.D., and Olle Stendahl, eds. , Phagocytosis of bacteria and bacterial pathogenicity. 1st ed. . Cambridge Books Online. , 2006.
14. van Furth, R. and Z.A. Cohn, The origin and kinetics of mononuclear phagocytes. J Exp Med, 1968. **128**(3): p. 415-35.
15. Hashimoto, D., A. Chow, C. Noizat, P. Teo, M.B. Beasley, M. Leboeuf, C.D. Becker, P. See, J. Price, D. Lucas, M. Greter, A. Mortha, S.W. Boyer, E.C. Forsberg, M. Tanaka, N. van Rooijen, A. Garcia-Sastre, E.R. Stanley, F. Ginhoux, P.S. Frenette, and M. Merad, Tissue-resident macrophages self-maintain locally throughout adult life with minimal contribution from circulating monocytes. Immunity, 2013. **38**(4): p. 792-804.
16. Mosser, D.M. and J.P. Edwards, Exploring the full spectrum of macrophage activation. Nat Rev Immunol, 2008. **8**(12): p. 958-69.
17. Mills, C.D., K. Kincaid, J.M. Alt, M.J. Heilman, and A.M. Hill, M-1/M-2 macrophages and the Th1/Th2 paradigm. J Immunol, 2000. **164**(12): p. 6166-73.
18. Hristodorov, D., R. Mladenov, V. von Felbert, M. Huhn, R. Fischer, S. Barth, and T. Thepen, Targeting CD64 mediates elimination of M1 but not M2 macrophages in vitro and in cutaneous inflammation in mice and patient biopsies. MAbs, 2015. **7**(5): p. 853-862.
19. Mantovani, A., A. Sica, S. Sozzani, P. Allavena, A. Vecchi, and M. Locati, The chemokine system in diverse forms of macrophage activation and polarization. Trends Immunol, 2004. **25**(12): p. 677-86.
20. Xue, J., S.V. Schmidt, J. Sander, A. Draffehn, W. Krebs, I. Quester, D. De Nardo, T.D. Gohel, M. Emde, L. Schmidleithner, H. Ganesan, A. Nino-Castro, M.R. Mallmann, L. Labzin, H. Theis, M. Kraut, M. Beyer, E. Latz, T.C. Freeman, T. Ulas, and J.L. Schultze, Transcriptome-based

network analysis reveals a spectrum model of human macrophage activation. Immunity, 2014. **40**(2): p. 274-88.
21. Martinez, F.O., A. Sica, A. Mantovani, and M. Locati, Macrophage activation and polarization. Front Biosci, 2008. **13**: p. 453-61.
22. Bondeson, J., S.D. Wainwright, S. Lauder, N. Amos, and C.E. Hughes, The role of synovial macrophages and macrophage-produced cytokines in driving aggrecanases, matrix metalloproteinases, and other destructive and inflammatory responses in osteoarthritis. Arthritis Res Ther, 2006. **8**(6): p. R187.
23. Vlahos, R. and S. Bozinovski, Role of alveolar macrophages in chronic obstructive pulmonary disease. Front Immunol, 2014. **5**: p. 435.
24. Lin, S., M. Qiu, and J. Chen, IL-4 modulates macrophage polarization in ankylosing spondylitis. Cell Physiol Biochem, 2015. **35**(6): p. 2213-22.
25. Moore, K.J., F.J. Sheedy, and E.A. Fisher, Macrophages in atherosclerosis: a dynamic balance. Nat Rev Immunol, 2013. **13**(10): p. 709-21.
26. Leung, D.Y., M. Boguniewicz, M.D. Howell, I. Nomura, and Q.A. Hamid, New insights into atopic dermatitis. J Clin Invest, 2004. **113**(5): p. 651-7.
27. Khanna, S., S. Biswas, Y. Shang, E. Collard, A. Azad, C. Kauh, V. Bhasker, G.M. Gordillo, C.K. Sen, and S. Roy, Macrophage dysfunction impairs resolution of inflammation in the wounds of diabetic mice. PLoS One, 2010. **5**(3): p. e9539.
28. Wendelsdorf, K., J. Bassaganya-Riera, R. Hontecillas, and S. Eubank, Model of colonic inflammation: immune modulatory mechanisms in inflammatory bowel disease. J Theor Biol, 2010. **264**(4): p. 1225-39.
29. Lissner, D., M. Schumann, A. Batra, L.I. Kredel, A.A. Kuhl, U. Erben, C. May, J.D. Schulzke, and B. Siegmund, Monocyte and M1 cacrophage-induced barrier defect contributes to chronic intestinal inflammation in IBD. Inflamm Bowel Dis, 2015. **21**(6): p. 1297-305.
30. Duffield, J.S., Macrophages and immunologic inflammation of the kidney. Semin Nephrol, 2010. **30**(3): p. 234-54.
31. Wang, Y. and D.C. Harris, Macrophages in renal disease. J Am Soc Nephrol, 2011. **22**(1): p. 21-7.
32. Amedei, A., D. Prisco, and M.M. D'Elios, Multiple sclerosis: the role of cytokines in pathogenesis and in therapies. Int J Mol Sci, 2012. **13**(10): p. 13438-60.
33. Vogel, D.Y., E.J. Vereyken, J.E. Glim, P.D. Heijnen, M. Moeton, P. van der Valk, S. Amor, C.E. Teunissen, J. van Horssen, and C.D. Dijkstra, Macrophages in inflammatory multiple sclerosis lesions have an intermediate activation status. J Neuroinflammation, 2013. **10**: p. 35.
34. Gea-Sorli, S. and D. Closa, Role of macrophages in the progression of acute pancreatitis. World J Gastrointest Pharmacol Ther, 2010. **1**(5): p. 107-11.
35. Li, J., H.C. Hsu, and J.D. Mountz, Managing macrophages in rheumatoid arthritis by reform or removal. Curr Rheumatol Rep, 2012. **14**(5): p. 445-54.
36. Chizzolini, C., J.M. Dayer, and P. Miossec, Cytokines in chronic rheumatic diseases: is everything lack of homeostatic balance? Arthritis Res Ther, 2009. **11**(5): p. 246.
37. Quiding-Jarbrink, M., S. Raghavan, and M. Sundquist, Enhanced M1 macrophage polarization in human helicobacter pylori-associated atrophic gastritis and in vaccinated mice. PLoS One, 2010. **5**(11): p. e15018.
38. Jou, I.M., C.F. Lin, K.J. Tsai, and S.J. Wei, Macrophage-mediated inflammatory disorders. Mediators Inflamm, 2013. **2013**: p. 316482.
39. El-Gabalawy, H., L.C. Guenther, and C.N. Bernstein, Epidemiology of immune-mediated inflammatory diseases: incidence, prevalence, natural history, and comorbidities. J Rheumatol Suppl, 2010. **85**: p. 2-10.
40. Trengove, M.C. and A.C. Ward, SOCS proteins in development and disease. Am J Clin Exp Immunol, 2013. **2**(1): p. 1-29.
41. Qin, H., Y. Liu, T. Fox, A. Harms, D. Standaert, and E. Benveniste, Function of M1-polarized macrophages in the pathogenesis of Parkinson's disease (INC6P.300). The Journal of Immunology, 2015. **194**(1 Supplement): p. 192.2.
42. Decramer, M., W. Janssens, and M. Miravitlles, Chronic obstructive pulmonary disease. Lancet, 2012. **379**(9823): p. 1341-51.

43. Shaykhiev, R., A. Krause, J. Salit, Y. Strulovici-Barel, B.G. Harvey, T.P. O'Connor, and R.G. Crystal, Smoking-dependent reprogramming of alveolar macrophage polarization: implication for pathogenesis of chronic obstructive pulmonary disease. J Immunol, 2009. **183**(4): p. 2867-83.
44. Woodruff, P.G., L.L. Koth, Y.H. Yang, M.W. Rodriguez, S. Favoreto, G.M. Dolganov, A.C. Paquet, and D.J. Erle, A distinctive alveolar macrophage activation state induced by cigarette smoking. Am J Respir Crit Care Med, 2005. **172**(11): p. 1383-92.
45. Glick, R., D.R. Bish, and E. Agca, Optimization-based decision support to assist in logistics planning for hospital evacuations. J Emerg Manag, 2013. **11**(4): p. 261-70.
46. Ginhoux, F. and S. Jung, Monocytes and macrophages: developmental pathways and tissue homeostasis. Nat Rev Immunol, 2014. **14**(6): p. 392-404.
47. Trinchieri, G., Interleukin-12: a proinflammatory cytokine with immunoregulatory functions that bridge innate resistance and antigen-specific adaptive immunity. Annu Rev Immunol, 1995. **13**: p. 251-76.
48. Vignali, D.A. and V.K. Kuchroo, IL-12 family cytokines: immunological playmakers. Nat Immunol, 2012. **13**(8): p. 722-8.
49. Trinchieri, G., Interleukin-12 and the regulation of innate resistance and adaptive immunity. Nat Rev Immunol, 2003. **3**(2): p. 133-46.
50. Gabay, C., Interleukin-6 and chronic inflammation. Arthritis Res Ther, 2006. **8 Suppl 2**: p. S3.
51. Nishimoto, N. and T. Kishimoto, Interleukin 6: from bench to bedside. Nat Clin Pract Rheumatol, 2006. **2**(11): p. 619-26.
52. Rossi, J.F., Z.Y. Lu, M. Jourdan, and B. Klein, Interleukin-6 as a therapeutic target. Clin Cancer Res, 2015. **21**(6): p. 1248-57.
53. Bradley, J.R., TNF-mediated inflammatory disease. J Pathol, 2008. **214**(2): p. 149-60.
54. Espat, N.J., E.M. Copeland, and L.L. Moldawer, Tumor necrosis factor and cachexia: a current perspective. Surg Oncol, 1994. **3**(5): p. 255-62.
55. Sedger, L.M. and M.F. McDermott, TNF and TNF-receptors: From mediators of cell death and inflammation to therapeutic giants - past, present and future. Cytokine Growth Factor Rev, 2014. **25**(4): p. 453-72.
56. Garlanda, C., C.A. Dinarello, and A. Mantovani, The interleukin-1 family: back to the future. Immunity, 2013. **39**(6): p. 1003-18.
57. Dinarello, C.A., Immunological and inflammatory functions of the interleukin-1 family. Annu Rev Immunol, 2009. **27**: p. 519-50.
58. Masters, S.L., A. Simon, I. Aksentijevich, and D.L. Kastner, Horror autoinflammaticus: the molecular pathophysiology of autoinflammatory disease (*). Annu Rev Immunol, 2009. **27**: p. 621-68.
59. Fleetwood, A.J., A.D. Cook, and J.A. Hamilton, Functions of granulocyte-macrophage colony-stimulating factor. Crit Rev Immunol, 2005. **25**(5): p. 405-28.
60. Francisco-Cruz, A., M. Aguilar-Santelises, O. Ramos-Espinosa, D. Mata-Espinosa, B. Marquina-Castillo, J. Barrios-Payan, and R. Hernandez-Pando, Granulocyte-macrophage colony-stimulating factor: not just another haematopoietic growth factor. Med Oncol, 2014. **31**(1): p. 774.
61. Gasson, J.C., Molecular physiology of granulocyte-macrophage colony-stimulating factor. Blood, 1991. **77**(6): p. 1131-45.
62. Mosser, D.M. and X. Zhang, Interleukin-10: new perspectives on an old cytokine. Immunol Rev, 2008. **226**: p. 205-18.
63. Braat, H., P. Rottiers, D.W. Hommes, N. Huyghebaert, E. Remaut, J.P. Remon, S.J. van Deventer, S. Neirynck, M.P. Peppelenbosch, and L. Steidler, A phase I trial with transgenic bacteria expressing interleukin-10 in Crohn's disease. Clin Gastroenterol Hepatol, 2006. **4**(6): p. 754-9.
64. Asadullah, K., W.D. Docke, M. Ebeling, M. Friedrich, G. Belbe, H. Audring, H.D. Volk, and W. Sterry, Interleukin 10 treatment of psoriasis: clinical results of a phase 2 trial. Arch Dermatol, 1999. **135**(2): p. 187-92.
65. Luzina, I.G., A.D. Keegan, N.M. Heller, G.A. Rook, T. Shea-Donohue, and S.P. Atamas, Regulation of inflammation by interleukin-4: a review of "alternatives". J Leukoc Biol, 2012. **92**(4): p. 753-64.

66. Brown, M.A. and J. Hural, Functions of IL-4 and control of its expression. Crit Rev Immunol, 1997. **17**(1): p. 1-32.
67. La Flamme, A.C., M. Kharkrang, S. Stone, S. Mirmoeini, D. Chuluundorj, and R. Kyle, Type II-activated murine macrophages produce IL-4. PLoS One, 2012. **7**(10): p. e46989.
68. Wynn, T.A., IL-13 effector functions. Annu Rev Immunol, 2003. **21**: p. 425-56.
69. Seyfizadeh, N., N. Seyfizadeh, T. Gharibi, and Z. Babaloo, Interleukin-13 as an important cytokine: A review on its roles in some human diseases. Acta Microbiol Immunol Hung, 2015. **62**(4): p. 341-78.
70. Gold, L.I., The role for transforming growth factor-beta (TGF-beta) in human cancer. Crit Rev Oncog, 1999. **10**(4): p. 303-60.
71. Travis, M.A. and D. Sheppard, TGF-beta activation and function in immunity. Annu Rev Immunol, 2014. **32**: p. 51-82.
72. O'Kane, S. and M.W. Ferguson, Transforming growth factor beta s and wound healing. Int J Biochem Cell Biol, 1997. **29**(1): p. 63-78.
73. Sherry, B., P. Tekamp-Olson, C. Gallegos, D. Bauer, G. Davatelis, S.D. Wolpe, F. Masiarz, D. Coit, and A. Cerami, Resolution of the two components of macrophage inflammatory protein 1, and cloning and characterization of one of those components, macrophage inflammatory protein 1 beta. J Exp Med, 1988. **168**(6): p. 2251-9.
74. Lillard, J.W., Jr., U.P. Singh, P.N. Boyaka, S. Singh, D.D. Taub, and J.R. McGhee, MIP-1alpha and MIP-1beta differentially mediate mucosal and systemic adaptive immunity. Blood, 2003. **101**(3): p. 807-14.
75. Luster, A.D., J.C. Unkeless, and J.V. Ravetch, Gamma-interferon transcriptionally regulates an early-response gene containing homology to platelet proteins. Nature, 1985. **315**(6021): p. 672-6.
76. O'Donovan, N., M. Galvin, and J.G. Morgan, Physical mapping of the CXC chemokine locus on human chromosome 4. Cytogenet Cell Genet, 1999. **84**(1-2): p. 39-42.
77. Dufour, J.H., M. Dziejman, M.T. Liu, J.H. Leung, T.E. Lane, and A.D. Luster, IFN-gamma-inducible protein 10 (IP-10; CXCL10)-deficient mice reveal a role for IP-10 in effector T cell generation and trafficking. J Immunol, 2002. **168**(7): p. 3195-204.
78. Landmann, R., H.P. Knopf, S. Link, S. Sansano, R. Schumann, and W. Zimmerli, Human monocyte CD14 is upregulated by lipopolysaccharide. Infect Immun, 1996. **64**(5): p. 1762-9.
79. Nimmerjahn, F. and J.V. Ravetch, Fcgamma receptors: old friends and new family members. Immunity, 2006. **24**(1): p. 19-28.
80. Lu, J., J.L. Ellsworth, N. Hamacher, S.W. Oak, and P.D. Sun, Crystal structure of Fcgamma receptor I and its implication in high affinity gamma-immunoglobulin binding. J Biol Chem, 2011. **286**(47): p. 40608-13.
81. Harrison, P.T. and J.M. Allen, High affinity IgG binding by FcgammaRI (CD64) is modulated by two distinct IgSF domains and the transmembrane domain of the receptor. Protein Eng, 1998. **11**(3): p. 225-32.
82. Lee, S.J., S. Evers, D. Roeder, A.F. Parlow, J. Risteli, L. Risteli, Y.C. Lee, T. Feizi, H. Langen, and M.C. Nussenzweig, Mannose receptor-mediated regulation of serum glycoprotein homeostasis. Science, 2002. **295**(5561): p. 1898-901.
83. Schlesinger, P.H., T.W. Doebber, B.F. Mandell, R. White, C. DeSchryver, J.S. Rodman, M.J. Miller, and P. Stahl, Plasma clearance of glycoproteins with terminal mannose and N-acetylglucosamine by liver non-parenchymal cells. Studies with beta-glucuronidase, N-acetyl-beta-D-glucosaminidase, ribonuclease B and agalacto-orosomucoid. Biochem J, 1978. **176**(1): p. 103-9.
84. Szolnoky, G., Z. Bata-Csorgo, A.S. Kenderessy, M. Kiss, A. Pivarcsi, Z. Novak, K. Nagy Newman, G. Michel, T. Ruzicka, L. Marodi, A. Dobozy, and L. Kemeny, A mannose-binding receptor is expressed on human keratinocytes and mediates killing of Candida albicans. J Invest Dermatol, 2001. **117**(2): p. 205-13.
85. Dupasquier, M., P. Stoitzner, H. Wan, D. Cerqueira, A. van Oudenaren, J.S. Voerman, K. Denda-Nagai, T. Irimura, G. Raes, N. Romani, and P.J. Leenen, The dermal microenvironment induces the expression of the alternative activation marker CD301/mMGL in mononuclear phagocytes, independent of IL-4/IL-13 signaling. J Leukoc Biol, 2006. **80**(4): p. 838-49.

86. Adorini, L., Cytokine-based immunointervention in the treatment of autoimmune diseases. Clin Exp Immunol, 2003. **132**(2): p. 185-92.
87. Lindsley, C.W., 2014 global prescription medication statistics: strong growth and CNS well represented. ACS Chem Neurosci, 2015. **6**(4): p. 505-6.
88. Schabert, V.F., C. Watson, S.R. Gandra, S. Goodman, K.M. Fox, and D.J. Harrison, Annual costs of tumor necrosis factor inhibitors using real-world data in a commercially insured population in the United States. J Med Econ, 2012. **15**(2): p. 264-75.
89. Wojtal, K.A., G. Rogler, M. Scharl, L. Biedermann, P. Frei, M. Fried, A. Weber, J.J. Eloranta, G.A. Kullak-Ublick, and S.R. Vavricka, Fc gamma receptor CD64 modulates the inhibitory activity of infliximab. PLoS One, 2012. **7**(8): p. e43361.
90. Hristodorov, D., R. Mladenov, H. Brehm, R. Fischer, S. Barth, and T. Thepen, Recombinant H22(scFv) blocks CD64 and prevents the capture of anti-TNF monoclonal antibody. A potential strategy to enhance anti-TNF therapy. MAbs, 2014. **6**(5): p. 1283-9.
91. Mills, C.D., M1 and M2 macrophages: oracles of health and disease. Crit Rev Immunol, 2012. **32**(6): p. 463-88.
92. Perussia, B., E.T. Dayton, R. Lazarus, V. Fanning, and G. Trinchieri, Immune interferon induces the receptor for monomeric IgG1 on human monocytic and myeloid cells. J Exp Med, 1983. **158**(4): p. 1092-113.
93. Repp, R., T. Valerius, A. Sendler, M. Gramatzki, H. Iro, J.R. Kalden, and E. Platzer, Neutrophils express the high affinity receptor for IgG (Fc gamma RI, CD64) after in vivo application of recombinant human granulocyte colony-stimulating factor. Blood, 1991. **78**(4): p. 885-9.
94. Kiyoshi, M., J.M. Caaveiro, T. Kawai, S. Tashiro, T. Ide, Y. Asaoka, K. Hatayama, and K. Tsumoto, Structural basis for binding of human IgG1 to its high-affinity human receptor FcgammaRI. Nat Commun, 2015. **6**: p. 6866.
95. van der Poel, C.E., R.M. Spaapen, J.G. van de Winkel, and J.H. Leusen, Functional characteristics of the high affinity IgG receptor, FcgammaRI. J Immunol, 2011. **186**(5): p. 2699-704.
96. Bruhns, P., Properties of mouse and human IgG receptors and their contribution to disease models. Blood, 2012. **119**(24): p. 5640-9.
97. Thepen, T., M. Huhn, G. Melmer, M.K. Tur, and S. Barth, Fcgamma receptor 1 (CD64), a target beyond cancer. Curr Pharm Des, 2009. **15**(23): p. 2712-8.
98. Ribbert, T., T. Thepen, M.K. Tur, R. Fischer, M. Huhn, and S. Barth, Recombinant, ETA'-based CD64 immunotoxins: improved efficacy by increased valency, both in vitro and in vivo in a chronic cutaneous inflammation model in human CD64 transgenic mice. Br J Dermatol, 2010. **163**(2): p. 279-286.
99. Hristodorov, D., R. Mladenov, R. Fischer, S. Barth, and T. Thepen, Fully human MAP-fusion protein selectively targets and eliminates proliferating CD64(+) M1 macrophages. Immunol Cell Biol, 2016. **94**(5): p. 470-8.
100. Cremer, C., H. Braun, R. Mladenov, L. Schenke, X. Cong, E. Jost, T.H. Brummendorf, R. Fischer, P. Carloni, S. Barth, and T. Nachreiner, Novel angiogenin mutants with increased cytotoxicity enhance the depletion of pro-inflammatory macrophages and leukemia cells ex vivo. Cancer Immunol Immunother, 2015.
101. Guyre, P.M., R.F. Graziano, B.A. Vance, P.M. Morganelli, and M.W. Fanger, Monoclonal antibodies that bind to distinct epitopes on Fc gamma RI are able to trigger receptor function. J Immunol, 1989. **143**(5): p. 1650-5.
102. Graziano, R.F., P.R. Tempest, P. White, T. Keler, Y. Deo, H. Ghebremariam, K. Coleman, L.C. Pfefferkorn, M.W. Fanger, and P.M. Guyre, Construction and characterization of a humanized anti-gamma-Ig receptor type I (Fc gamma RI) monoclonal antibody. J Immunol, 1995. **155**(10): p. 4996-5002.
103. Thepen, T., A.J. van Vuuren, R.C. Kiekens, C.A. Damen, W.C. Vooijs, and J.G. van De Winkel, Resolution of cutaneous inflammation after local elimination of macrophages. Nat Biotechnol, 2000. **18**(1): p. 48-51.
104. Zhong, R.K., J.G. van de Winkel, T. Thepen, L.D. Schultz, and E.D. Ball, Cytotoxicity of anti-CD64-ricin a chain immunotoxin against human acute myeloid leukemia cells in vitro and in SCID mice. J Hematother Stem Cell Res, 2001. **10**(1): p. 95-105.
105. Ravetch, J.V. and J.P. Kinet, Fc receptors. Annu Rev Immunol, 1991. **9**: p. 457-492.

106. Challa, D.K., R. Velmurugan, R.J. Ober, and E. Sally Ward, FcRn: from molecular interactions to regulation of IgG pharmacokinetics and functions. Curr Top Microbiol Immunol, 2014. **382**: p. 249-72.
107. Tur, M.K., M. Huhn, T. Thepen, M. Stocker, R. Krohn, S. Vogel, E. Jost, R. Osieka, J.G. van de Winkel, R. Fischer, R. Finnern, and S. Barth, Recombinant CD64-specific single chain immunotoxin exhibits specific cytotoxicity against acute myeloid leukemia cells. Cancer Res, 2003. **63**(23): p. 8414-8419.
108. Berges, N., G. Hehmann-Titt, D. Hristodorov, G. Melmer, T. Thepen, and S. Barth, Human cytolytic fusion proteins: modified versions of human Granzyme B and Angiogenin have the potential to replace bacterial toxins in targeted therapies against CD64+ diseases. Antibodies, 2014. **3**(1): p. 92-115.
109. Thepen, T. and S. Barth, ADC's for Chronic Inflammatory Disease. Milestones in Drug Therapy (MDT) - Springer, 2016. **Book Chapter (in press)**.
110. Klimka, A., S. Barth, B. Matthey, R.C. Roovers, H. Lemke, H. Hansen, J.W. Arends, V. Diehl, H.R. Hoogenboom, and A. Engert, An anti-CD30 single-chain Fv selected by phage display and fused to Pseudomonas exotoxin A (Ki-4(scFv)-ETA') is a potent immunotoxin against a Hodgkin-derived cell line. Br J Cancer, 1999. **80**(8): p. 1214-22.
111. Deng, Q. and J.T. Barbieri, Molecular mechanisms of the cytotoxicity of ADP-ribosylating toxins. Annu Rev Microbiol, 2008. **62**: p. 271-88.
112. Fet, N.G., A. Fiebeler, U. Klinge, J.K. Park, S. Barth, T. Thepen, and R.H. Tolba, Reduction of activated macrophages after ischaemia-reperfusion injury diminishes oxidative stress and ameliorates renal damage. Nephrol Dial Transplant, 2012. **27**(8): p. 3149-3155.
113. Hristodorov, D., R. Mladenov, V. von Felbert, M. Huhn, R. Fischer, S. Barth, and T. Thepen, Targeting CD64 mediates elimination of M1 but not M2 macrophages in vitro and in cutaneous inflammation in mice and patient biopsies. mAbs, 2015: p. 00-00.
114. Pastan, I., R. Hassan, D.J. FitzGerald, and R.J. Kreitman, Immunotoxin treatment of cancer. Annu Rev Med, 2007. **58**: p. 221-37.
115. Schiffer, S., D. Hristodorov, R. Mladenov, E. Aslanian , M. Huhn, R. Fischer, S. Barth, and T. Thepen, Species-dependent functionality of the human cytolytic fusion proteins Granzyme B-H22(scFv) and H22(scFv)-Angiogenin in macrophages. Antibodies, 2013. **2**: p. 9-18.
116. Hristodorov, D., R. Mladenov, R. Fischer, S. Barth, and T. Thepen, Fully human MAP-fusion protein selectively targets and eliminates proliferating CD64 M1 macrophages. Immunol Cell Biol, 2016.
117. Biswas, S.K. and A. Mantovani, Macrophage plasticity and interaction with lymphocyte subsets: cancer as a paradigm. Nat Immunol, 2010. **11**(10): p. 889-96.
118. Sica, A. and A. Mantovani, Macrophage plasticity and polarization: in vivo veritas. J Clin Invest, 2012. **122**(3): p. 787-95.
119. Bonizzi, G. and M. Karin, The two NF-kappaB activation pathways and their role in innate and adaptive immunity. Trends Immunol, 2004. **25**(6): p. 280-8.
120. Pauleau, A.L., R. Rutschman, R. Lang, A. Pernis, S.S. Watowich, and P.J. Murray, Enhancer-mediated control of macrophage-specific arginase I expression. J Immunol, 2004. **172**(12): p. 7565-73.
121. Liao, X., N. Sharma, F. Kapadia, G. Zhou, Y. Lu, H. Hong, K. Paruchuri, G.H. Mahabeleshwar, E. Dalmas, N. Venteclef, C.A. Flask, J. Kim, B.W. Doreian, K.Q. Lu, K.H. Kaestner, A. Hamik, K. Clement, and M.K. Jain, Kruppel-like factor 4 regulates macrophage polarization. J Clin Invest, 2011. **121**(7): p. 2736-49.
122. Wormald, S. and D.J. Hilton, Inhibitors of cytokine signal transduction. J Biol Chem, 2004. **279**(2): p. 821-4.
123. Krebs, D.L. and D.J. Hilton, SOCS proteins: negative regulators of cytokine signaling. Stem Cells, 2001. **19**(5): p. 378-87.
124. Kario, E., M.D. Marmor, K. Adamsky, A. Citri, I. Amit, N. Amariglio, G. Rechavi, and Y. Yarden, Suppressors of cytokine signaling 4 and 5 regulate epidermal growth factor receptor signaling. J Biol Chem, 2005. **280**(8): p. 7038-48.
125. Kubo, M., T. Hanada, and A. Yoshimura, Suppressors of cytokine signaling and immunity. Nat Immunol, 2003. **4**(12): p. 1169-76.

126. Fenner, J.E., R. Starr, A.L. Cornish, J.G. Zhang, D. Metcalf, R.D. Schreiber, K. Sheehan, D.J. Hilton, W.S. Alexander, and P.J. Hertzog, Suppressor of cytokine signaling 1 regulates the immune response to infection by a unique inhibition of type I interferon activity. Nat Immunol, 2006. **7**(1): p. 33-9.
127. Qing, Y., A.P. Costa-Pereira, D. Watling, and G.R. Stark, Role of tyrosine 441 of interferon-gamma receptor subunit 1 in SOCS-1-mediated attenuation of STAT1 activation. J Biol Chem, 2005. **280**(3): p. 1849-53.
128. Spence, S., A. Fitzsimons, C.R. Boyd, J. Kessler, D. Fitzgerald, J. Elliott, J.N. Gabhann, S. Smith, A. Sica, E. Hams, S.P. Saunders, C.A. Jefferies, P.G. Fallon, D.F. McAuley, A. Kissenpfennig, and J.A. Johnston, Suppressors of cytokine signaling 2 and 3 diametrically control macrophage polarization. Immunity, 2013. **38**(1): p. 66-78.
129. Machado, F.S., J.E. Johndrow, L. Esper, A. Dias, A. Bafica, C.N. Serhan, and J. Aliberti, Anti-inflammatory actions of lipoxin A4 and aspirin-triggered lipoxin are SOCS-2 dependent. Nat Med, 2006. **12**(3): p. 330-4.
130. Arnold, C.E., C.S. Whyte, P. Gordon, R.N. Barker, A.J. Rees, and H.M. Wilson, A critical role for suppressor of cytokine signalling 3 in promoting M1 macrophage activation and function in vitro and in vivo. Immunology, 2014. **141**(1): p. 96-110.
131. Ueki, K., T. Kondo, and C.R. Kahn, Suppressor of cytokine signaling 1 (SOCS-1) and SOCS-3 cause insulin resistance through inhibition of tyrosine phosphorylation of insulin receptor substrate proteins by discrete mechanisms. Mol Cell Biol, 2004. **24**(12): p. 5434-46.
132. Powis, G. and W.R. Montfort, Properties and biological activities of thioredoxins. Annu Rev Pharmacol Toxicol, 2001. **41**: p. 261-95.
133. Collet, J.F. and J. Messens, Structure, function, and mechanism of thioredoxin proteins. Antioxid Redox Signal, 2010. **13**(8): p. 1205-16.
134. Powis, G. and W.R. Montfort, Properties and biological activities of thioredoxins. Annu Rev Biophys Biomol Struct, 2001. **30**: p. 421-55.
135. Sachi, Y., K. Hirota, H. Masutani, K. Toda, T. Okamoto, M. Takigawa, and J. Yodoi, Induction of ADF/TRX by oxidative stress in keratinocytes and lymphoid cells. Immunol Lett, 1995. **44**(2-3): p. 189-93.
136. Spindel, O.N., C. World, and B.C. Berk, Thioredoxin interacting protein: redox dependent and independent regulatory mechanisms. Antioxid Redox Signal, 2012. **16**(6): p. 587-96.
137. Billiet, L., C. Furman, G. Larigauderie, C. Copin, K. Brand, J.C. Fruchart, and M. Rouis, Extracellular human thioredoxin-1 inhibits lipopolysaccharide-induced interleukin-1beta expression in human monocyte-derived macrophages. J Biol Chem, 2005. **280**(48): p. 40310-8.
138. Son, A., N. Kato, T. Horibe, Y. Matsuo, M. Mochizuki, A. Mitsui, K. Kawakami, H. Nakamura, and J. Yodoi, Direct association of thioredoxin-1 (TRX) with macrophage migration inhibitory factor (MIF): regulatory role of TRX on MIF internalization and signaling. Antioxid Redox Signal, 2009. **11**(10): p. 2595-605.
139. El Hadri, K., D.F. Mahmood, D. Couchie, I. Jguirim-Souissi, F. Genze, V. Diderot, T. Syrovets, O. Lunov, T. Simmet, and M. Rouis, Thioredoxin-1 promotes anti-inflammatory macrophages of the M2 phenotype and antagonizes atherosclerosis. Arterioscler Thromb Vasc Biol, 2012. **32**(6): p. 1445-52.
140. Mitsui, A., J. Hamuro, H. Nakamura, N. Kondo, Y. Hirabayashi, S. Ishizaki-Koizumi, T. Hirakawa, T. Inoue, and J. Yodoi, Overexpression of human thioredoxin in transgenic mice controls oxidative stress and life span. Antioxid Redox Signal, 2002. **4**(4): p. 693-6.
141. Pineda Torra, I., P. Gervois, and B. Staels, Peroxisome proliferator-activated receptor alpha in metabolic disease, inflammation, atherosclerosis and aging. Curr Opin Lipidol, 1999. **10**(2): p. 151-9.
142. Mahmood, D.F., A. Abderrazak, D. Couchie, O. Lunov, V. Diderot, T. Syrovets, M.N. Slimane, F. Gosselet, T. Simmet, M. Rouis, and K. El Hadri, Truncated thioredoxin (Trx-80) promotes pro-inflammatory macrophages of the M1 phenotype and enhances atherosclerosis. J Cell Physiol, 2013. **228**(7): p. 1577-83.
143. Kerr, M.A., The structure and function of human IgA. Biochem J, 1990. **271**(2): p. 285-96.
144. Morton, H.C. and P. Brandtzaeg, CD89: the human myeloid IgA Fc receptor. Arch Immunol Ther Exp (Warsz), 2001. **49**(3): p. 217-29.

145. Hamre, R., I.N. Farstad, P. Brandtzaeg, and H.C. Morton, Expression and modulation of the human immunoglobulin A Fc receptor (CD89) and the FcR gamma chain on myeloid cells in blood and tissue. Scand J Immunol, 2003. **57**(6): p. 506-16.
146. Janssen, H. and R. Becker, Quality and costs of the management of chronic wounds – contradictory or compatible? Wunden, 2008. **12**(08): p. 920-925.
147. Sambrook, J. and D.W. Russell, *Molecular Cloning: A Laboratory Manual*. 2001: Cold Spring Harbor Laboratory Press.
148. Coligan, J.E., A.M. Kruisbeek, D.H. Margulies, E.M. Shevach, and W. Strober, *Current Protocols in Immunology*. 1991: John Wiley & Sons.
149. Stocker, M., M.K. Tur, S. Sasse, A. Krussmann, S. Barth, and A. Engert, Secretion of functional anti-CD30-angiogenin immunotoxins into the supernatant of transfected 293T-cells. Protein Expr Purif, 2003. **28**(2): p. 211-9.
150. Placzek, F., L. Barba-Lapersonne, and N. Malhomme, [A nursing consultation about chronic wounds in the hospital]. Rev Infirm, 1997(26): p. 41-6.
151. Ferwerda, B., M.B. McCall, M.C. de Vries, J. Hopman, B. Maiga, A. Dolo, O. Doumbo, M. Daou, D. de Jong, L.A. Joosten, R.A. Tissingh, F.A. Reubsaet, R. Sauerwein, J.W. van der Meer, A.J. van der Ven, and M.G. Netea, Caspase-12 and the inflammatory response to Yersinia pestis. PLoS One, 2009. **4**(9): p. e6870.
152. Barth, S., M. Huhn, B. Matthey, A. Klimka, E.A. Galinski, and A. Engert, Compatible-solute-supported periplasmic expression of functional recombinant proteins under stress conditions. Appl Environ Microbiol, 2000. **66**(4): p. 1572-9.
153. Campitiello, E., A. Della Corte, A. Fattopace, D. D'Acunzi, and S. Canonico, The use of artificial dermis in the treatment of chronic and acute wounds: regeneration of dermis and wound healing. Acta Biomed, 2005. **76 Suppl 1**: p. 69-71.
154. Scudiero, D.A., R.H. Shoemaker, K.D. Paull, A. Monks, S. Tierney, T.H. Nofziger, M.J. Currens, D. Seniff, and M.R. Boyd, Evaluation of a soluble tetrazolium/formazan assay for cell growth and drug sensitivity in culture using human and other tumor cell lines. Cancer Res, 1988. **48**(17): p. 4827-33.
155. Stroisch, T., Generation and evaluation of H22(scFv)-fused immunomodulatory proteins. Master Thesis, 2014.
156. Weichsel, A., J.R. Gasdaska, G. Powis, and W.R. Montfort, Crystal structures of reduced, oxidized, and mutated human thioredoxins: evidence for a regulatory homodimer. Structure, 1996. **4**(6): p. 735-51.
157. Guettinger, Y., K. Barbin, M. Peipp, J. Bruenke, M. Dechant, H. Horner, D. Thierschmidt, T. Valerius, R. Repp, G.H. Fey, and B. Stockmeyer, A recombinant bispecific single-chain fragment variable specific for HLA class II and Fc alpha RI (CD89) recruits polymorphonuclear neutrophils for efficient lysis of malignant B lymphoid cells. J Immunol, 2010. **184**(3): p. 1210-7.
158. Mladenov, R., D. Hristodorov, C. Cremer, L. Hein, F. Kreutzer, T. Stroisch, J. Niesen, H. Brehm, T. Blume, T.H. Brummendorf, E. Jost, T. Thepen, R. Fischer, B. Stockmeyer, S. Barth, and C. Stein, The Fc-alpha receptor is a new target antigen for immunotherapy of myeloid leukemia. Int J Cancer, 2015. **137**(11): p. 2729-38.
159. Barth, S., M. Huhn, B. Matthey, S. Tawadros, R. Schnell, T. Schinkothe, V. Diehl, and A. Engert, Ki-4(scFv)-ETA', a new recombinant anti-CD30 immunotoxin with highly specific cytotoxic activity against disseminated Hodgkin tumors in SCID mice. Blood, 2000. **95**(12): p. 3909-14.
160. Amoury, M., T. Blume, H. Brehm, J. Niesen, N. Tenhaef, S. Barth, S. Gattenlohner, W. Helfrich, J. Fitting, T. Nachreiner, and A. Pardo, SNAP-tag based agents for preclinical in vitro imaging in malignant diseases. Curr Pharm Des, 2013. **19**(30): p. 5429-36.
161. Heap, G.A. and D.A. van Heel, The genetics of chronic inflammatory diseases. Human molecular genetics, 2009. **18**(R1): p. R101-6.
162. Roszer, T., Understanding the mysterious M2 macrophage through activation markers and effector mechanisms. Mediators Inflamm, 2015. **2015**: p. 816460.
163. Labonte, A.C., A.C. Tosello-Trampont, and Y.S. Hahn, The role of macrophage polarization in infectious and inflammatory diseases. Mol Cells, 2014. **37**(4): p. 275-85.

164. Liu, Y.C., X.B. Zou, Y.F. Chai, and Y.M. Yao, Macrophage polarization in inflammatory diseases. Int J Biol Sci, 2014. **10**(5): p. 520-9.
165. Ranganathan, P.V., C. Jayakumar, and G. Ramesh, Netrin-1-treated macrophages protect the kidney against ischemia-reperfusion injury and suppress inflammation by inducing M2 polarization. Am J Physiol Renal Physiol, 2013. **304**(7): p. F948-57.
166. Gea-Sorli, S. and D. Closa, In vitro, but not in vivo, reversibility of peritoneal macrophages activation during experimental acute pancreatitis. BMC Immunol, 2009. **10**: p. 42.
167. Takeyama, Y., J. Nishikawa, T. Ueda, Y. Hori, M. Yamamoto, and Y. Kuroda, Involvement of peritoneal macrophage in the induction of cytotoxicity due to apoptosis in ascitic fluid associated with severe acute pancreatitis. J Surg Res, 1999. **82**(2): p. 163-71.
168. Sica, A., P. Invernizzi, and A. Mantovani, Macrophage plasticity and polarization in liver homeostasis and pathology. Hepatology, 2014. **59**(5): p. 2034-42.
169. Louvet, A., F. Teixeira-Clerc, M.N. Chobert, V. Deveaux, C. Pavoine, A. Zimmer, F. Pecker, A. Mallat, and S. Lotersztajn, Cannabinoid CB2 receptors protect against alcoholic liver disease by regulating Kupffer cell polarization in mice. Hepatology, 2011. **54**(4): p. 1217-26.
170. Mandal, P., B.T. Pratt, M. Barnes, M.R. McMullen, and L.E. Nagy, Molecular mechanism for adiponectin-dependent M2 macrophage polarization: link between the metabolic and innate immune activity of full-length adiponectin. J Biol Chem, 2011. **286**(15): p. 13460-9.
171. Fukushima, J., Y. Kamada, H. Matsumoto, Y. Yoshida, H. Ezaki, T. Takemura, Y. Saji, T. Igura, S. Tsutsui, S. Kihara, T. Funahashi, I. Shimomura, S. Tamura, S. Kiso, and N. Hayashi, Adiponectin prevents progression of steatohepatitis in mice by regulating oxidative stress and Kupffer cell phenotype polarization. Hepatol Res, 2009. **39**(7): p. 724-38.
172. Olefsky, J.M. and C.K. Glass, Macrophages, inflammation, and insulin resistance. Annu Rev Physiol, 2010. **72**: p. 219-46.
173. Odegaard, J.I., R.R. Ricardo-Gonzalez, A. Red Eagle, D. Vats, C.R. Morel, M.H. Goforth, V. Subramanian, L. Mukundan, A.W. Ferrante, and A. Chawla, Alternative M2 activation of Kupffer cells by PPARdelta ameliorates obesity-induced insulin resistance. Cell Metab, 2008. **7**(6): p. 496-507.
174. Papackova, Z., E. Palenickova, H. Dankova, J. Zdychova, V. Skop, L. Kazdova, and M. Cahova, Kupffer cells ameliorate hepatic insulin resistance induced by high-fat diet rich in monounsaturated fatty acids: the evidence for the involvement of alternatively activated macrophages. Nutr Metab (Lond), 2012. **9**: p. 22.
175. Nakagawa, Y. and K. Chiba, Role of microglial m1/m2 polarization in relapse and remission of psychiatric disorders and diseases. Pharmaceuticals (Basel), 2014. **7**(12): p. 1028-48.
176. Mackenzie, I.S., S.V. Morant, G.A. Bloomfield, T.M. MacDonald, and J. O'Riordan, Incidence and prevalence of multiple sclerosis in the UK 1990-2010: a descriptive study in the General Practice Research Database. J Neurol Neurosurg Psychiatry, 2014. **85**(1): p. 76-84.
177. Koch-Henriksen, N. and P.S. Sorensen, The changing demographic pattern of multiple sclerosis epidemiology. Lancet Neurol, 2010. **9**(5): p. 520-32.
178. Loma, I. and R. Heyman, Multiple sclerosis: pathogenesis and treatment. Curr Neuropharmacol, 2011. **9**(3): p. 409-16.
179. Mikita, J., N. Dubourdieu-Cassagno, M.S. Deloire, A. Vekris, M. Biran, G. Raffard, B. Brochet, M.H. Canron, J.M. Franconi, C. Boiziau, and K.G. Petry, Altered M1/M2 activation patterns of monocytes in severe relapsing experimental rat model of multiple sclerosis. Amelioration of clinical status by M2 activated monocyte administration. Mult Scler, 2011. **17**(1): p. 2-15.
180. Klawiter, E.C., A.H. Cross, and R.T. Naismith, The present efficacy of multiple sclerosis therapeutics: Is the new 66% just the old 33%? Neurology, 2009. **73**(12): p. 984-90.
181. Simpson, D., S. Noble, and C. Perry, Glatiramer acetate: a review of its use in relapsing-remitting multiple sclerosis. CNS Drugs, 2002. **16**(12): p. 825-50.
182. Racke, M.K., A.E. Lovett-Racke, and N.J. Karandikar, The mechanism of action of glatiramer acetate treatment in multiple sclerosis. Neurology, 2010. **74 Suppl 1**: p. S25-30.
183. Weber, M.S., T. Prod'homme, S. Youssef, S.E. Dunn, C.D. Rundle, L. Lee, J.C. Patarroyo, O. Stuve, R.A. Sobel, L. Steinman, and S.S. Zamvil, Type II monocytes modulate T cell-mediated central nervous system autoimmune disease. Nat Med, 2007. **13**(8): p. 935-43.
184. Ziegler-Heitbrock, L., The CD14+ CD16+ blood monocytes: their role in infection and inflammation. J Leukoc Biol, 2007. **81**(3): p. 584-92.

185. Fingerle, G., A. Pforte, B. Passlick, M. Blumenstein, M. Strobel, and H.W. Ziegler-Heitbrock, The novel subset of CD14+/CD16+ blood monocytes is expanded in sepsis patients. Blood, 1993. **82**(10): p. 3170-6.
186. Nahrendorf, M. and F.K. Swirski, Monocyte and macrophage heterogeneity in the heart. Circ Res, 2013. **112**(12): p. 1624-33.
187. Pinto, A.R., J.W. Godwin, and N.A. Rosenthal, Macrophages in cardiac homeostasis, injury responses and progenitor cell mobilisation. Stem Cell Res, 2014. **13**(3 Pt B): p. 705-14.
188. Jetten, N., S. Verbruggen, M.J. Gijbels, M.J. Post, M.P. De Winther, and M.M. Donners, Anti-inflammatory M2, but not pro-inflammatory M1 macrophages promote angiogenesis in vivo. Angiogenesis, 2014. **17**(1): p. 109-18.
189. Gargiulo, S., P. Gamba, G. Testa, D. Rossin, F. Biasi, G. Poli, and G. Leonarduzzi, Relation between TLR4/NF-kappaB signaling pathway activation by 27-hydroxycholesterol and 4-hydroxynonenal, and atherosclerotic plaque instability. Aging Cell, 2015. **14**(4): p. 569-81.
190. Stewart, C.R., L.M. Stuart, K. Wilkinson, J.M. van Gils, J. Deng, A. Halle, K.J. Rayner, L. Boyer, R. Zhong, W.A. Frazier, A. Lacy-Hulbert, J. El Khoury, D.T. Golenbock, and K.J. Moore, CD36 ligands promote sterile inflammation through assembly of a Toll-like receptor 4 and 6 heterodimer. Nat Immunol, 2010. **11**(2): p. 155-61.
191. Kadl, A., A.K. Meher, P.R. Sharma, M.Y. Lee, A.C. Doran, S.R. Johnstone, M.R. Elliott, F. Gruber, J. Han, W. Chen, T. Kensler, K.S. Ravichandran, B.E. Isakson, B.R. Wamhoff, and N. Leitinger, Identification of a novel macrophage phenotype that develops in response to atherogenic phospholipids via Nrf2. Circ Res, 2010. **107**(6): p. 737-46.
192. Morrell, C.N., Reactive oxygen species: finding the right balance. Circ Res, 2008. **103**(6): p. 571-2.
193. Gelderman, K.A., M. Hultqvist, L.M. Olsson, K. Bauer, A. Pizzolla, P. Olofsson, and R. Holmdahl, Rheumatoid arthritis: the role of reactive oxygen species in disease development and therapeutic strategies. Antioxid Redox Signal, 2007. **9**(10): p. 1541-67.
194. Lettesjo, H., E. Nordstrom, H. Strom, B. Nilsson, B. Glinghammar, L. Dahlstedt, and E. Moller, Synovial fluid cytokines in patients with rheumatoid arthritis or other arthritic lesions. Scand J Immunol, 1998. **48**(3): p. 286-92.
195. Hampel, U., S. Sesselmann, P. Iserovich, S. Sel, F. Paulsen, and R. Sack, Chemokine and cytokine levels in osteoarthritis and rheumatoid arthritis synovial fluid. J Immunol Methods, 2013. **396**(1-2): p. 134-9.
196. Gohel, M.S., R.A. Windhaber, J.F. Tarlton, M.R. Whyman, and K.R. Poskitt, The relationship between cytokine concentrations and wound healing in chronic venous ulceration. J Vasc Surg, 2008. **48**(5): p. 1272-7.
197. Salmon-Ehr, V., L. Ramont, G. Godeau, P. Birembaut, M. Guenounou, P. Bernard, and F.X. Maquart, Implication of interleukin-4 in wound healing. Lab Invest, 2000. **80**(8): p. 1337-43.
198. King, A., S. Balaji, L.D. Le, T.M. Crombleholme, and S.G. Keswani, Regenerative Wound Healing: The role of interleukin-10. Adv Wound Care (New Rochelle), 2014. **3**(4): p. 315-323.
199. Santamaria, P., Cytokines and chemokines in autoimmune disease: an overview. Adv Exp Med Biol, 2003. **520**: p. 1-7.
200. Miller, A.M. and I.B. McInnes, Cytokines as therapeutic targets to reduce cardiovascular risk in chronic inflammation. Curr Pharm Des, 2011. **17**(1): p. 1-8.
201. Cesari, M., B.W. Penninx, A.B. Newman, S.B. Kritchevsky, B.J. Nicklas, K. Sutton-Tyrrell, R.P. Tracy, S.M. Rubin, T.B. Harris, and M. Pahor, Inflammatory markers and cardiovascular disease (The Health, Aging and Body Composition [Health ABC] Study). Am J Cardiol, 2003. **92**(5): p. 522-8.
202. Waehre, T., A. Yndestad, C. Smith, T. Haug, S.H. Tunheim, L. Gullestad, S.S. Froland, A.G. Semb, P. Aukrust, and J.K. Damas, Increased expression of interleukin-1 in coronary artery disease with downregulatory effects of HMG-CoA reductase inhibitors. Circulation, 2004. **109**(16): p. 1966-72.
203. Martin, P.L. and P.J. Bugelski, Concordance of preclinical and clinical pharmacology and toxicology of monoclonal antibodies and fusion proteins: soluble targets. Br J Pharmacol, 2012. **166**(3): p. 806-22.
204. Reichert, J.M., Antibodies to watch in 2015. MAbs, 2015. **7**(1): p. 1-8.
205. Fischer, A., FDA approves new psoriasis drug Cosentyx. 2015.

206. Canavan, T.N., C.A. Elmets, W.L. Cantrell, J.M. Evans, and B.E. Elewski, Anti-IL-17 Medications Used in the Treatment of Plaque Psoriasis and Psoriatic Arthritis: A Comprehensive Review. Am J Clin Dermatol, 2016. **17**(1): p. 33-47.
207. NCT00691964, Clinical trial number NCT00691964 for "Study comparing the efficacy and safety of ABT-874 to etanercept and placebo in subjects with moderate to severe chronic plaque psoriasis" at ClinicalTrials.gov. 2013.
208. Gottlieb, A.B., C. Leonardi, F. Kerdel, S. Mehlis, M. Olds, and D.A. Williams, Efficacy and safety of briakinumab vs. etanercept and placebo in patients with moderate to severe chronic plaque psoriasis. Br J Dermatol, 2011. **165**(3): p. 652-60.
209. NCT00086671, Clinical trial number NCT00086671 for "Safety and effectiveness of two doses of ABT-874 as compared to placebo in subjects with multiple sclerosis (MS)" at ClinicalTrials.gov. 2013.
210. Vollmer, T.L., D.R. Wynn, M.S. Alam, and J. Valdes, A phase 2, 24-week, randomized, placebo-controlled, double-blind study examining the efficacy and safety of an anti-interleukin-12 and -23 monoclonal antibody in patients with relapsing-remitting or secondary progressive multiple sclerosis. Mult Scler, 2011. **17**(2): p. 181-91.
211. NCT00562887, Clinical trial number NCT00562887 for "Dose ranging study comparing the efficacy, safety and pharmacokinetics of intravenous infusions of ABT-874 vs placebo in subjects with active Crohn's disease" at ClinicalTrials.gov. 2011.
212. Ding, C., J. Xu, and J. Li, ABT-874, a fully human monoclonal anti-IL-12/IL-23 antibody for the potential treatment of autoimmune diseases. Curr Opin Investig Drugs, 2008. **9**(5): p. 515-22.
213. Thaci, D., E.L. Simpson, L.A. Beck, T. Bieber, A. Blauvelt, K. Papp, W. Soong, M. Worm, J.C. Szepietowski, H. Sofen, M. Kawashima, R. Wu, S.P. Weinstein, N.M. Graham, G. Pirozzi, A. Teper, E.R. Sutherland, V. Mastey, N. Stahl, G.D. Yancopoulos, and M. Ardeleanu, Efficacy and safety of dupilumab in adults with moderate-to-severe atopic dermatitis inadequately controlled by topical treatments: a randomised, placebo-controlled, dose-ranging phase 2b trial. Lancet, 2016. **387**(10013): p. 40-52.
214. NCT01979016, Clinical trial number NCT01979016 for "Study to determine the safety and effectiveness of Dupilumab (REGN668/SAR231893) for treatment of atopic dermatitis (AD)" at ClinicalTrials.gov. 2015.
215. Bannon, P., S. Wood, T. Restivo, L. Campbell, M.J. Hardman, and K.A. Mace, Diabetes induces stable intrinsic changes to myeloid cells that contribute to chronic inflammation during wound healing in mice. Dis Model Mech, 2013. **6**(6): p. 1434-47.
216. Khallou-Laschet, J., A. Varthaman, G. Fornasa, C. Compain, A.T. Gaston, M. Clement, M. Dussiot, O. Levillain, S. Graff-Dubois, A. Nicoletti, and G. Caligiuri, Macrophage plasticity in experimental atherosclerosis. PLoS One, 2010. **5**(1): p. e8852.
217. Mills, C.D., Anatomy of a discovery: m1 and m2 macrophages. Front Immunol, 2015. **6**: p. 212.
218. Thepen, T., A.J. van Vuuren, R.C. Kiekens, C.A. Damen, W.C. Vooijs, and J.G. van De Winkel, Resolution of cutaneous inflammation after local elimination of macrophages. Nat Biotechnol, 2000. **18**: p. 48-51.
219. Martinez, F.O., L. Helming, and S. Gordon, Alternative activation of macrophages: an immunologic functional perspective. Annu Rev Immunol, 2009. **27**: p. 451-83.
220. Balce, D.R., B. Li, E.R. Allan, J.M. Rybicka, R.M. Krohn, and R.M. Yates, Alternative activation of macrophages by IL-4 enhances the proteolytic capacity of their phagosomes through synergistic mechanisms. Blood, 2011. **118**(15): p. 4199-208.
221. Yates, R.M., A. Hermetter, G.A. Taylor, and D.G. Russell, Macrophage activation downregulates the degradative capacity of the phagosome. Traffic, 2007. **8**(3): p. 241-50.
222. Dale, D.C., L. Boxer, and W.C. Liles, The phagocytes: neutrophils and monocytes. Blood, 2008. **112**(4): p. 935-45.
223. Gordon, S. and P.R. Taylor, Monocyte and macrophage heterogeneity. Nat Rev Immunol, 2005. **5**(12): p. 953-64.
224. Mantovani, A., S.K. Biswas, M.R. Galdiero, A. Sica, and M. Locati, Macrophage plasticity and polarization in tissue repair and remodelling. J Pathol, 2013. **229**(2): p. 176-85.
225. Schiffer, S., R. Rosinke, E. Jost, G. Hehmann-Titt, M. Huhn, G. Melmer, S. Barth, and T. Thepen, Targeted ex vivo reduction of CD64-positive monocytes in chronic myelomonocytic

leukemia and acute myelomonocytic leukemia using human granzyme B-based cytolytic fusion proteins. Int J Cancer, 2014. **135**(6): p. 1497-508.
226. Guyre, C.A., M.E. Barreda, S.L. Swink, and M.W. Fanger, Colocalization of Fc gamma RI-targeted antigen with class I MHC: implications for antigen processing. J Immunol, 2001. **166**(4): p. 2469-78.
227. Rock, K.L., A new foreign policy: MHC class I molecules monitor the outside world. Immunol Today, 1996. **17**(3): p. 131-7.
228. Brode, S. and P.A. Macary, Cross-presentation: dendritic cells and macrophages bite off more than they can chew! Immunology, 2004. **112**(3): p. 345-51.
229. Platzer, B., M. Stout, and E. Fiebiger, Antigen cross-presentation of immune complexes. Front Immunol, 2014. **5**: p. 140.
230. Varkouhi, A.K., M. Scholte, G. Storm, and H.J. Haisma, Endosomal escape pathways for delivery of biologicals. J Control Release, 2011. **151**(3): p. 220-8.
231. Cremer, C., T. Vierbuchen, L. Hein, R. Fischer, S. Barth, and T. Nachreiner, Angiogenin mutants as novel effector molecules for the generation of fusion proteins with increased cytotoxic potential. J Immunother, 2015. **38**(3): p. 85-95.
232. Nicholson, S.E. and D.J. Hilton, The SOCS proteins: a new family of negative regulators of signal transduction. J Leukoc Biol, 1998. **63**(6): p. 665-8.
233. Stout, R.D., S.K. Watkins, and J. Suttles, Functional plasticity of macrophages: in situ reprogramming of tumor-associated macrophages. J Leukoc Biol, 2009. **86**(5): p. 1105-9.
234. Malyshev, I. and Y. Malyshev, Current concept and update of the macrophage plasticity concept: intracellular mechanisms of reprogramming and M3 macrophage "switch" phenotype. Biomed Res Int, 2015. **2015**: p. 341308.
235. Lund, T., B. Fosby, O. Korsgren, H. Scholz, and A. Foss, Glucocorticoids reduce pro-inflammatory cytokines and tissue factor in vitro and improve function of transplanted human islets in vivo. Transpl Int, 2008. **21**(7): p. 669-78.
236. Tollet-Egnell, P., A. Flores-Morales, A. Stavreus-Evers, L. Sahlin, and G. Norstedt, Growth hormone regulation of SOCS-2, SOCS-3, and CIS messenger ribonucleic acid expression in the rat. Endocrinology, 1999. **140**(8): p. 3693-704.
237. Turnley, A.M., Role of SOCS2 in growth hormone actions. Trends Endocrinol Metab, 2005. **16**(2): p. 53-8.
238. Hu, J., O. Winqvist, A. Flores-Morales, A.C. Wikstrom, and G. Norstedt, SOCS2 influences LPS induced human monocyte-derived dendritic cell maturation. PLoS One, 2009. **4**(9): p. e7178.
239. Park, S.H., K.E. Kim, H.Y. Hwang, and T.Y. Kim, Regulatory effect of SOCS on NF-kappaB activity in murine monocytes/macrophages. DNA Cell Biol, 2003. **22**(2): p. 131-9.
240. Oh, J., S.H. Kim, S. Ahn, and C.E. Lee, Suppressors of cytokine signaling promote Fas-induced apoptosis through downregulation of NF-kappaB and mitochondrial Bfl-1 in leukemic T cells. J Immunol, 2012. **189**(12): p. 5561-71.
241. Arner, E.S. and A. Holmgren, Physiological functions of thioredoxin and thioredoxin reductase. Eur J Biochem, 2000. **267**(20): p. 6102-9.
242. Arner, E.S. and A. Holmgren, The thioredoxin system in cancer. Semin Cancer Biol, 2006. **16**(6): p. 420-6.
243. Karlenius, T.C. and K.F. Tonissen, Thioredoxin and cancer: A role for thioredoxin in all states of tumor oxygenation. Cancers (Basel), 2010. **2**(2): p. 209-32.
244. Takagi, Y., A. Mitsui, A. Nishiyama, K. Nozaki, H. Sono, Y. Gon, N. Hashimoto, and J. Yodoi, Overexpression of thioredoxin in transgenic mice attenuates focal ischemic brain damage. Proc Natl Acad Sci U S A, 1999. **96**(7): p. 4131-6.
245. Welsh, S.J., W.T. Bellamy, M.M. Briehl, and G. Powis, The redox protein thioredoxin-1 (Trx-1) increases hypoxia-inducible factor 1alpha protein expression: Trx-1 overexpression results in increased vascular endothelial growth factor production and enhanced tumor angiogenesis. Cancer Res, 2002. **62**(17): p. 5089-95.
246. Tanabe, N., Y. Hoshino, S. Marumo, H. Kiyokawa, S. Sato, D. Kinose, K. Uno, S. Muro, T. Hirai, J. Yodoi, and M. Mishima, Thioredoxin-1 protects against neutrophilic inflammation and emphysema progression in a mouse model of chronic obstructive pulmonary disease exacerbation. PLoS One, 2013. **8**(11): p. e79016.

247. Sato, A., Y. Hoshino, T. Hara, S. Muro, H. Nakamura, M. Mishima, and J. Yodoi, Thioredoxin-1 ameliorates cigarette smoke-induced lung inflammation and emphysema in mice. J Pharmacol Exp Ther, 2008. **325**(2): p. 380-8.
248. Soderberg, A., B. Sahaf, and A. Rosen, Thioredoxin reductase, a redox-active selenoprotein, is secreted by normal and neoplastic cells: presence in human plasma. Cancer Res, 2000. **60**(8): p. 2281-9.
249. Nakamura, H., Extracellular functions of thioredoxin. Novartis Found Symp, 2008. **291**: p. 184-92; discussion 192-5, 221-4.
250. An, N. and Y. Kang, Thioredoxin and hematologic malignancies. Adv Cancer Res, 2014. **122**: p. 245-79.
251. Sakurai, A., K. Yuasa, Y. Shoji, S. Himeno, M. Tsujimoto, M. Kunimoto, N. Imura, and S. Hara, Overexpression of thioredoxin reductase 1 regulates NF-kappa B activation. J Cell Physiol, 2004. **198**(1): p. 22-30.
252. Hayashi, T., Y. Ueno, and T. Okamoto, Oxidoreductive regulation of nuclear factor kappa B. Involvement of a cellular reducing catalyst thioredoxin. J Biol Chem, 1993. **268**(15): p. 11380-8.
253. Laskin, D.L., V.R. Sunil, C.R. Gardner, and J.D. Laskin, Macrophages and tissue injury: agents of defense or destruction? Annu Rev Pharmacol Toxicol, 2011. **51**: p. 267-88.
254. Pekkari, K. and A. Holmgren, Truncated thioredoxin: physiological functions and mechanism. Antioxid Redox Signal, 2004. **6**(1): p. 53-61.
255. Thiele, M. and J. Bernhagen, Link between macrophage migration inhibitory factor and cellular redox regulation. Antioxid Redox Signal, 2005. **7**(9-10): p. 1234-48.
256. Mongardon, N., V. Lemiale, D. Borderie, A. Burke-Gaffney, S. Perbet, N. Marin, J. Charpentier, F. Pene, J.D. Chiche, J.P. Mira, and A. Cariou, Plasma thioredoxin levels during post-cardiac arrest syndrome: relationship with severity and outcome. Crit Care, 2013. **17**(1): p. R18.
257. Sido, B., T. Giese, F. Autschbach, F. Lasitschka, J. Braunstein, and S.C. Meuer, Potential role of thioredoxin in immune responses in intestinal lamina propria T lymphocytes. Eur J Immunol, 2005. **35**(2): p. 408-17.
258. Valerius, T., B. Stockmeyer, A.B. van Spriel, R.F. Graziano, I.E. van den Herik-Oudijk, R. Repp, Y.M. Deo, J. Lund, J.R. Kalden, M. Gramatzki, and J.G. van de Winkel, FcalphaRI (CD89) as a novel trigger molecule for bispecific antibody therapy. Blood, 1997. **90**(11): p. 4485-92.
259. van Egmond, M., E. van Garderen, A.B. van Spriel, C.A. Damen, E.S. van Amersfoort, G. van Zandbergen, J. van Hattum, J. Kuiper, and J.G. van de Winkel, FcalphaRI-positive liver Kupffer cells: reappraisal of the function of immunoglobulin A in immunity. Nat Med, 2000. **6**(6): p. 680-5.
260. Ben Mkaddem, S., E. Rossato, N. Heming, and R.C. Monteiro, Anti-inflammatory role of the IgA Fc receptor (CD89): from autoimmunity to therapeutic perspectives. Autoimmun Rev, 2013. **12**(6): p. 666-9.
261. Morton, H.C., M. van Egmond, and J.G. van de Winkel, Structure and function of human IgA Fc receptors (Fc alpha R). Crit Rev Immunol, 1996. **16**(4): p. 423-40.
262. Monteiro, R.C., Role of IgA and IgA fc receptors in inflammation. J Clin Immunol, 2010. **30**(1): p. 1-9.
263. Peipp, M. and T. Valerius, Bispecific antibodies targeting cancer cells. Biochem Soc Trans, 2002. **30**(4): p. 507-11.
264. Dechant, M., T. Beyer, T. Schneider-Merck, W. Weisner, M. Peipp, J.G. van de Winkel, and T. Valerius, Effector mechanisms of recombinant IgA antibodies against epidermal growth factor receptor. J Immunol, 2007. **179**(5): p. 2936-43.
265. Schiffer, S., S. Letzian, E. Jost, R. Mladenov, D. Hristodorov, M. Huhn, R. Fischer, S. Barth, and T. Thepen, Granzyme M as a novel effector molecule for human cytolytic fusion proteins: CD64-specific cytotoxicity of Gm-H22(scFv) against leukemic cells. Cancer Lett, 2013. **341**(2): p. 178-85.
266. Mantovani, A., T. Schioppa, C. Porta, P. Allavena, and A. Sica, Role of tumor-associated macrophages in tumor progression and invasion. Cancer Metastasis Rev, 2006. **25**(3): p. 315-22.

267. Erazo-Oliveras, A., N. Muthukrishnan, R. Baker, T.Y. Wang, and J.P. Pellois, Improving the endosomal escape of cell-penetrating peptides and their cargos: strategies and challenges. Pharmaceuticals (Basel), 2012. **5**(11): p. 1177-209.
268. Fuchs, H., C. Bachran, and D. Flavell, Diving through membranes: molecular cunning to enforce the endosomal escape of antibody-targeted anti-tumor toxins. Antibodies, 2013. **2**(2): p. 209.
269. Rawat, A., B. Vaidya, K. Khatri, A.K. Goyal, P.N. Gupta, S. Mahor, R. Paliwal, S. Rai, and S.P. Vyas, Targeted intracellular delivery of therapeutics: an overview. Pharmazie, 2007. **62**(9): p. 643-58.
270. Torchilin, V.P., Recent approaches to intracellular delivery of drugs and DNA and organelle targeting. Annu Rev Biomed Eng, 2006. **8**: p. 343-75.
271. Keller, J., I. Heisler, R. Tauber, and H. Fuchs, Development of a novel molecular adapter for the optimization of immunotoxins. J Control Release, 2001. **74**(1-3): p. 259-61.
272. Salojin, K.V., I.B. Owusu, K.A. Millerchip, M. Potter, K.A. Platt, and T. Oravecz, Essential role of MAPK phosphatase-1 in the negative control of innate immune responses. J Immunol, 2006. **176**(3): p. 1899-907.
273. Nakagawa, R., T. Naka, H. Tsutsui, M. Fujimoto, A. Kimura, T. Abe, E. Seki, S. Sato, O. Takeuchi, K. Takeda, S. Akira, K. Yamanishi, I. Kawase, K. Nakanishi, and T. Kishimoto, SOCS-1 participates in negative regulation of LPS responses. Immunity, 2002. **17**(5): p. 677-87.
274. Rogliani, P., L. Calzetta, J. Ora, and M.G. Matera, Canakinumab for the treatment of chronic obstructive pulmonary disease. Pulm Pharmacol Ther, 2015. **31**: p. 15-27.
275. Lachmann, H.J., I. Kone-Paut, J.B. Kuemmerle-Deschner, K.S. Leslie, E. Hachulla, P. Quartier, X. Gitton, A. Widmer, N. Patel, P.N. Hawkins, and C.S.G. Canakinumab in, Use of canakinumab in the cryopyrin-associated periodic syndrome. N Engl J Med, 2009. **360**(23): p. 2416-25.
276. NCT02497469, Clinical trial number NCT02497469 for "An efficacy and safety study of Vedolizumab intravenous (IV) compared to Adalimumab subcutaneous (SC) in participants with ulcerative colitis" at ClinicalTrials.gov. 2015.
277. Lapadula, G., A. Marchesoni, A. Armuzzi, C. Blandizzi, R. Caporali, S. Chimenti, R. Cimaz, L. Cimino, P. Gionchetti, G. Girolomoni, P. Lionetti, A. Marcellusi, F.S. Mennini, and C. Salvarani, Adalimumab in the treatment of immune-mediated diseases. Int J Immunopathol Pharmacol, 2014. **27**(1 Suppl): p. 33-48.
278. Streit, M., Z. Beleznay, and L.R. Braathen, Topical application of the tumour necrosis factor-alpha antibody infliximab improves healing of chronic wounds. Int Wound J, 2006. **3**(3): p. 171-9.
279. Kornbluth, A., Infliximab approved for use in Crohn's disease: a report on the FDA GI Advisory Committee conference. Inflamm Bowel Dis, 1998. **4**(4): p. 328-9.
280. Blumenauer, B., M. Judd, G. Wells, A. Burls, A. Cranney, M. Hochberg, and P. Tugwell, Infliximab for the treatment of rheumatoid arthritis. Cochrane Database Syst Rev, 2002(3): p. CD003785.
281. Oldfield, V., S. Dhillon, and G.L. Plosker, Tocilizumab: a review of its use in the management of rheumatoid arthritis. Drugs, 2009. **69**(5): p. 609-32.
282. Bugelski, P.J. and P.L. Martin, Concordance of preclinical and clinical pharmacology and toxicology of therapeutic monoclonal antibodies and fusion proteins: cell surface targets. Br J Pharmacol, 2012. **166**(3): p. 823-46.
283. Smolen, J.S., M.E. Weinblatt, S. Sheng, Y. Zhuang, and B. Hsu, Sirukumab, a human anti-interleukin-6 monoclonal antibody: a randomised, 2-part (proof-of-concept and dose-finding), phase II study in patients with active rheumatoid arthritis despite methotrexate therapy. Ann Rheum Dis, 2014. **73**(9): p. 1616-25.
284. Sanford, M. and K. McKeage, Secukinumab: first global approval. Drugs, 2015. **75**(3): p. 329-38.
285. Mease, P.J., I.B. McInnes, B. Kirkham, A. Kavanaugh, P. Rahman, D. van der Heijde, R. Landewe, P. Nash, L. Pricop, J. Yuan, H.B. Richards, S. Mpofu, and F.S. Group, Secukinumab Inhibition of Interleukin-17A in Patients with Psoriatic Arthritis. N Engl J Med, 2015. **373**(14): p. 1329-39.

286. Farahnik, B., K. Beroukhim, T.H. Zhu, M. Abrouk, M. Nakamura, R. Singh, K. Lee, T. Bhutani, and J. Koo, Ixekizumab for the Treatment of Psoriasis: A Review of Phase III Trials. Dermatol Ther (Heidelb), 2016. **6**(1): p. 25-37.
287. Tsuda, K., T. Tanimoto, S. Takenouchi, S. Sakaue, and T. Komatsu, Ixekizumab for psoriasis. Lancet, 2016. **387**(10015): p. 225-6.
288. Lebwohl, M., B. Strober, A. Menter, K. Gordon, J. Weglowska, L. Puig, K. Papp, L. Spelman, D. Toth, F. Kerdel, A.W. Armstrong, G. Stingl, A.B. Kimball, H. Bachelez, J.J. Wu, J. Crowley, R.G. Langley, T. Blicharski, C. Paul, J.P. Lacour, S. Tyring, L. Kircik, S. Chimenti, K. Callis Duffin, J. Bagel, J. Koo, G. Aras, J. Li, W. Song, C.E. Milmont, Y. Shi, N. Erondu, P. Klekotka, B. Kotzin, and A. Nirula, Phase 3 Studies Comparing Brodalumab with Ustekinumab in Psoriasis. N Engl J Med, 2015. **373**(14): p. 1318-28.
289. Gordon, K.B., K.C. Duffin, R. Bissonnette, J.C. Prinz, Y. Wasfi, S. Li, Y.K. Shen, P. Szapary, B. Randazzo, and K. Reich, A Phase 2 Trial of Guselkumab versus Adalimumab for Plaque Psoriasis. N Engl J Med, 2015. **373**(2): p. 136-44.
290. Panaccione, R., W.J. Sandborn, G.L. Gordon, S.D. Lee, A. Safdi, S. Sedghi, B.G. Feagan, S. Hanauer, W. Reinisch, J.F. Valentine, B. Huang, and R. Carcereri, Briakinumab for treatment of Crohn's disease: results of a randomized trial. Inflamm Bowel Dis, 2015. **21**(6): p. 1329-40.
291. Papp, K.A., M. Sundaram, Y. Bao, D.A. Williams, Y. Gu, J.E. Signorovitch, Y. Wang, J.M. Valdes, and P.M. Mulani, Effects of briakinumab treatment for moderate to severe psoriasis on health-related quality of life and work productivity and activity impairment: results from a randomized phase III study. J Eur Acad Dermatol Venereol, 2014. **28**(6): p. 790-8.
292. Harris, K.A., S. Horst, A. Gadani, A. Nohl, K. Annis, C. Duley, D. Beaulieu, L. Ghazi, and D.A. Schwartz, Patients with Refractory Crohn's Disease Successfully Treated with Ustekinumab. Inflamm Bowel Dis, 2016. **22**(2): p. 397-401.
293. Legendre, C.M., C. Licht, P. Muus, L.A. Greenbaum, S. Babu, C. Bedrosian, C. Bingham, D.J. Cohen, Y. Delmas, K. Douglas, F. Eitner, T. Feldkamp, D. Fouque, R.R. Furman, O. Gaber, M. Herthelius, M. Hourmant, D. Karpman, Y. Lebranchu, C. Mariat, J. Menne, B. Moulin, J. Nurnberger, M. Ogawa, G. Remuzzi, T. Richard, R. Sberro-Soussan, B. Severino, N.S. Sheerin, A. Trivelli, L.B. Zimmerhackl, T. Goodship, and C. Loirat, Terminal complement inhibitor eculizumab in atypical hemolytic-uremic syndrome. N Engl J Med, 2013. **368**(23): p. 2169-81.
294. Rosario, M., N.L. Dirks, M.R. Gastonguay, A.A. Fasanmade, T. Wyant, A. Parikh, W.J. Sandborn, B.G. Feagan, W. Reinisch, and I. Fox, Population pharmacokinetics-pharmacodynamics of vedolizumab in patients with ulcerative colitis and Crohn's disease. Aliment Pharmacol Ther, 2015. **42**(2): p. 188-202.
295. Murray P.J. and Wynn T.A., Protective and pathogenic functions of macrophage subsets, Nat Rev Immunol, 2011. **11**(11): p.723-737.

VI Appendix

VI.1. Index of figures

VI.2. Index of tables

VI.3. List of monoclonal antibody candidates for treatment of IMIDs

Name of mAb	Target	Evaluation stage	Indication	Reference
Canakinumab	IL-1β	FDA approved, Phase I	FDA approved - Cryopyrin-associated periodic syndromes; autoinflammatory syndromes Phase I - COPD, gout and coronary artery disease	[274, 275]
Adalimumab	TNF-α	FDA approved	Crohn's disease, ulcerative colitis, RA, psoriatic arthritis, AS, moderate to severe chronic psoriasis and juvenile idiopathic arthritis.	[276, 277]
Infliximab	TNF-α	FDA approved	Crohn's disease, ulcerative colitis, psoriasis, psoriatic arthritis, AS and RA	[278-280]
Tocilizumab	IL-6R	FDA approved	RA, systemic juvenile idiopathic arthritis	[52, 281, 282]
Sirukumab	IL-6	Phase II,III	RA	[283]
Secukinumab	IL-17A	FDA approved, Phase II, III	FDA approved - psoriasis Phase III- AS and psoriatic arthritis Phase II - MS	[205, 284, 285]
Ixekizumab	IL-17	Phase II	Psoriasis	[286, 287]
Brodalumab	IL-17R	Phase III	Psoriasis	[288]
Guselkumab	IL-23	Phase II	Psoriasis	[289]
Tildrakizumab	IL-23	Phase III	Psoriasis	[289]
Briakinumab	IL-12/23	Phase II, III	Phase II – MS, Crohn's disease Phase III - Psoriasis	[290, 291]
Ustekinumab	IL-12/23	FDA approved, Phase II, III	FDA approved - psoriatic arthritis Phase II – MS, Crohn´s disease and sarcoidosis Phase III - psoriasis	[288, 292]
Eculizumab	C5	FDA approved	FDA approved - atypical hemolytic uremic syndrome.	[293]
Dupilumab	IL-4Rα	Phase II	Asthma, atopic dermatitis	[213]
Vedolizumab	integrin $\alpha_4\beta_7$	FDA approved	Ulcerative colitis and Crohn's disease	[294]

VI.4. List of Abbreviations

Ab	antibody
Ag	antigen
AD	atopic dermatitis
ADC	antibody-drug conjugate
ADCC	antibody dependent cellular cytotoxicity
AMML	acute myeloid monocytic leukemia
AP	alkaline phosphatase
APC	antigen presenting cell
appr.	approximately
AS	ankylosing spondylitis
ATCC	American type culture collection
BSA	bovine serum albumin
bsscFv	bispecific single chain variable fragment
CD	cluster of differentiation
CDR	complementarity determining region
CDW	chronic diabetic wound
CIS	cytokine-induced STAT inhibitor
COPD	chronic obstructive pulmonary disease
CML	chronic myeloid leukemia
CMML	chronic myeloid monocytic leukemia
CXCL	C-X-C (motif) ligand
DC	dendritic cell
DMSO	dimethyl sulfoxide
DNA	deoxyribonucleic acid
DPBS	Dulbecco's phosphate-buffered saline
DSMZ	Deutsche Sammlung von Mikroorganismen und Zellkulturen
DTT	dithiothreitol
EDTA	ethylenediaminetetraacetic acid
eGFP	enhanced green-fluorescent protein
EGFR	epidermal growth factor receptor
E-Sel	e-selectin
ETA`	exotoxin A (truncated version)
FACS	fluorescence-activated cell sorting
Fc	fragment crystallizable
FC	flow cytometry
FCS	fetal calf serum
FDA	Food and Drug Administration
FITC	fluorescein isothiocyanate
g	relative centrifuge force
GM-CSF	granulocyte macrophage colony stimulating factor
h	hour(s)
HAB	human antibody blocking
hCD64	human cluster of differentiation number 64

hCFP	human cytolytic fusion protein
His-tag	poly-histidine tag sequence
HTS	high throughput screening
H22	humanized anti-CD64 antibody (fragment) clone 22
IBD	inflammatory bowel disease
ICAM	intercellular adhesion molecule
Ig (G,A)	immunoglobulin G, A, etc.
IFN-γ	interferon gamma
IHC	immunohistochemistry
IL	interleukin
IMAC	immobilized metalion affinity chromatography
IME	institute for molecular biology and applied immunology
IMID	immune-mediated inflammatory disease
IT	immunotoxin
ITAM	immunoreceptor tyrosine activation motifs
IC_{50}	inhibitory concentration at 50% survival
IPTG	isopropyl-beta-D-thiogalactopyranoside
IP-10	IFN-γ-inducible protein 10
IRF-3	interferon regulatory factor 3
JAK	janus kinase
KC	Kuepfer cells
kD	kilodalton
K_D	dissociation constant
KLF	Kruppel-like factor
LAP	latency-associated peptide
LB	lysogeny broth
LPS	lipopolysaccharides
mAbs	monoclonal antibodies
MAP	microtubuli-associated protein
MCP	monocyte chemoattractant protein-1
MIF	macrophages migration inhibitory factor
min	minute(s)
MFI	mean fluorescent intensity
MHC	major histocompatibility complex
ML	myeloid leukemia
MO	monocytes
MPS	mononuclear phagocyte system
MS	multiple sclerosis
МΦ	macrophages
m22	murine monoclonal antibody against CD64 (clone 22)
NADPH	Nicotinamide adenine dinucleotide phosphate
NBT/BCIP	nitro blue tetrazolium chloride/5-bromo-4-chloro-3-indolyl phosphate
Nf-κB	Nuclear Factor Kappa B (cells)
NK	natural killer cell

nm	nanometer
NO	nitric oxide
NTA	nitrilotriacetic acid
NRF2	nuclear respiratory factor 2
NΘ	neutrophils
ori	origin of replication
PAGE	polyacrylamide gel electrophoresis
PBMC	peripheral blood mononuclear cells
PBS	phosphate buffer saline
PBST	phosphate buffer saline + 0.05% Tween 20
PCR	polymerization chain reaction
PI	propidium iodide
PE	phycoerythrin
pH	negative logarithm of the concentration of hydrogen ions in solution
PPARγ	peroxisome proliferator-activated receptor gamma
RA	rheumatoid arthritis
RBC	red blood cells
RNA	ribonucleic acid
RPMI	Roswell Park Memorial Institute
RT	room temperature (~21°C)
rpm	rotations per minute
RNS	reactive nitric species
ROS	reactive oxygen species
scFv	single chain variable fragment
sIgA	secretory immunoglobulin A
STAT	signal transducer and activator of transcription
SEC	size exclusion chromatography
SDS	sodium dodecyl sulphate
SOCS	suppressor of cytokine signaling
SOC	super optimal broth
SEM	standard error of mean
SD	standard deviation
SLE	systemic lupus erythematosus
SLS	sodium laureth sulfate
T1D	type 1 diabetes
T2D	type 2 diabetes
TAE	tris-acetate-EDTA
TAM	tumor associated macrophage
TB	terrific broth
TEMED	tetramethylethylenediamine
TGF	transforming growth factor
TGS	tris-glycine-SDS
Th	T helper lymphocyte
TLR	toll-like receptor

TNF	tumor necrosis factor
TRP-14	thioredoxin-related protein 14 kDa
Trx	thioredoxin
TRIS	Tris(hydroxymethyl)aminomethane
Tween20	polyoxyethylene (20) sorbitan monolaurate
U	units
UV	ultraviolet
v/v	volume/volume
VEGF	vascular endothelial growth factor
XTT	sodium 3'-[1-(phenylaminocarbonyl)-3,4-tetrazolium] bis(4-methoxy-6-nitro)benzenesulfonic acid hydrate
WB	western blot
w/v	weight/volume

VI.5. Vector maps of generated fusion proteins

VI.5.1. Vectors for eukaryotic expression of both MIMPs

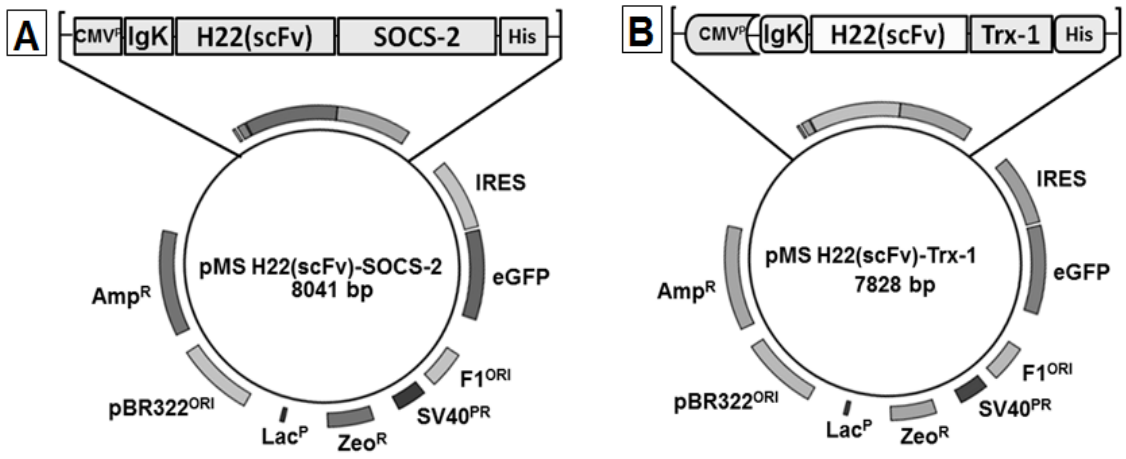

Figure 41: Schematic drawing of the H22(scFv)-SOCS-2 (A) and H22(scFv)-Trx-1 (B) encoding pMS-plasmid.
The backbone of the pMS plasmid is the pSecTag2. The strong constitutive CMV-promoter (CMVp) guarantees an overexpression of the engineered construct and also the co-expression of the enhanced green fluorescent protein (eGFP) enabled by internal ribosomal entry site (IRES). Further selection of efficiently transfected HEK293T-cells was conducted using a Zeocin resistance gene (ZeoR) under control of the SV40-promoter region (SV40PR). The supernatant expression of the engineered MIMPs was achieved using the human IgK-leader (IgK). The mRNA stabilization was invigorated by a synthetic intervening sequence (IVS). For plasmid propagation in *E. coli* was used a bacterial origin of replication (pBR322) and an ampicillin resistance gene (AmpR). The recombinant proteins were fused to a His6-tag to allow easy protein enrichment by IMAC (II.2.2.3.2) and binding detection (II.2.4.1.1)

VI.5.2. Vectors for prokaryotic expression of the CD89(scFv)- ETA'

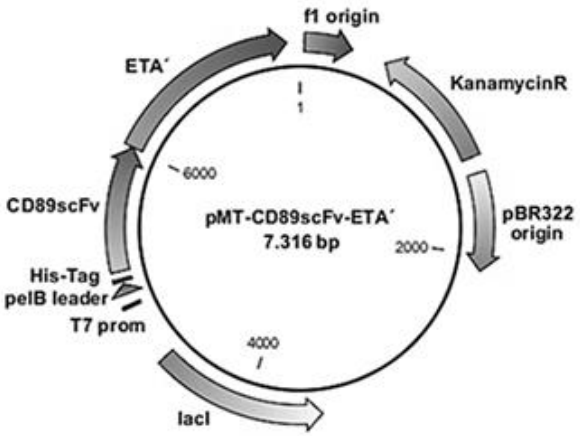

Figure 42: Schematic drawing of the CD89(scFv)-ETA' encoding pMT vector.
The CD89(scFv) comprising the VL and VH sequences was separated by a (G4S)4 linker. The resulting scFv sequence was cloned into the pMT vector containing the sequence of ETA', which is a truncated version of Pseudomonas exotoxin A containing domains Ib, II and III. For plasmid propagation in *E. coli* was used a bacterial origin of replication (pBR322) and an kanamycin resistance gene (KanamycinR). The mRNA of the recombinant IT has been transcribed by the inducible T7 polymerase recognizing the T7 promotor (T7prom). The recombinant expression was targeted at the periplasmic space using the PelB leader sequence. The recombinant proteins were fused to a His_6-tag to allow easy protein enrichment by IMAC (II.2.2.3.2) and binding detection (II.2.4.1.1)

VI.6. Sequences of generated constructs

VI.6.1. Sequence of H22(scFv)-SOCS-2

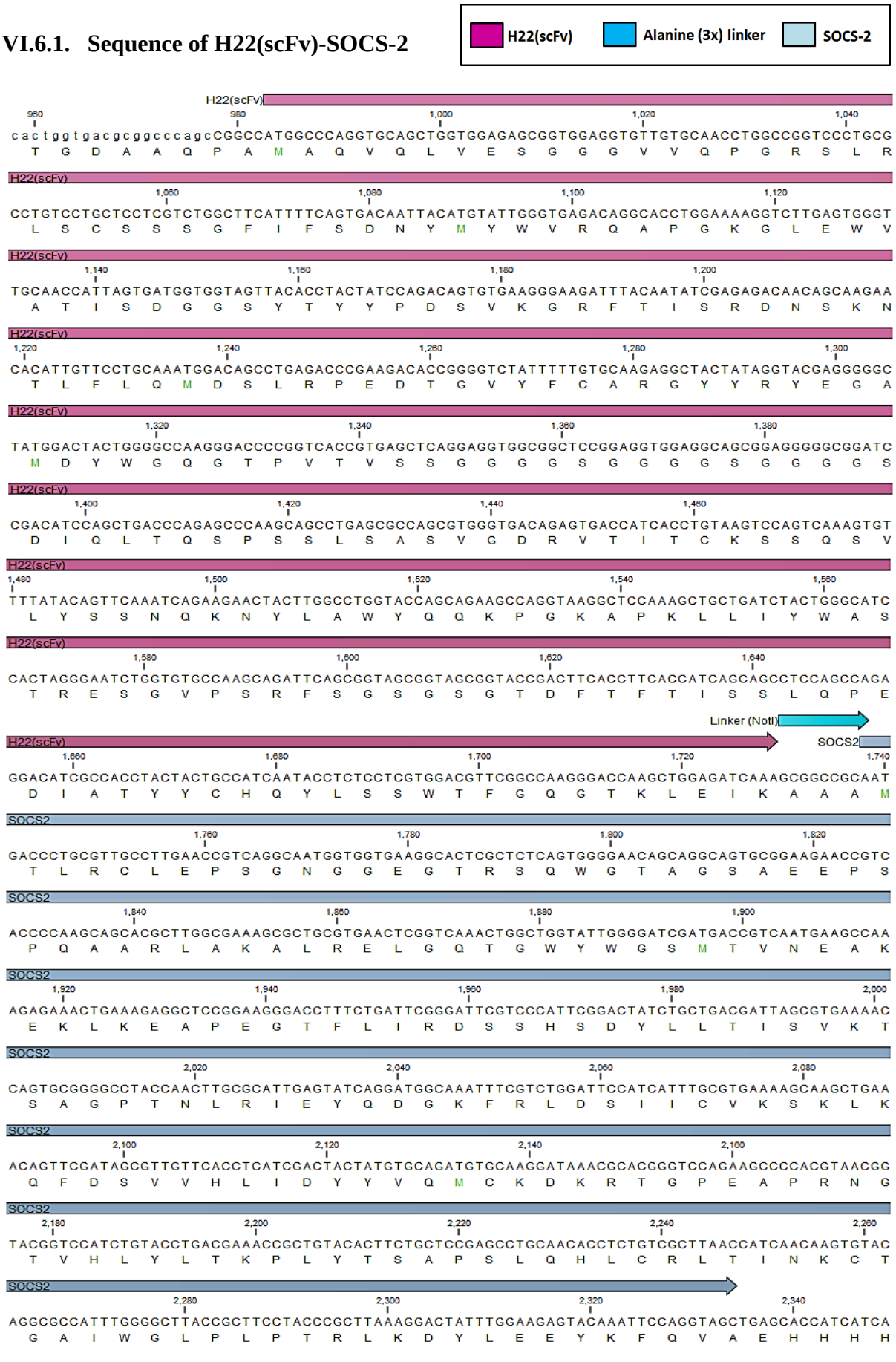

VI.6.2. Sequence of H22(scFv)-Trx-1

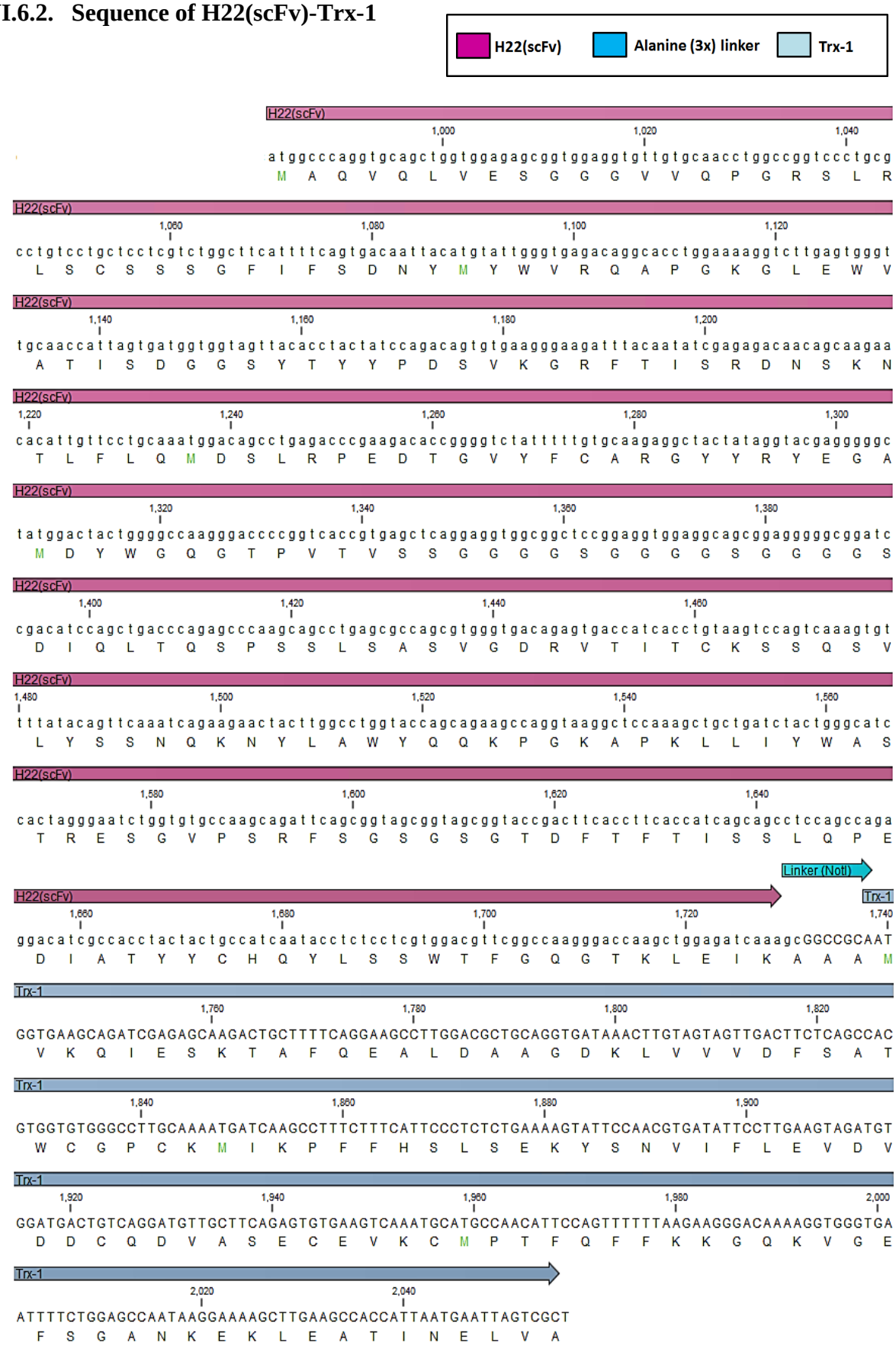

VI.6.3. Sequences of CD89(scFv)- ETA'

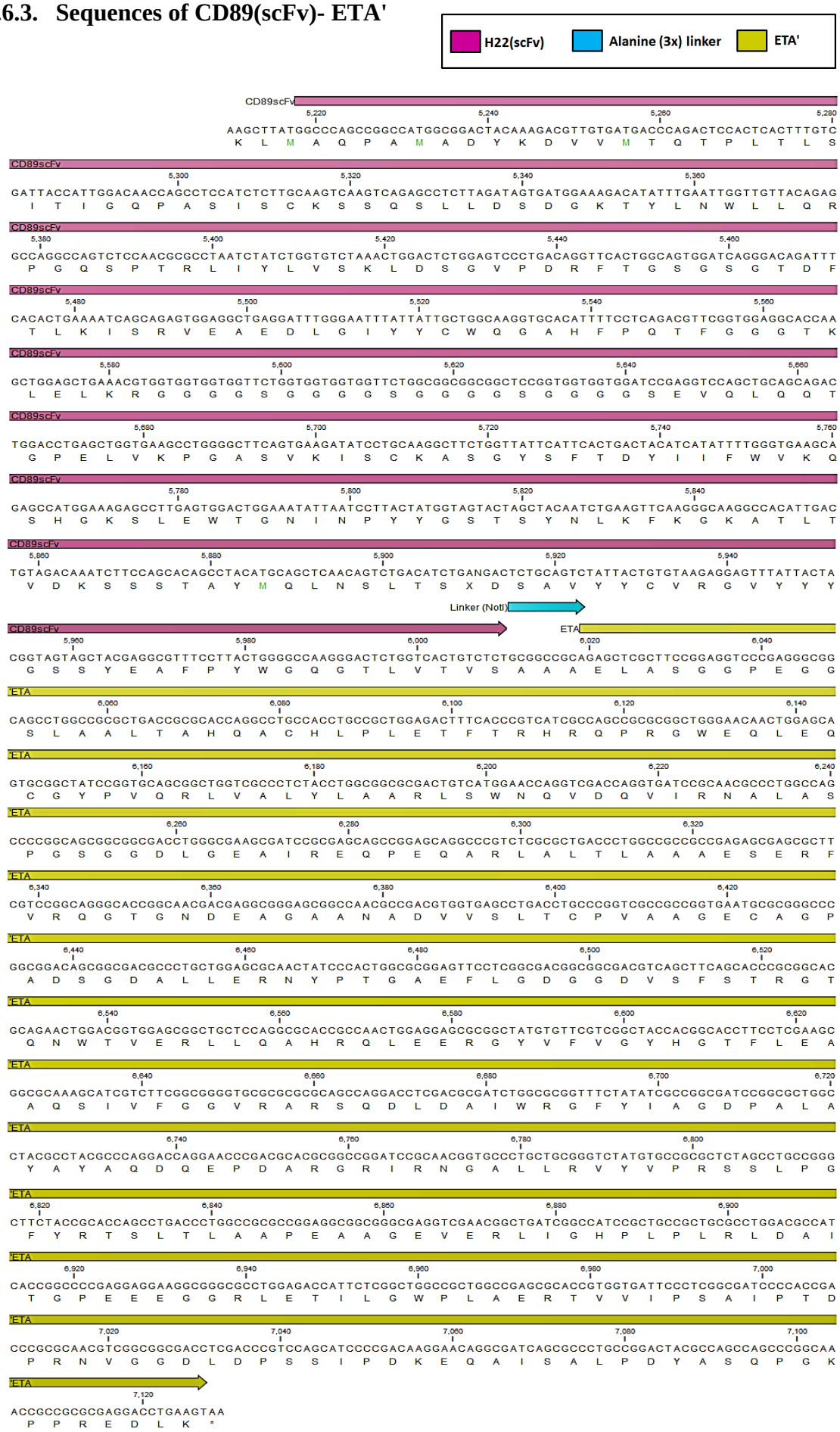

Curriculum Vitae

Personal information

Birthday: 17 April 1986

Place of birth: St. Zagora (Bulgaria)

Nationalities: German / Bulgarian

Academic background

Jan. 2013 – to date
Fraunhofer IME / RWTH Aachen University
- Doctorate (Dr. rer nat) at Fraunhofer IME, Aachen
- "SkinHeal" project within Fraunhofer Society

Oct. 2009 – Oct. 2012
RWTH Aachen University (Germany)
- Molecular and applied biotechnology
- Master of Science, Grade: 1.8
- Master thesis: 1.0

Oct. 2006 – Sep. 2009
RWTH Aachen University (Germany)
- Biotechnology
- Bachelor of Science, Grade: 2.3
- Bachelor thesis: 1.3

Sep. 2000 – Jun. 2005
Foreign-language high school "Romain Rolland", St. Zagora (Bulgaria)
- High school diploma, Grade: 1.1
- Profiles: German, English und natural science

Work and project experience

Aug. 2012 – Mar. 2013
Research associate
Antibodies-online GmbH
- Quality und product management

Nov. 2009 – Jun. 2011
Student assistant
Biotechnology chair, RWTH Aachen
- "BioNoCo" – Research program of DFG

1st Research project: "Asymmetric reduction of ketones with recombinant *E. coli* whole cells in neat substrates"

2nd Research project: "Analysis of Two Variants of Carbonyl Reductases from *Candida parapsilosis* species"

Prizes and Awards

2015 – to date
Scholarship at Jürgen Manchot Foundation

Nov. 2014
"Best Keynote Talk" Award - PhD Seminar - Fraunhofer IME

Additional skills

Animal training	FELASA Cat. B certificate
EDP and IT	MS Office, Cyflogic, WinMDI, BD CellQuest Pro, Graphpad Prism, WinMDI, Origin Pro 7, BioEdit, EndNote, CLC Main Workbench, Adobe Design Premium CS, Aida Image Analyzer, BioEdit, SeqManager, Unicorn, Quantity One, HistoCAD, Clone Manager

Languages

German	Fluent (Goethe Institute and TestDaF Institute)
English	Fluent (Language courses at RWTH Aachen University)
Bulgarian	Mother Tongue

Volunteer commitments

2014-2016	Chairman of election office in Aachen/Vaals for parliamentary elections in Bulgaria
2009 – 2015	Translations for municipal of Kazanlak, Bulgaria

Extracurricular activities

Volleyball, “Der Grillmeister”, Sci-Fi

Achievements during the PhD study at Fraunhofer IME

Filed patent applications

Oct. 2014	**Mladenov R.**, Stein C., Barth S., Fischer R. – "Anti-CD89 cytotoxic complex" (WO2016/150496).
Oct. 2013	Hristodorov D., **Mladenov R.**, Thepen T., Barth S. – "A microtubuli-modifying compound" (WO/2014/064187).
May. 2013	Hristodorov D., **Mladenov R.**, Thepen T., Barth S. – "Targeted modulation of macrophages" (WO/2014/191391).

Publications related to the topic of the PhD thesis

Feb. 2016	**Mladenov, R.**[†], Hristodorov, D.[†], *et al* Fully human MAP-fusion protein specifically targets and eliminates proliferating CD64+ M1 macrophages. Immunology and cell biology, doi:10.1038/icb.2016.4 (accepted).
Dec. 2015	Cremer C., Braun H., **Mladenov**, **R.**, *et al* - Novel angiogenin mutants with increased cytotoxicity enhance the depletion of pro-inflammatory macrophages and leukemia cells ex vivo. Cancer Immunol Immunother 64(12):1575-1586.
Jul. 2015	Hristodorov, D.[†], **Mladenov**, **R.**[†], *et al* – Targeting CD64 mediates elimination of M1 but not M2 macrophages in vitro and in cutaneous inflammation in mice and patient biopsies. mAbs, 7(5), 853-862.
Dec. 2015	**Mladenov**, **R.**, Hristodorov D., *et al* – The Fc-alpha receptor is a new target antigen for immunotherapy of myeloid leukemia. Int J Cancer, 137(11), 2729-2738.
Nov. 2014	Hristodorov, D., **Mladenov**, **R.**, *et al* – Recombinant H22(scFv) blocks CD64 and prevents the capture of anti-TNF monoclonal antibody: A potential strategy to enhance anti-TNF therapy. mAbs, 6(5), 1283-1289.
Jan. 2013	Schiffer, S., Hristodorov, D., **Mladenov, R.**, *et al* – Species-dependent functionality of the human cytolytic fusion proteins Granzyme B-H22(scFv) and H22(scFv)-Angiogenin in macrophages, Antibodies, 2, 9-18.
Sep. 2012	Hristodorov, D., **Mladenov, R.**, *et al.* - Macrophage-targeted therapy: CD64-based immunotoxins for treatment of chronic inflammatory diseases. (Review). Toxins (Basel). 4(9):676-694.

Topic-unrelated publications during the PhD study

Aug. 2016	**Mladenov R.**, Hristodorov D., *et al.* - CD64-directed microtubule associated protein tau kills leukemic blasts ex vivo. Oncotarget, 2016, doi: 10.18632/oncotarget.11568 (accepted).
Apr. 2016	Amoury M., **Mladenov R.**, *et al.* - A novel approach for targeted elimination of CSPG4-positive triple negative breast cancer using a MAP-tau based fusion protein. Int J Cancer, doi: 10.1002/ijc.30119 (accepted).

[†] shared first authors

Mar. 2016	Amoury M., Kolberg K., Pham, A.T., Hristodorov D., **Mladenov R**., *et al.* - Granzyme B-based cytolytic fusion protein targeting EpCAM specifically kills triple negative breast cancer cells in vitro and inhibits tumor growth in a subcutaneous mouse tumor model. Cancer Lett, 372(2):201-209.
Sep. 2015	Brehm, H., Hristodorov, D., Pardo, A., **Mladenov**, **R**., *et al.* – Targeted killing of rhabdomyosarcoma cells by a MAP-based human cytolytic fusion protein. Cancer Lett, 365(2), 149-155.
Oct. 2014	Brehm, H., Niesen, J., **Mladenov**, **R**., *et al.* – A CSPG4-specific immunotoxin kills rhabdomyosarcoma cells and binds to primary tumor tissues. Cancer Lett, 352(2), 228-235.
Sep. 2014	Hristodorov, D., Amoury, M., **Mladenov**, **R**., *et al.* – EpCAM-selective elimination of carcinoma cells by a covel MAP-based cytolytic fusion protein. Molecular Cancer Therapy, 13(9), 2194-2202.
Jan. 2014	Hristodorov, D., Nordlohne, J., **Mladenov**, **R**., *et al.* – Human microtubule-associated protein tau mediates targeted killing of CD30(+) lymphoma cells in vitro and inhibits tumour growth in vivo. British Journal of Haematology, 164(2), 251-257.
Dec. 2013	Schiffer, S., Letzian, S., Jost, E., **Mladenov**, **R**., *et al.* – Granzyme M as a novel effector molecule for human cytolytic fusion proteins: CD64-specific cytotoxicity of Gm-H22(scFv) against leukemic cells. Cancer Lett, 341(2), 178-185.
Sep. 2013	Hristodorov, D., **Mladenov, R**., *et al.* – Microtubule-associated protein tau facilitates the targeted killing of proliferating cancer cells in vitro and in a xenograft mouse tumour model in vivo. Br J Cancer, 109(6), 1570-1578.

Posters

Jun. 2015	Gordon Research Conferences (Phagocytes) in Boston, Massachusetts, and Waterville, New Hampshire, USA
Jun. 2014	Biomedica Summit in Maastricht, Holland.
Sep. 2013	43. Annual Meeting of Germany Society for Immunology

Speaker

Sep. 2013	Talk (20 min) at the 43. Annual Meeting of Germany Society for Immunology

Awards, Certificates and Scholarships

2015 – 2016	Scholarship at Jürgen Manchot Foundation
Sep. 2014	"Best Keynote Talk" Award - PhD Seminar - Fraunhofer IME
2013	FELASA Cat. B certificate in animal training

Technical supervision

2014	Master thesis of Tim Stroisch – "Generation and evaluation of H22(scFv)-fused immunomodulatory proteins" (1.0)